Comparison of Linear, Nonlinear, Hysteretic, and Probabilistic MR Damper Models

By

Russell Richards

Thesis submitted to the Faculty of the
Virginia Polytechnic Institute and State University
in partial fulfillment of the requirements for the degree of

Master of Science
In
Mechanical Engineering

APPROVED:

Corina Sandu, Co-Advisor Steve Southward, Co-Advisor
Mehdi Ahmadian, Committee Member

February 26, 2007
Blacksburg, Virginia

Keywords: Magnetorheological Fluid, Active Dampers, Shock Absorber Characterization

Comparison of Linear, Nonlinear, Hysteretic, and Probabilistic MR Damper Models

Russell Richards

Abstract

Magnetorheolgical (MR) fluid dampers have the capability of changing their effective damping force depending on the current input to the damper. A number of factors in the construction of the damper, as well as the properties of the fluid and the electromagnet, create a dynamic response of the damper that cannot be fully described with a static model dependent on current and velocity. This study will compare different techniques for modeling the force response of the damper in the current-velocity space.

To ensure that all the dynamic response characteristics of the damper are captured in data collection, random input signals were used for velocity and current inputs. By providing a normally distributed random signal for velocity to a shock dynamometer and a uniformly distributed random signal for current to a Lord rheonetic seat damper, the force response could be measured.

The data from this test is analyzed as a two dimensional signal, a three dimensional force plot in the current velocity plane, and as a probability density function. Four models are created to fit the data. The first is a linear model dependent solely on current. The second is a nonlinear model dependent on both current and velocity. The third model takes the nonlinear model and includes a filter that affects the force response of the model with time. Each of these three approaches are compared based on the total error in the force response and the models' ability to match the PDF of the data. Finally, a fourth model is created for the damper that improves the nonlinear model by making one parameter a probability parameter defined by a PDF calculated from the data. However, because it is a probability model, the error cannot be found through comparison to the data.

Acknowledgements

I would like to thank my advisors, Dr. Corina Sandu and Dr. Steve Southward, for all their help and support in my pursuit of a Master's degree. Throughout this process they have provided support and encouragement in my research and my studies. Their advice and their enthusiasm were critical to the success of this effort. I would also like to thank Dr. Mehdi Ahmadian for serving on my advisory committee, as well as his readiness to lend a hand. I would also like to thank Shawn Emmons for all his efforts to aid me in the experimentation phase of the research.

Of course I could never have made it without the support of friends and family. My parents deserve many thanks for their encouragement, their interest in my work, and all their aid both with my studies and financially. Finally, I would like to give my thanks and all my love to my Fiancée, who has endured my stress and long hours with unwavering support. This work is a realization of the efforts of everyone.

Table of Contents

List of Figures

List of Tables

1 Introduction

This thesis presents a magnetorheological (MR) damper characterization study. The main objective of the study was to better understand, through mathematical modeling, the behavior of an MR damper under random excitation. This new approach will enable the implementation of better control strategies, as well as provide the basis for developing computer models that will more accurately predict the force response of the damper.

This chapter presents the background, research motivation of the study, and introduces the content of the project.

1.1 Background and Motivation

Magnetorheolgical (MR) dampers have the capability of enabling semi-active control of the motion of a system of interest, such as a sprung mass. Due to the properties of the MR fluid, MR dampers have the ability to vary damping force in real time using much less energy than fully-active systems. The most common application of MR dampers is in automotive shock absorbers. By changing the damping characteristics of the damper, the suspension can be semi-actively controlled for improved ride and handling. Other MR damper applications include vibration absorbers for large structures, fluid clutches, and gun recoil absorbers [1].

It is important for all applications of MR dampers to have consistent control over the output force. However, there is currently little information available in the literature on the controllability of MR dampers. Characterization of the dampers has been done using discrete, constant values of current to control the output force. In addition, the relationship between velocity and force is treated in the same manner as for passive dampers, where any hysteresis or nonlinear effects that result in a discontinuous relationship are averaged out of the data. The relationship between current, velocity, and force is generally plotted in a two dimensional space, an example being the research done by Goncalves [2]. The representation of test data in this way does not provide any information regarding the possible variations in the output force. In reality, the hysteresis

due to damper construction, the fluid characteristics, and the lag in the response time due to current cause the current, velocity, and force plot to have an additional dimension which in this study will be identified as thickness. In this context, thickness describes the range of possible force values for the same current and velocity inputs, thus quantifying the stochastic behavior of the MR damper.

1.2 Research Goals and Approach

To improve the current way of modeling and characterizing MR dampers, this thesis will present three dimensional data of current, velocity, and force. It is the goal of this work to develop a damper model that will aid in controllability studies, enable new control methods to improve the accuracy of the force response, and improve existing damper models for simulation purposes. This will be accomplished by running experimental tests where both velocity and current vary with time over the range of interest of both parameters. The data collected will still be presented as dependent on velocity and current, but a stochastic approach will be taken to characterize any thickness in the current, velocity, and force graph.

1.3 Thesis Outline

This thesis contains five chapters which are followed by a list of references and appendices. The next chapter reports on a literature review of previous theses, journals, and papers that pertain to the research addressed in the current study. It will include an overview of passive dampers with details on their construction and characterization methods. Next, a description of active and semi-active dampers, focusing on MR fluid technology and its advantages, will be discussed. Further details on current techniques employed to characterize MR dampers, as well as on control methods and MR damper applications will be given. Chapter 2 will conclude with an analysis of statistic methods of describing a data set. Chapter 3 presents the experiment performed in this study. This will include the details of the input signals for velocity and current used in the experiment. It will also cover the experimental set up, the testing procedures, and some

conclusions regarding the design of this experiment. Chapter 4 covers an analysis of the test data collected, presents a discrete model relating force to velocity and current, displays the stochastic nature of the experimental results, and explains a probability analysis of the stochastic model. Finally, Chapter 5 presents the conclusions drawn from this work and explores some ideas for the future applications of these results.

2 Literature Review

This section presents background information on damper technology and statistical analysis needed to introduce the concepts in this thesis. The information here is a summary of important information found in a comprehensive literature review. Journal articles, thesis, and books were searched for topics relating to shock absorbers, dampers, active damper, magnetorheological dampers, MR damper models, probability models, and stochastic models. Each result of this search was examined for relevance to the subject. The following sections review the information that was found, organized by subject.

2.1 Passive Damper Technology

Dampers, more commonly known as shock absorbers, are used in vehicle applications to control excessive motions of the vehicle in ride conditions, roll, and pitch. Though called a shock absorber, they do not absorb forces applied to the system in the literal sense but serve the purpose of dissipating energy from the vertical motion of the wheels and body. In this study the device will be referred to as a damper, as this is the more appropriate term for its application. The first dampers appeared on automobiles in 1910. Originally, they were frictional, or Coulomb dampers. By 1925 hydraulic dampers became widespread. Active dampers, which will be discussed in the following section, are a more recent invention, with its beginnings in the 1980s [3].

Dampers today are most often hydraulic with telescopic construction, which provides easy packaging for linear damping application. The three basic types of hydraulic telescopic dampers are shown in Figure 2-1 [3]. Each type of construction is a solution to the different volumes on each side of the piston. Because of the area of the rod at its circular cross section, the change in volume on one side of the damper with the rod is less than on the side without the rod. That is,

$$\begin{aligned} \Delta V_u &= \left(A_{tube} - A_{rod}\right)d \\ \Delta V_l &= A_{tube}d \end{aligned} \tag{2.1}$$

where,

ΔV_u is the volume in the upper chamber
ΔV_l is the volume in the lower chamber
A_{tube} is the circular cross sectional area of the tube
A_{rod} is the circular cross sectional area of the rod
d is the distance travelled by the piston

Though this is not a problem with the through-rod damper, the fact that there is a second seal under pressure makes this construction method less reliable. Double tube and monotube construction mitigate the effect of the change in volume by including a volume of compressible gas after the fluid.

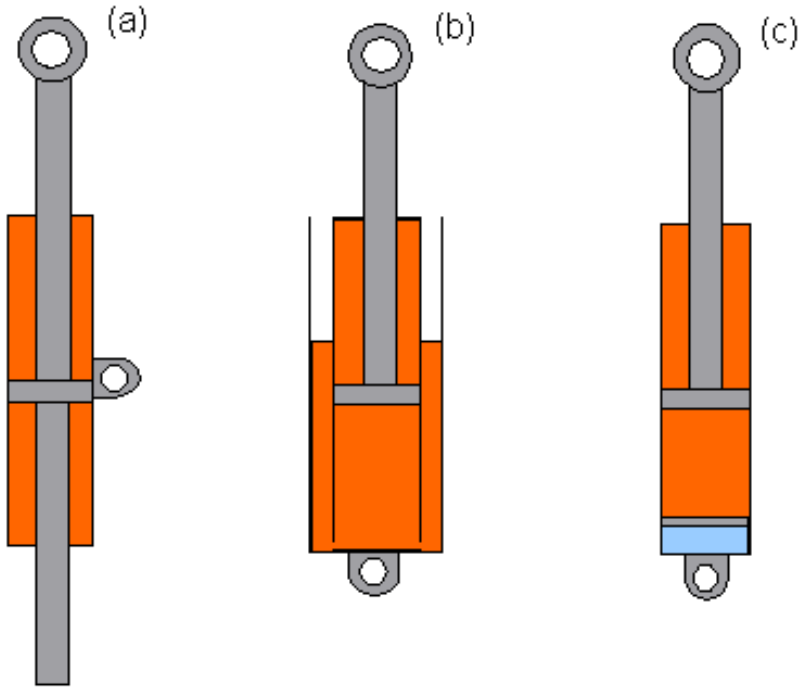

Figure 2-1. Three basic types of telescopic damper. Type (a) is a through-rod, type (b) is a double tube, and type (c) is a monotube.

Of these three types of telescopic dampers, the monotube and double tube are the most prevalent in automotive applications. Additional considerations about the construction of these dampers are the fluid type and the valve construction. Typical fluid for automotive dampers is mineral oil, whose properties are shown in Table 2-1 below. These can be used for flow calculations to determine the properties of the damper.

Though beyond the scope of this paper, there are some important conclusions about flow characteristics in dampers. First, if the flow were ideal, i.e. incompressible and frictionless, then the force exerted by the damper would be dependant on velocity alone. However, this is not the case. The flow in a damper will generally be turbulent for which friction effects are not trivial. Further, there are pressure losses at the valves based on an orifice model of the flow. This is compounded by the fact that due to size limitations valves are not often shaped to minimize such losses. The final flow consideration is cavitation. This occurs when the damper velocity is too high for the fluid and vapor bubbles appear. The fluid is now compressible and the dependence on fluid viscosity no longer applies. This phenomenon can damage internal parts of the damper so often "blow-off" valves are incorporated into the design. These increase the flow when the damper exceeds a certain velocity. In either case, the damper only exhibits predictable behavior below a designed maximum speed.

The force in the damper from fluid effects other than viscosity can be grouped in with friction between the seals and the piston and rod as nonlinear effects. In a passive damper these are any physical properties of the damper or damper fluid that cause the relationship between relative velocity and output force to be nonlinear. Some nonlinear effects vary with the position of the damper, and some are dependent on the direction the damper is traveling. In this study the word hysteresis will be used to describe any nonlinear effects that depend on the previous position and velocity of the damper.

2.2 Active and Semi-Active Damper Technology

Starting in the 1980s, special interest was paid to new active damper technologies. A true active system would be able to output the appropriate force to control the motion of the sprung mass throughout the range of inputs. These systems are complex and expensive because they require force actuators. Semi-active damping is a more practical and economical solution. Rather than control the force output by the damper over the entire range of inputs, semi-active control works by increasing or decreasing the effective damping coefficient of the damper; only dissipative forces (relative to the velocity of the damper) can be produced.

Recently, the most popular method of semi-active damping employs using magnetorheological fluid. Magnetorheological (MR) fluids change their apparent viscosity when a magnetic field is applied. MR fluid is made up of a carrier liquid, usually a standard passive damper fluid, which contains 20-40 percent by volume iron particles the measure 3-10 microns in diameter [4]. In addition, many MR fluids contain additives to keep the iron particles suspended. Without the magnetic field, the fluid behaves like a Newtonian liquid. When a magnetic field passes through the fluid, the iron particles act as dipoles and align along constant flux lines. When the particles are aligned, the apparent viscosity increases. The term apparent viscosity is used here because the viscosity of the base fluid is unaffected. However, the chains of iron particles have a yield strength that increases the force needed to achieve the same flow rate as an unactivated fluid. In this case the activated fluid can be closely modeled as Bingham Plastic [4].

The yield strength of an MR fluid is 50-100 kPa for applied magnetic fields of 150-250 kA/m [5]. This is a much higher yield strength than a comparable electro-rheological fluids, and the MR fluid is not very sensitive to temperature or contaminates. These improved properties of the MR fluid resulted in the technology being widely applied in the past decade.

Most applications use the fluid in one of three modes: valve mode, squeeze mode, and shear mode. In squeeze mode a thin layer or MR fluid is suspended between the two poles of paramagnetic substance [6].

Shear mode is a similar configuration to squeeze mode, but the force acts along the plates. This configuration is commonly used in rotating clutches, MR brakes, and rotational dampers [7].

The configuration pertinent to this experiment and applied primarily in telescopic dampers is the valve mode. For this case, the field is applied so that the chains of iron particles are perpendicular to the direction of flow. In order to pass through the valve, the chains must be broken [7]. Because of the large volume of fluid, the magnetic field is only applied at local points near the valves.

A typical schematic of an MR damper is shown in Figure 2-6 [1]. Much of the construction of an MR damper is similar to a passive damper. The damper in this figure

is of monotube construction. The top of the damper, at the right side of the figure, the damper has a floating piston design used to compensate for the unequal change in volume of the fluid at either side of the valve. The rod is at the opposite end, and attached to the piston assembly. The "valve" of the MR damper is where the major difference with a passive damper lies. Instead of a small orifice, the valve has a long, narrow fluid gap. Like a valve in a passive damper, there are flow effects such as turbulence and the possibility of cavitation at the entrance and exit of the fluid gap.

Control of damping force comes from two electromagnetic coils located in the piston. These coils create a magnetic field that passes through the MR fluid traveling through the fluid gap. Where the lines of constant flux of the magnetic field are perpendicular to the flow in the fluid gap, the iron particles in the fluid align and cause the fluid to exhibit yield strength, thereby increasing the effective damping.

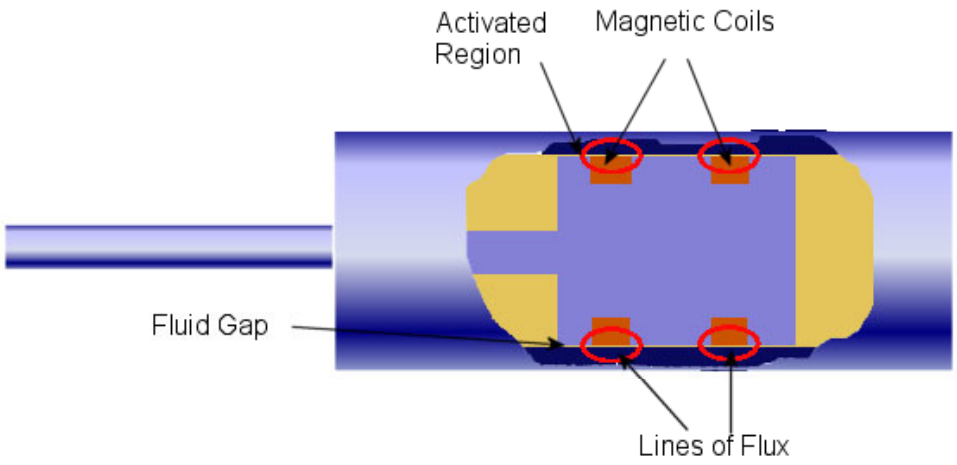

Figure 2-2. Typical schematic of an MR damper. Note that the activated region is very small compared to the volume of fluid. The lines of constant flux approximate straight lines due to the very small fluid gap [1].

2.3 Existing Magnetorheological Damper Models

There are many different approaches to modeling an MR damper. Nonlinear effects inherent to the damper such as the yield strength of the fluid when activated in valve mode require a nonlinear model. In addition, effects previously discussed

including friction, turbulent flow, and cavitation contribute to additional nonlinearities and time dependence that may be included in the model. There are two approaches to modeling an MR damper. The first is a simple nonparametric model, where empirical data is used to define the behavior of an MR damper. The second is parametric models, where there has been a significant amount of study devoted to creating a model. This is the focus of the modeling efforts in this thesis.

The nonparametric model used by Paré defines the response of an MR damper as any point contained within a performance 'envelope' [7]. In this case, the force response of the damper is found at two different currents which represent the maximum and minimum damping. Both curves are plotted versus velocity, which can be seen in research by Paré and Ahmadian [8]. The damper is defined as having a response that falls between the two curves.

A number of parametric models have been proposed to describe the force response of an MR damper. The Bouc-Wen model is a popular approach to damper modeling because it includes hysteresis and a phenomenological approach to the yield characteristics of the damper fluid [8]. A more involved model from Spencer et al. [9] based on the results of damping testing on a Lord MR damper. The physical model of the damper has a seven equation, fourteen parameter equation of motion. The first three equations are,

$$f = c_1\dot{y} + k_1(x - x_0)$$

$$\dot{y} = \frac{1}{c_0 + c_1}\left[\alpha z + c_0\dot{x} + k_0(x - y)\right]$$

$$\dot{z} = -\gamma|\dot{x} - \dot{y}||z|z|^{n-1} - \beta(\dot{x} - \dot{y})|z|^n + A(\dot{x} - \dot{y})$$

With the parameters defined as

$$\alpha = \alpha_a + \alpha_b u$$

$$c_1 = c_{1a} + c_{1b} u$$

$$c_0 = c_{0a} + c_{0b} u$$

$$\dot{u} = -\eta(u - v)$$

Parametric models have the ability of accurately characterizing an MR damper. However, models such as the Spencer model are difficult to solve numerically, due to sharp transition nonlinearity. This is detrimental to real time control applications.

A simpler model is the three element model created by Powell [10]. It is a model that represents a physical system of a viscous damper, a nonlinear spring, and a frictional damper in parallel. The equation for damper force is,

$$f = c\dot{x} + kx + F\sin(x)$$

where k, c, and F are parameters that are dependant on the vibration frequency, displacement amplitude, and input current. The lack of flexibility of the parameters limits the effectiveness of the three parameter model in this study.

For this study it is important to have a model that requires a minimum number of input parameters. From observation, it is also known that the period of the velocity excitation must be preserved in the force output of the model. Another consideration is ensuring that the function has a shape consistent with the preyield/postyield rheological domain characteristics of the MR damper. The difference in force response in ER and MR fluids is observed as a bend in the force versus velocity curve for a damper [11]. The simplest equation that contains this feature is a combination of the exponential function and the sign function [12]. Applying this to a damper gives the equation

$$f = sign(v) \times \left(1 - e^{-|v|/k}\right)$$

where k is a constant that determines the transition between the preyield and postyield regions.

2.4 Active Damper Control Techniques

One of the most commonly used control techniques for MR dampers is the Skyhook method. Skyhook control uses a switching technique to control the sprung mass where the damper is either fully stiff or fully soft depending on the velocity of the body and the relative velocity of the damper [3]. Specifically, it is controlled by

$$F_{dd} = \begin{cases} Gv_1 & v_1 v_{12} > 0 \\ 0 & v_1 v_{12} \le 0 \end{cases} \tag{2.3}$$

where,

F_{dd} = desired damping force, N
G = Skyhook Gain, $N/m/s$
v_1 = velocity of the sprung mass, m/s
v_{12} = damper velocity, m/s

Basically, the damper will be at its maximum damping characteristic when the velocity of the sprung mass and the relative velocity of the damper are in the same direction, and at its minimum damping when the velocities are in opposite directions. This method of control is intended to decrease the velocity of the sprung mass [3].

An alternative to Skyhook control, though not often used in automotive applications, is Groundhook control, which works on the same principle but uses the velocity of the unsprung mass instead of the sprung mass. A more recent control method is to use a hybrid of the two. The resulting control algorithm is based on the following relations

$$F_{dd} = G\left(\alpha\sigma_{sky} - (1-\alpha)\sigma_{ground}\right)$$
$$\sigma_{sky} = \begin{cases} v_1 & v_1 v_{12} > 0 \\ 0 & v_1 v_{12} \le 0 \end{cases} \quad \sigma_{ground} = \begin{cases} v_2 & v_2 v_{12} < 0 \\ 0 & v_2 v_{12} \ge 0 \end{cases} \tag{2.4}$$

where,

v_2 = velocity of the unsprung mass, m/s
α = weighing factor
σ_{sky_1} = Skyhook switch variable, m/s
σ_{ground_1} = Groundhook switch variable, m/s

All three major control systems are dependent on current and velocity. As a result, these are the measured variables on an automotive suspension. It is advantageous to have a model for the damper that is dependent on the same variables, in order for a new control system to be implemented with proven equipment. In addition, dynamics of the damper model that depend on variables not found in the control system increase the complexity of evaluating the control system.

2.5 Stochastic Modeling

The probability model is based on a establishing a probability density function (PDF) of the data. A PDF is a function of the input values to the model and parameters

associated with the probability function that is known to describe the data. Any discrete data set is not sufficient for a full error study on the PDF, but a large data set would be appropriate for a probability study. There are two types of PDF fitting. If the type of PDF function is known, (Gaussian, χ-distribution, etc.) then the data can be used to find the parameters for the PDF model, normally mean and variance. This parametric approach to solving the PDF can be performed using traditional error minimization methods. With a priori knowledge of the mechanics that are causing the dynamic effects, or with an expected shape of the distribution of the data, parametric modeling of the data will yield the PDF of the function. Nonparametric models make no such assumptions about how the data is distributed. [12]

Parametric estimation is accomplished through minimizing the error between the PDF and the empirical distribution of the data. This error can be defined as the distance between the two, L,

$$L_p\left(f,\hat{f}\right)=\left(\int\left|\hat{f}-f\right|^p dx\right)^{1/p},\ 0<p<\infty$$

A more popular method is to find the Mean Square Error,

$$MSE\left(f,\hat{f}\right)=E\left[\hat{f}-f\right]^2$$

which for an entire data set can be integrated to find the Mean Integrated Square Error,

$$MISE\left(f,\hat{f}\right)=E\int\left[\hat{f}-f\right]^2 dx$$

For discrete data sets can be written as the Average Square Error [13],

$$ASE\left(f,\hat{f}\right)=\frac{1}{n}\sum_{i=1}^{n}\left(\left[\hat{f}-f\right]^2\right)$$

MISE or ASE method of analyzing the error is useful in PDF estimations because it inherently deemphasizes the tail region of the PDF, focusing more on error in the higher probability region of interest [14].

A histogram estimate can be used to estimate the PDF from the empirical data. A histogram divides the range of data into bins, counting the number of data points that are within the range of each bin. The histogram is scaled [13] such that,

$$\hat{f}_{bin}(x)=\frac{1}{n}\frac{\text{count all } X_i \text{ in bin}}{\text{width of bins}}\forall\text{bins}$$

where n is the number of data points recorded. It is important how the bins are chosen for the data to be accurately represented. The advantage of a histogram is that it is numerically efficient, requiring a fixed number of operations per bin. The disadvantage of histograms is that because the number of bins is fixed there is no information about the slope of the PDF, limiting the types of operations that can be performed.

2.6 Summary

The following sections in this thesis will describe how the data was recorded, and how it was applied to minimize the error of different types of models. The information in this chapter will be used to select the most appropriate type of model. Despite the many nonlinear effects in an MR damper, the key to a useful damper model is simplicity and easy integration into models for control studies. This thesis also aims for consistency between models so that error comparisons are meaningful.

3 Experimental Procedures

To determine an appropriate model for an MR damper, data of the force response of the damper to a velocity and current must be collected. The experiment performed in this study was designed to collect data that would show a force response that contained the same effects as a damper would exhibit in a real world application. It was decided that the best way to accomplish this is to simultaneously apply a random current and velocity excitation to the damper. By making both signals random, there is a much higher likelihood that all the possible dynamics of the damper appear in the data collected.

The following chapter covers the methodology of the data collection experiment and a discussion of how the data collection process was completed. The first sections relate why the experiment was designed, and what considerations affected how the tests were run. The following section discusses the implementation of the experiment, including advantages to the method found and adjustments that needed to be made. Finally, this chapter concludes with a review of the test performed, with an emphasis on repeatability of the procedure described here.

3.1 Background Theory

In designing this experiment, the focus was on ensuring that the range of velocity and current values filled the entire space tested in an appropriate way. The space tested is defined by the rectangle in the velocity-current plot with bounds of maximum and minimum velocity and maximum and minimum current. One consideration in selecting velocity and current inputs for this experiment is that all sections of the rectangle have force measurements taken. Another consideration is that the points on the graph are approached from different directions. Because the purpose of this test is to analyze the variation in the force at each point of velocity and current, input signals must be selected such that they do not limit the effects of any dynamics that would cause a different force response in a real world application. Reproducing realistic dynamic effects and hysteresis is a primary concern in designing this experiment.

The next major concern for this experiment is to eliminate as much noise in the data as possible. After performing the experiment it is not possible to differentiate the noise in the data from variation in the data due to dynamic effects of the damper. Multiple data runs can show trends, but there is no way to analytically reduce low frequency noise. Therefore, it is particularly important that as many sources of noise be reduced as possible during the experiment.

3.2 Designing Appropriate Input Signals

In the previous section the important considerations for designing this experiment were outlined. The first step in the experiment is to create an input signal that fits the criteria as described to provide the best data. Several approaches were considered to select an appropriate set of input signals. The following subsections will deal with each criterion and how it was satisfied for this experiment.

Coupled Velocity-Current Input Considerations

To fill the entire velocity-current space, the function for velocity and current can be either a definite function or a random signal. The definite function has the advantage of a user defined shape. However, due to the nature of the shock dynamometer on which the tests are conducted and the finite length of a real damper, any applied function must be repeated. Also, such a function must be continuous. This produces a plot in the current-velocity space that occupies a circular area. By changing the amplitude and offset in both directions, this area can sequentially occupy a large space in the total area. The downfall of this approach is that points on the graph are approached from a consistent direction. This problem can be avoided by using a random continuous function instead of the definite function.

An important characteristic of a random function is that the derivative of the function is also random. This guarantees that each point in the current-velocity space is approached from a random direction. In Figure 3-1, the random distribution and direction of approach are shown using two randomly distributed functions for velocity and current. The advantage to the signal having a random position and direction in the

current-velocity space is that the dynamic effects including hysteresis are more likely to be present over the entire space. By definition, hysteresis is dependent on the previous condition of the system. If the previous condition is consistent for repeated positions in the current-velocity space, than not all of the hysteretic or dynamic effects can be seen in the response of the damper. Because this experiment intends to provide a more reliable model for real world conditions, it is important that the data contains all potential effects.

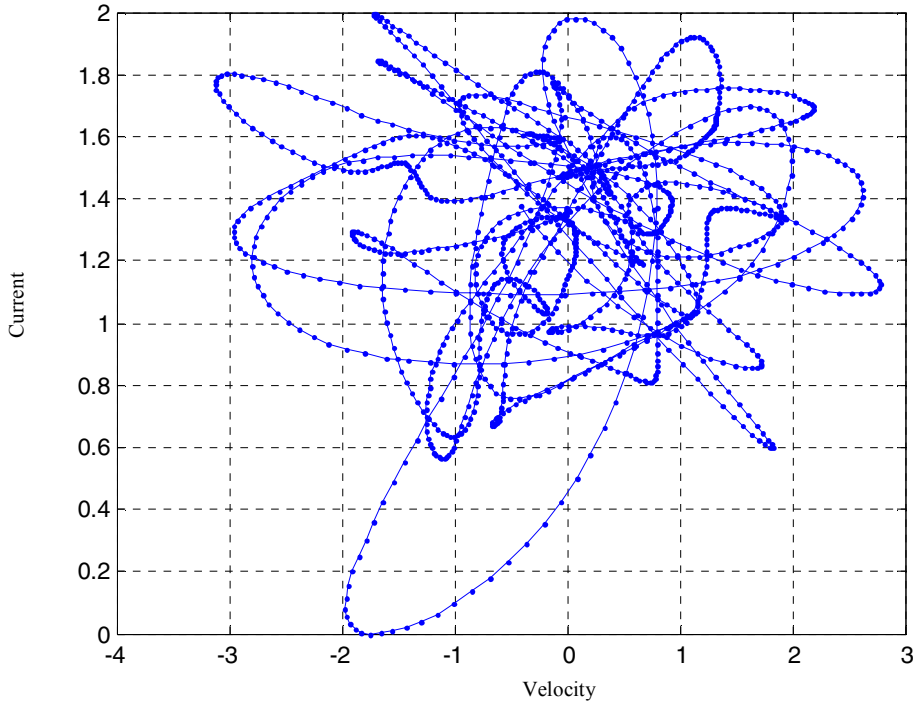

Figure 3-1. Velocity-current space containing a normally distributed random function for current and velocity. The plot has been scaled to the maximum range for each value and offset to fit within the bounds.

In this example, the length of time of the signals is only 10 seconds, and the signal is band limited to 15 Hz. The number of periods of the signal makes the path taken by coupled signals more clear, but also makes the outlying portion of the signal more prominent which in turn affects the location of the mean value of the signal. However, some trends in this short signal show what the strengths and limitations of a normally distributed random function are. As expected of a normal distribution, the majority of the data points are at the center of the plot. This is an advantage because the mean value can be set to a particular area of interest in the velocity-current space, and more data points

can be collected in that area. The disadvantage of using a normally distributed function is that the area it fills is bounded by a circle. Even with a much higher number of data points, the corners are still empty in this graph. Information about the behavior of the damper at the maximum current input and the maximum velocity, as well as information at the minimum current and velocity, cannot be gathered using this signal.

An alternative to using the normally distributed, random velocity-current function is using a uniform distribution. This signal type loses the control over adjusting the focus of the data points, but more closely fills the entire rectangular bounds of the current and velocity inputs. Figure 3-2 provides a direct comparison of the signals. The graph on the left shows the normal distribution, and the graph on the right is a uniform distribution. Both figures are band limited to the same frequency and have the same duration.

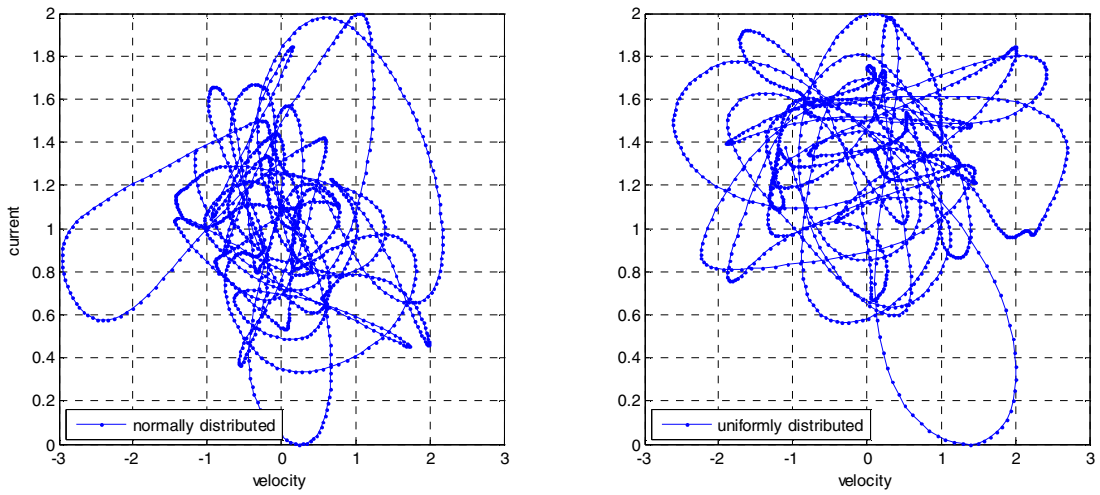

Figure 3-2. Comparison of normally distributed and uniformly distributed random signals for velocity and current. Both sets of signals are band limited to 15 Hz.

Additional Considerations for Velocity and Current

It is important to select the input signals needed for both velocity and current, it is important that the signals will allow the same dynamic effects that could be seen in a real world situation. This is best accomplished by approximating real inputs with the velocity and current signals. Examining measured road inputs, it can be seen that most velocities are close to zero with only a few higher magnitude spikes. The example studied here is from H. Wang's, "Road Profiler Performance Evaluation and Accuracy Criteria Analysis," where a sasmple profile of Virginia Tech's Smart Road clearly shows these

spikes. [15] Therefore, a normally distributed random signal will best serve as the velocity input.

The type of signal used for the current input the damper will not base its shape on what would typically be an input current for an automotive application. Both Skyhook and Groundhook control strategies result in a current that is normally at zero. This is an uninteresting case in this study because the current input may cause some dynamic effects in the force response of the damper. With no current input, the damper behaves like a passive damper. Passive damper characteristics have been studied in depth in previous works and are outside the scope of the research effort here. It is important that the data will show nonlinearities and dynamic effects that may occur regardless of the control algorithm used; the current signal should be spread over the entire range of interest. Therefore, a uniform random distribution was chosen to create the input signal. The absolute value of the generated signal is sent to the damper because the damper can only accept positive values of current.

The final considerations in determining the appropriate input signals to feed the damper are the cutoff frequencies for the filter smoothing the input signals, and the bounds of the current and velocity signal. The cutoff frequencies are based on limiting factors in the damper and the dynamometer used to perform the test. The cutoff frequency for the filter smoothing the velocity signal was set to 60 Hz, the maximum frequency that the dynamometer could replicate. The cutoff frequency for the current filter was based on specifications of the damper provided by Lord. The MR damper has a response time of 10 ms; the filter cutoff frequency was set to 8 Hz, which resulted in a frequency of twice that (16 Hz) near zero due to the absolute value operation. The bounds on the signals were set by limitations from the damper. The bounds for current were simply the minimum and maximum current the damper can accept, 0 and 2 A. The bounds for velocity were set by integrating the velocity signal using a first order filter, which gave the displacement of damper. To keep the displacement from exceeding the maximum safe stroke of the damper, the velocity bounds had to be approximately -6 and 6 in/s. Figure 3-4 shows an example of final input signals for velocity and current.

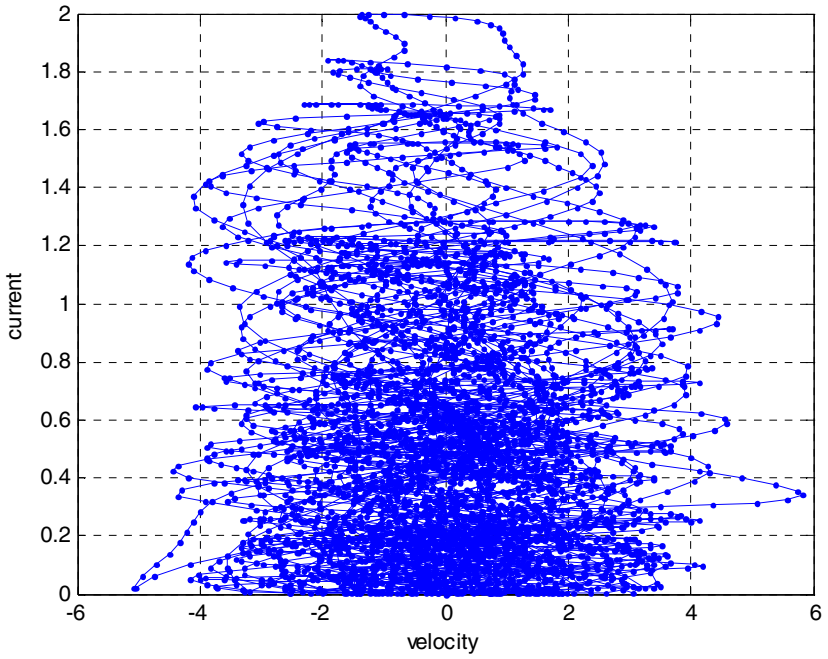

Figure 3-3. Sample input signals of velocity and current, showing the type of distribution used in the experiment. The frequency limitations of each signal account for the more rapid oscillation in velocity than current.

It is important to note from this figure that the actual distribution of the velocity and current signals is not exactly normal or uniform, respectively. By filtering the signals, the distribution is changed. The distribution of the actual signals can be seen in Figure 3-5. The plot on the left shows velocity; notice that the higher velocities have a higher occurrence than would be expected of a normal distribution. Conversely, the plot on the right of current shows a lower occurrence at higher values than a uniform distribution would have.

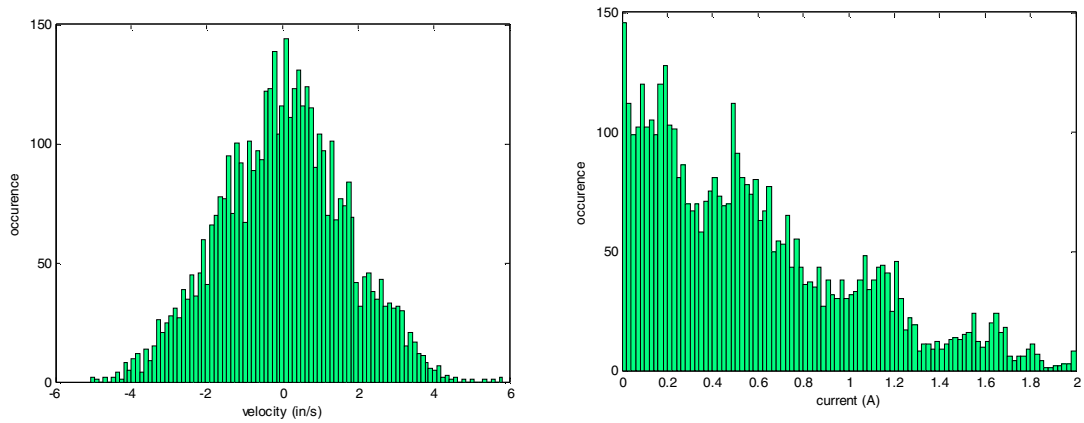

Figure 3-4. Plots showing the distribution of a sample velocity signal (left) and a sample current signal (right). The current signal especially shows the effect of a filter to the original uniform distribution.

3.3 Experimental Setup

The experiment was conducted using a Lord Rheonetic seat damper. A Roehrig Shock Dynamometer provided the driving displacement profile for the damper and was instrumented with outputs for relative velocity, force exerted by the damper, and temperature. The Roehrig 2K Electro-magnetic Actuator Damper Dynamometer was the model used for this test. The outputs from the Roehrig were calibrated; the full calibration results can be seen in Appendix B. For this experiment it was necessary to build a second system to input and record the current signal for the damper. To generate the signal the MatLab current input was entered into the Tektronix AFG 3000 Arbitrary Function Generator. This produced a voltage signal that was transformed into a current signal of the appropriate magnitude using an Advanced Motion Control transconductance amplifier. The amplifier output was connected to the leads of the damper and also recorded using a AAEC current probe.

The Tektronix Arbitrary Function Generator allows any shape signal can be input as an Excel file through a USB interface. The Tektronix has its own control over the scale and period of the signal. For this experiment the random signal generated in MatLab had to be scaled and offset so that the amplifier produced the appropriate output for the damper control signal. This was set using a Tektronix oscilloscope.

The output signals of velocity, force, and temperature from the Roehrig, the control signal from the Tektronix and the current measured at the input to the damper were recorded using the IOTech Wavebook. The full product specifications for the Wavebook can be seen in Appendix B.

3.4 Experimental Procedures

To begin the experiment, the random position file created in MatLab was loaded as the drive file of the Roehrig Damper Dynamometer. Because there was little temperature variation in the shock absorber there was no warm-up cycle used before each test. Since the current input file was not connected to the rest of the system, it could not be started simultaneously; therefore, the function generator was set to continuously loop the current input signal. The period for the signal was thirty seconds. The total time of data collection was also set to thirty seconds. Again, because of the set up, the data collection had to be triggered independently of the Roehrig drive file. The drive file created was the maximum length, or about thirty-two seconds, at 2000 Hz. This allowed the data acquisition to be triggered after the start of the drive file. This way the data would not include the very small velocities when the Roehrig is positioning the damper for the start of the test. Ten test runs for the damper were recorded.

3.5 Discussion of Experiment

The experiment had no obvious errors beyond the zero order error of the instruments used in data collection. The initial plots of force, current, and velocity seemed to show a very high correlation between current and force.

4 Results and Discussion

The results of the experiment showed a strong correlation between force, current, and velocity. Figure 4-1 shows the results of the experiment. The first plot shows the relative position of the damper. The second plot is the force output by the damper. The third and fourth plots are the input velocity and current signals, and the final plot is the temperature of the damper during the test.

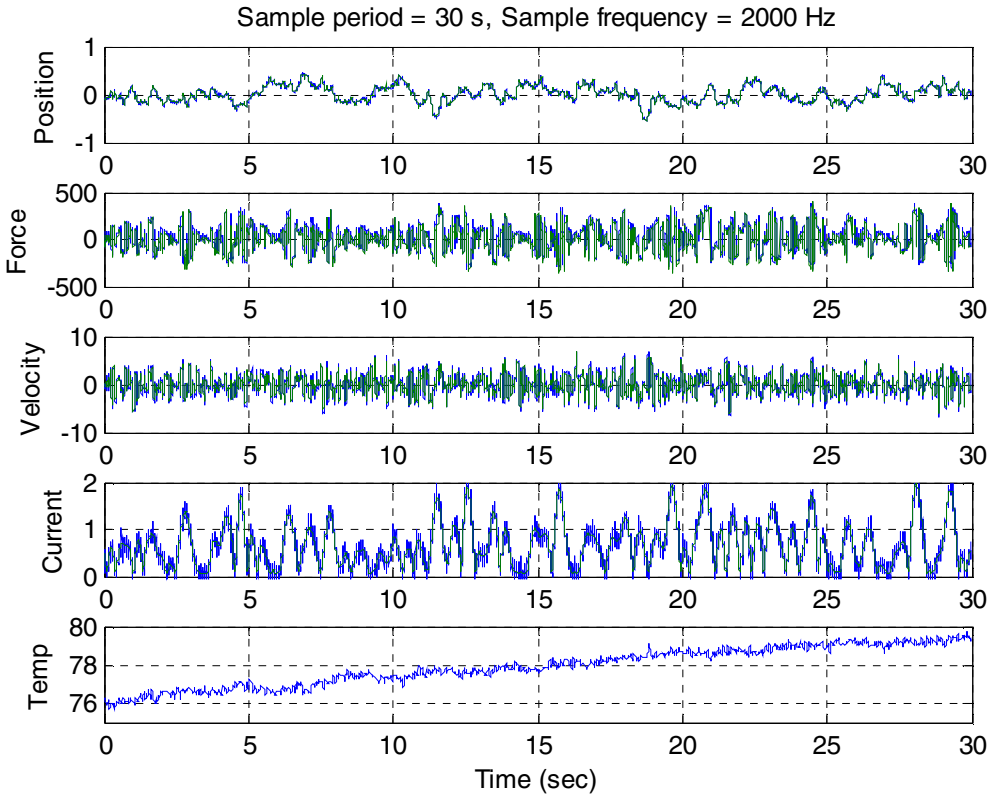

Figure 4-1. Relative position, force, and relative velocity of the damper; current input to the damper, and the original control signal.

Since damper force is dependent on current and velocity, information about the relationship can be more clearly shown in a three dimensional plot. This is shown in Figure 4-2 below. A clear increase in force can be seen as the current rises, and the data seems to show force dependence on velocity that is similar to a passive damper.

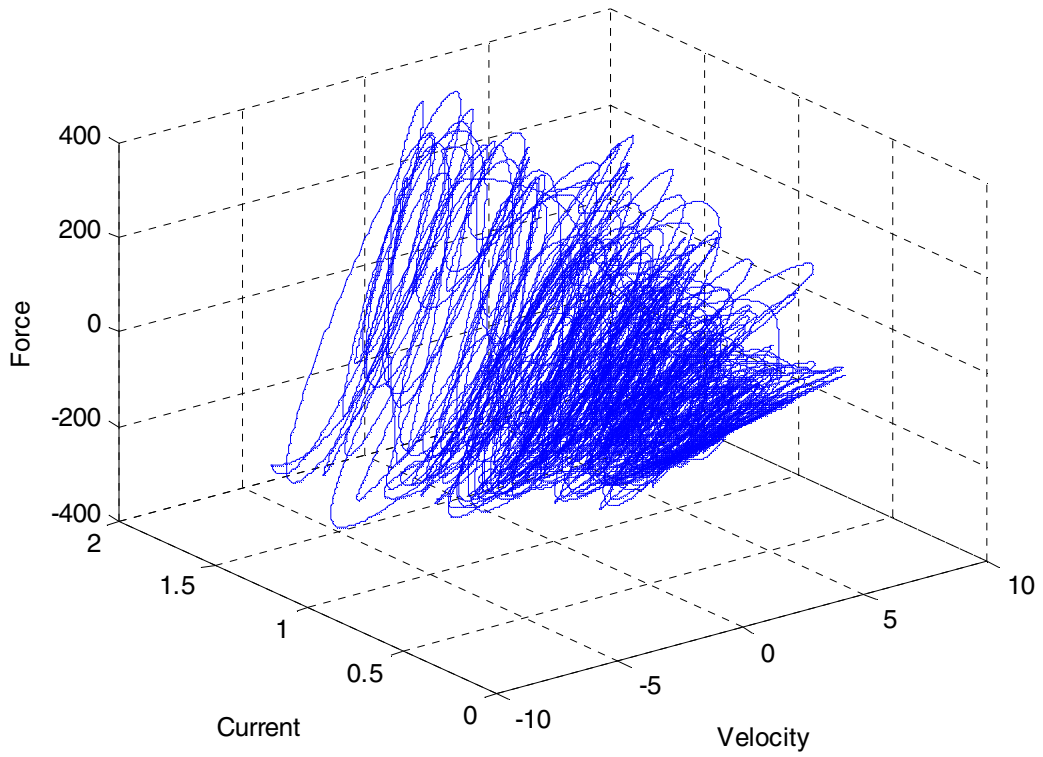

Figure 4-2. Relationship of force to current and velocity

Plotting the results of this experiment in 3D provides more information about how force relates to velocity and current. It is apparent that the surface has some thickness to it. There are dynamic effects that were described earlier which in this case cause a different shape for traces of the signal in an area of the graph. It is hard to determine the overall effect of the dynamic effects from this plot, however. An alternative to the three dimensional plot is a two dimensional projection showing the areas where most of the points lie.

This is best accomplished using a probability density function, or PDF. Because there is no indication of the type of function the PDF should be, it will be empirically estimated here by a histogram function. To create the histogram function for the experiment, the data was broken into 10 bins for current with a 0.2 amp range. All the data that falls into a bin can then be further broken down into velocity and force bins, and displayed as a PDF in two dimensions. The density is denoted by a color scale, with light green showing lower densities and dark blue showing the highest densities. The scale of

the PDFs is in percent of the total number of data points. This scale is based on the total number of data points taken in the experiment compared to haw many are at a certain location. Two PDFs are shown in Figures 4-3 and 4-4. It shows the densities for two areas of interest; currents near the maximum current of 2A, and at a lower current near 1A, respectively. At two amps, there is a very clear envelope that the possible force values fall within. The aspect of the plot that is most clear is the hysteresis that is seen in this plot in particular. There are two visible traces created by the highest density area. The values at high velocities are similar, but as the traces are followed towards zero velocity there are two distinct paths.

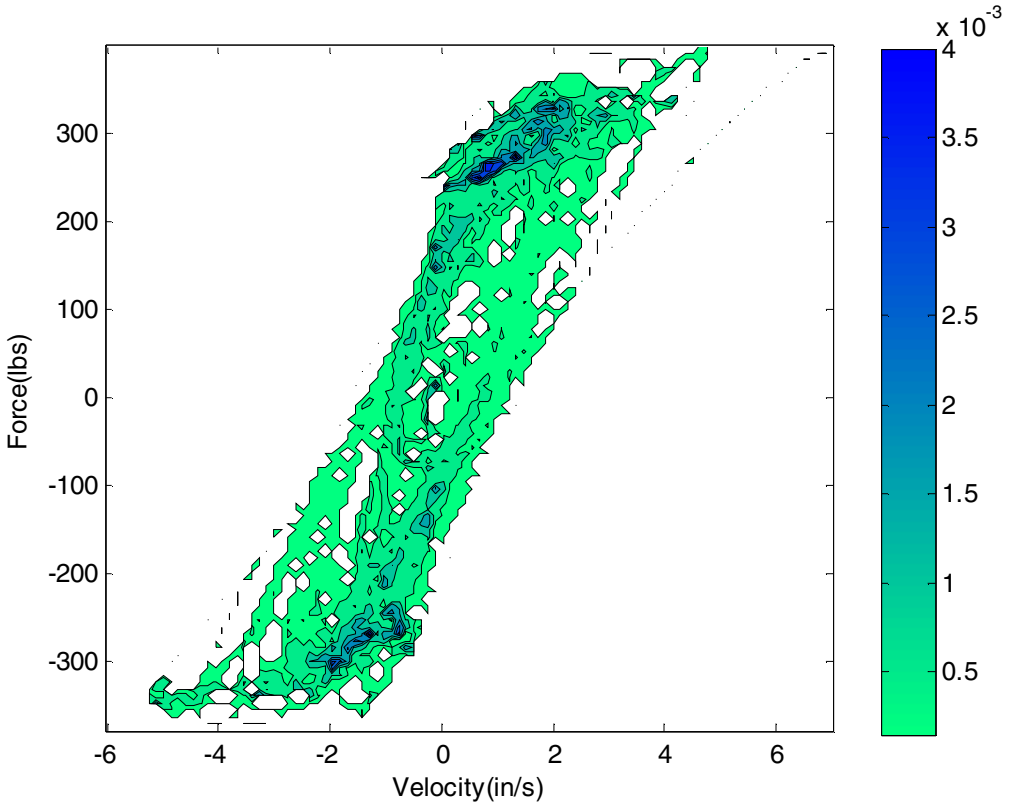

Figure 4-3. Plot of the PDF at a current range of 1.8 to 2.0 amps. The colors vary based on the percent of the total data points that fall in a certain point in the velocity-current-force space. Hysteresis is clearly visible for high current values.

Looking at a plot of a lower current in Figure 4-4 shows less obvious hysteresis. Rather than a void in between two higher areas of probability, the highest area of probability is in the center of the plot. The shape of the velocity-force plot at this current

has a similar shape to the plots sat higher currents. Also, as expected, the maximum force at this current is approximately proportionally lower at this current.

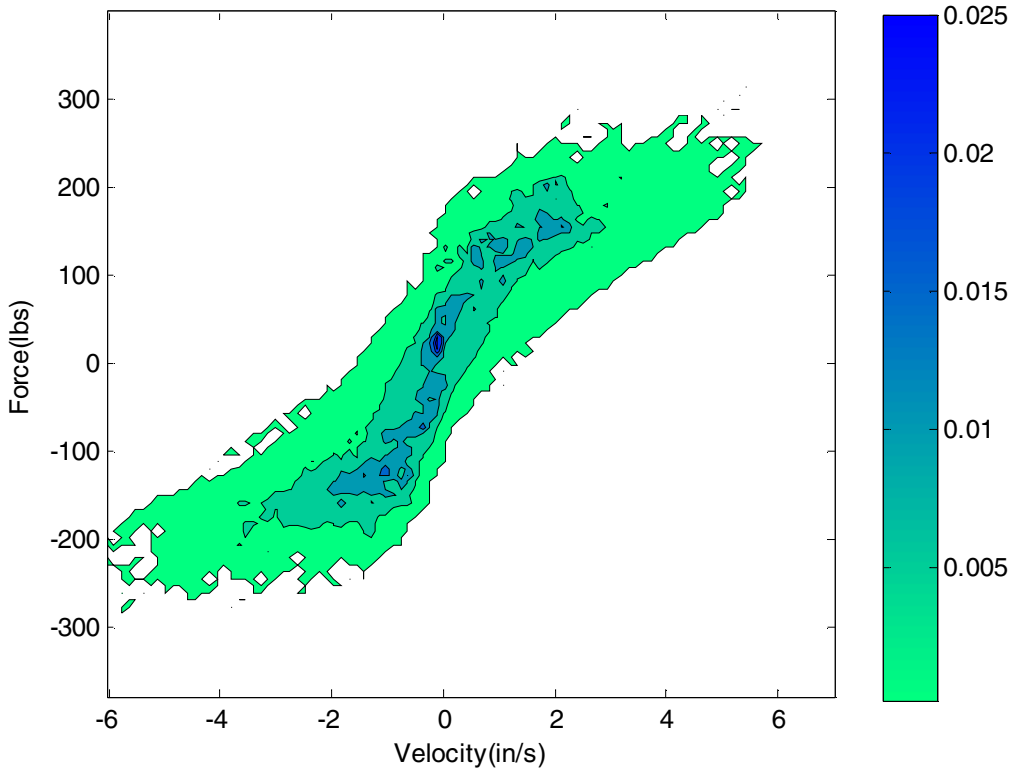

Figure 4-4. Plot of the PDF at a current range of 0.9 to 1.0 amps. The colors vary on a logarithmic scale to the number of points per 100th of each scale. The higher probability lines form a similar shape as the higher current plot without the same level of obvious hysteresis.

5 Comparison of Damper Models

The first step in examining the data is to find a deterministic model that will directly relate force to current and velocity. This will provide the basis for understanding the damper behavior and provide a comparison for the probability function of the force data. The function commonly used to model the force-velocity–current relationship is the inverse exponent. In addition to this function, the error was examined using a hyperbolic tangent [12]. Also, it is important to model current in the appropriate way. Magnets have saturation of field strength, so the relationship between current and force may not be linear.

The general model for current must be determined before the overall model can be created. The dependence of the force on current is not separable from the dependence on velocity in the data gathered in this experiment. So, to develop the general model for current dependence, previous data taken by Poyner [1] where the current and velocity were held constant was used. Because the data does not contain any dynamic effects, the velocity and current dependence are separable by simply recording the values of force along a line of constant current. For the purposes here it is sufficient to just look at a single current. Figure 5-1 shows the current dependence at 1 A from Poyner's data. This data was curve fit to polynomials of 2, 3, 4 and 5 terms. It was discovered that a four term (3^{rd} order) polynomial sufficiently describes the data. More than this is unnecessary because the total error does not decrease by a significant amount beyond this. However, the 3^{rd} order polynomial has much smaller error than the 1^{st} or 2^{nd} order equations.

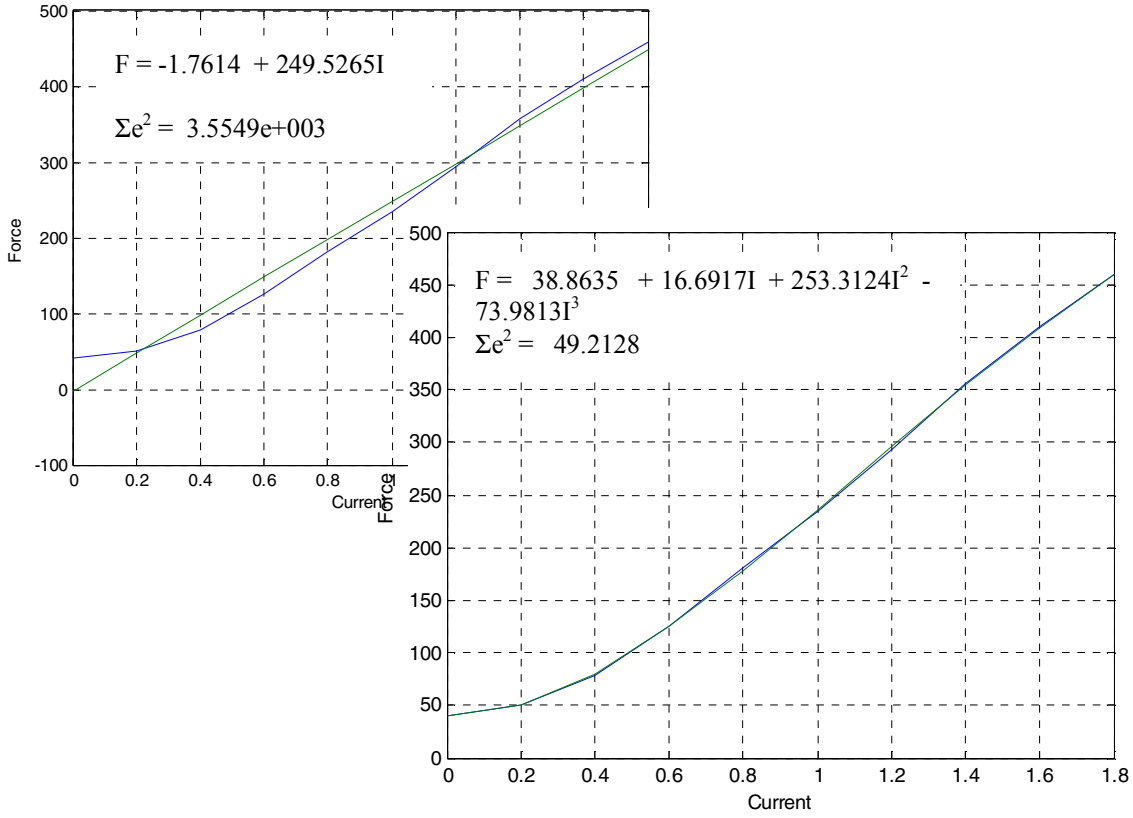

Figure 5-1. Force dependence on current. The data is from Poyner [1]. A linear model for current proved to have a much higher error than a third order polynomial.

For the final model of the damper a four term 3rd order polynomial will be used. To fit the data , the Matlab function *fmincon* was used. *Fmincon* finds the minimum value of a function of any number of variables. To find the parameters of the best-fit model for force, the variables passed into the function will be the parameters for the model, and the function that *fmincon* will optimize will be the sum of the error squared. Specifically, the *fmincon* solver will be sent the cost function,

$$\sum e^2 = \sum \left(F_i - \hat{F}(x, v_{rel\,i}, I_i) \right)^2 \tag{5.1}$$

where,

e = the error between calculated force and actual force

F = the experimental values of force recorded

$\hat{F}$ = the calculated value of force using the equation

x = the vector of parameters used in the equation

v_{rel} = the relative velocity of the damper

I = the current

i = the index of the data point from the experiment

The advantage of using *fmincon* is that it is a bounded search. This improves the accuracy and allows the user to check the results. The general algorithm for implementing this solver is shown in Figure 4-2. The solver is run using a very broad range of values that make physical sense. The results of the solver for parameter values are input as the "guess" of the actual values and the bounds for each parameter are set to ± 5% of the value. The solver is run again; if the values stay within the bounds this process is repeated, shrinking the boundaries further. If not, the previous solution is set as one bound and the opposite bound is set to expand the area searched. This is repeated until all parameter values are within a relatively small bounded area

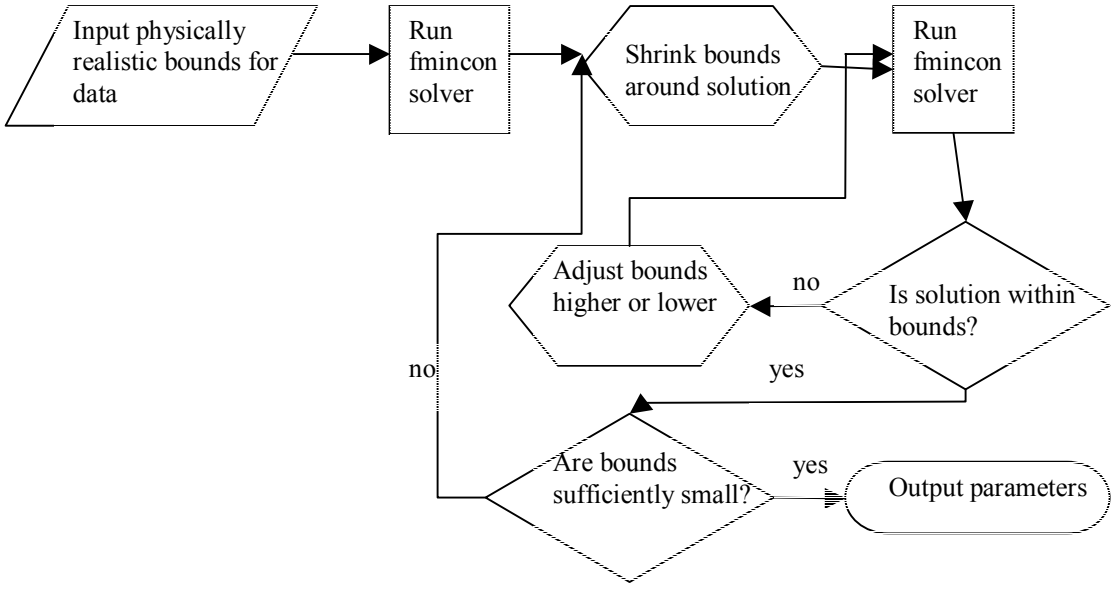

Figure 5-2. Flowchart for the Matlab optimization code using *fmincon*.

5.1 Linear Damper Model

The first model that will be optimized is a linear, current dependant model. This model is based on an "ideal" damper response. For MR dampers, the relationship between force and velocity will change when a current is applied. As a result, the envelope of force output is defined by an area rather than a line in the force velocity plane[4]. Expanding on Goncalves, [2] the ideal case of damper response would cover an area of all positive forces and positive velocities, and all negative forces at all negative velocities. That is, the damper force is independent of relative velocity. Therefore, the damper can be controlled to have any force-velocity characteristic, or any combination thereof. The reason for the restriction that the force must be of the same sign as the relative velocity (remembering the convention that this is a force that resists the direction of motion) is that a damper cannot store energy but only dissipate it.

The model that Goncalves uses to describe this behavior is an output force directly proportional to the input current. This general form is necessary to satisfy the condition that the damper is controllable over all real current inputs. The general form of the deterministic equation used is

$$F_d = \alpha I \qquad (5\text{-}2)$$

where,

F_d = the damper force
I = the current supplied to the damper
α = the constant linear coefficient for the model

by inputting the values found in Matlab, the final equation becomes

$$F_d = 127.4125I \qquad (5\text{-}3)$$

for the ideal linear model. The root mean square error for this model is 99.49 lbs. The equation was solved by minimizing this error. It is useful in directly comparing two different models, but has little obvious physical meaning and is not useful for anything beyond a direct comparison. By looking at the error in the same scale as the data, it is

more apparent how close each model is. The data for damper force ranges from 0 lbs to almost 400 lbs. The error for a linear model is an average of 70 lbs.

It is difficult to determine how well a model approximates a physical system numerically; valuable information about how the model performs can be found graphically. The first comparison is the output signal of the shock dynamometer with the model predicting the force output. This is shown in Figure 5-3. The blue line is the measured force and the green line is the predicted force. The plot shows ten seconds of the data collected, a short enough time interval to see detail in the signal but long enough that the force varies though a large percentage of its full range. It is clear that in the model the value of predicted force increases and decreases in the same pattern as the actual force output by the damper. However, the predicted force of the model does not have as high a maximum value, and overall the actual force seems to have a higher amplitude for any given period of time. This is consistent with what is expected. The model does not account for variations in force due to velocity. It is known that a real MR damper is dependent on velocity, which will cause the force to be either higher or lower than the model can predict depending on the velocity at that particular time. The model was solved by trying to minimize the error; as a consequence the output force is the average force at a given current. The real force has higher peaks at times when the velocity is higher than average.

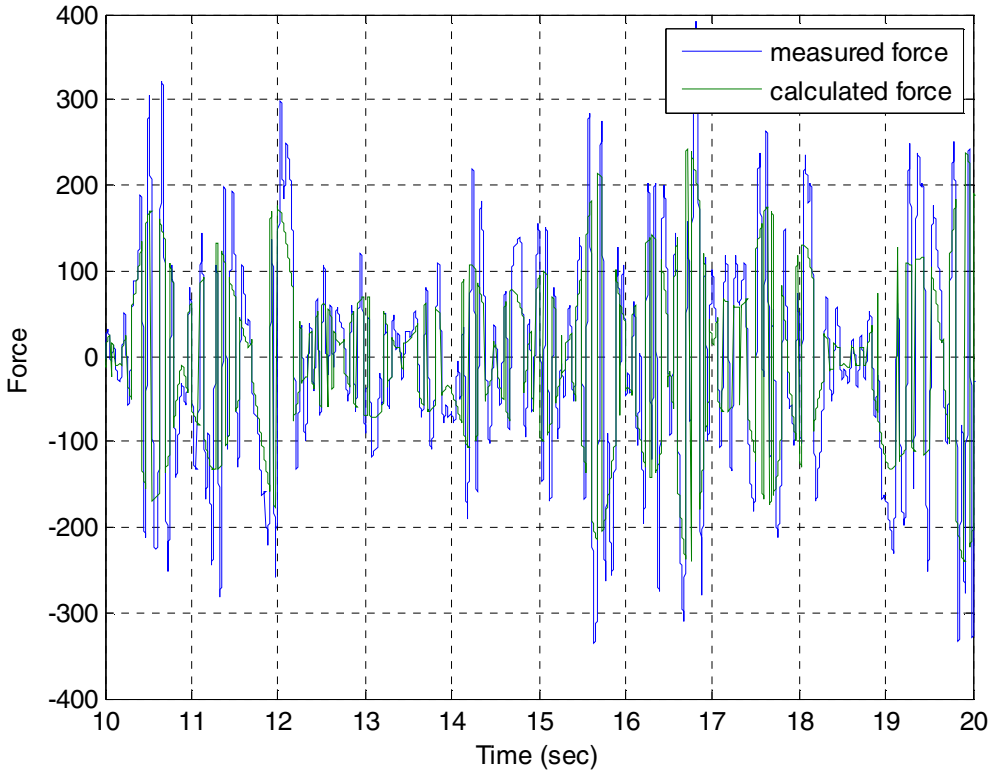

Figure 5-3. Plot of the actual measured force and the predicted force based on the ideal linear model of an MR damper. Notice the model cannot reproduce the peaks of the actual force.

Additional information about at what velocities are currents the force is modeled well can be determined using a 3 dimensional plot of the model. The model is depicted by a green surface in Figure 5-4, with the actual data plotted over in blue. The model is simply two planes, one being the negative of the other, and running purely vertical at a velocity of zero. It is easier to see that the force value is an average of the velocities at that particular current.

The next approach to modeling the force will be to include a velocity term. This model will not be an ideal representation and will therefore no longer have the limitation of applying over all possible values, just within the values measured. Consequently, the current will no longer have a linear relationship to force, but will adopt the polynomial model discussed in this section's introduction.

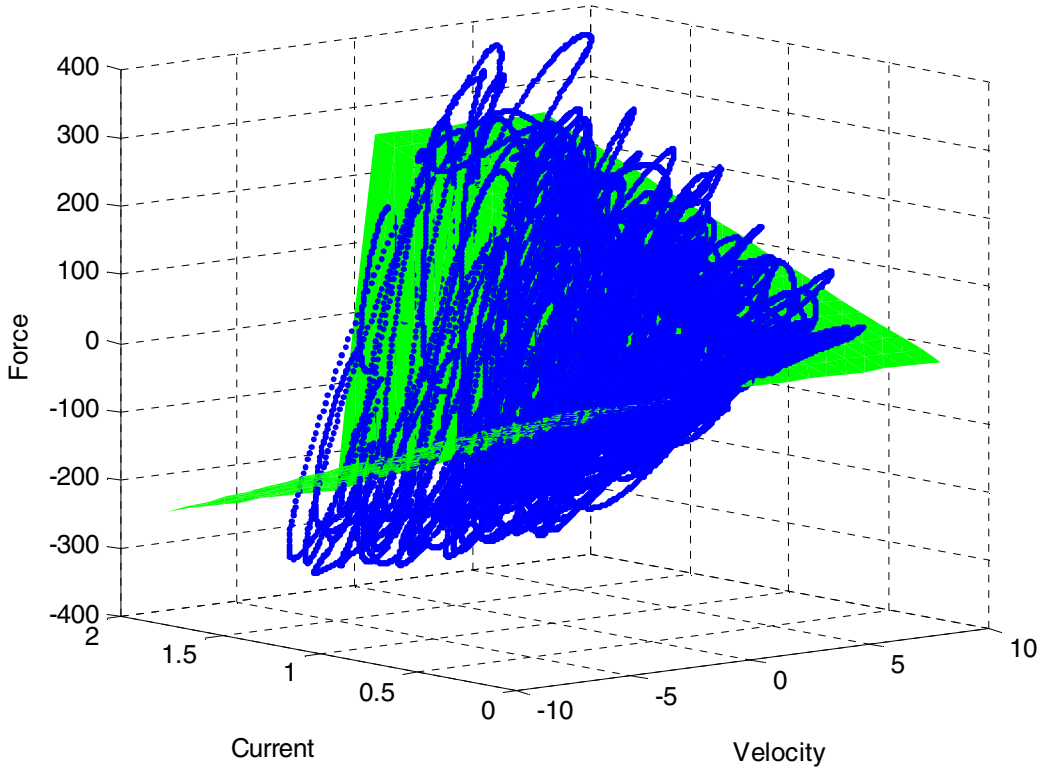

Figure 5-4. Plot of the linear model of the force, dependant only on current, shown as the green surface, with the force data plotted in blue.

5.2 Non-linear Damper Model

The cost function for *fmincon,* which is the total error, was evaluated once the parameters had been set for both the hyperbolic tangent and the exponential model of the damper. The differences were negligible, and because the exponential model is more computationally efficient for numerical models, the inverse exponent was used as the model to describe the current-velocity force dependency for further analysis.

The final equation that relates force to current and velocity uses the polynomial equation described previously to find the contribution of current to force, and the inverse exponent to find the contribution of velocity to force. The general form of the deterministic equation used is

$$F_d = \left(A_1 I^3 + A_2 I^2 + A_3 I + A_4\right)\left(\operatorname{sgn}\left(v_{rel}\right)\left(1 - e^{-\left|v_{rel}\right|/v_0}\right)\right) + c v_{rel} \qquad (5\text{-}2)$$

where,

F_d = the damper force

v_{rel} = the relative velocity of the damper

I = the current

A_n, v_0, c = the parameters for the equation

by inputting the values found in Matlab, the final equation becomes

$$F_d = \left(-22.96I^3 + 21.42I^2 + 194.3I + 7.462\right)\left(\operatorname{sgn}\left(v_{rel}\right)\left(1 - e^{-\left|v_{rel}\right|/1.173}\right)\right) + 7.53v_{rel} \qquad (5\text{-}3)$$

which has a total RMS error of 66.65 lbs, or an average of 45 lbs difference between the expected force and the actual force.

Examining the comparison of the real force output signal with what the model produces, Figure 5-5, reveals what looks to be a very close match. The two signals have the same shape, appear to have the same amplitude and frequency content, and do not seem to exhibit any difference in behavior. The actual force seems to have a few places where it exceeds the predicted force, but it generally looks like a strong model from this point.

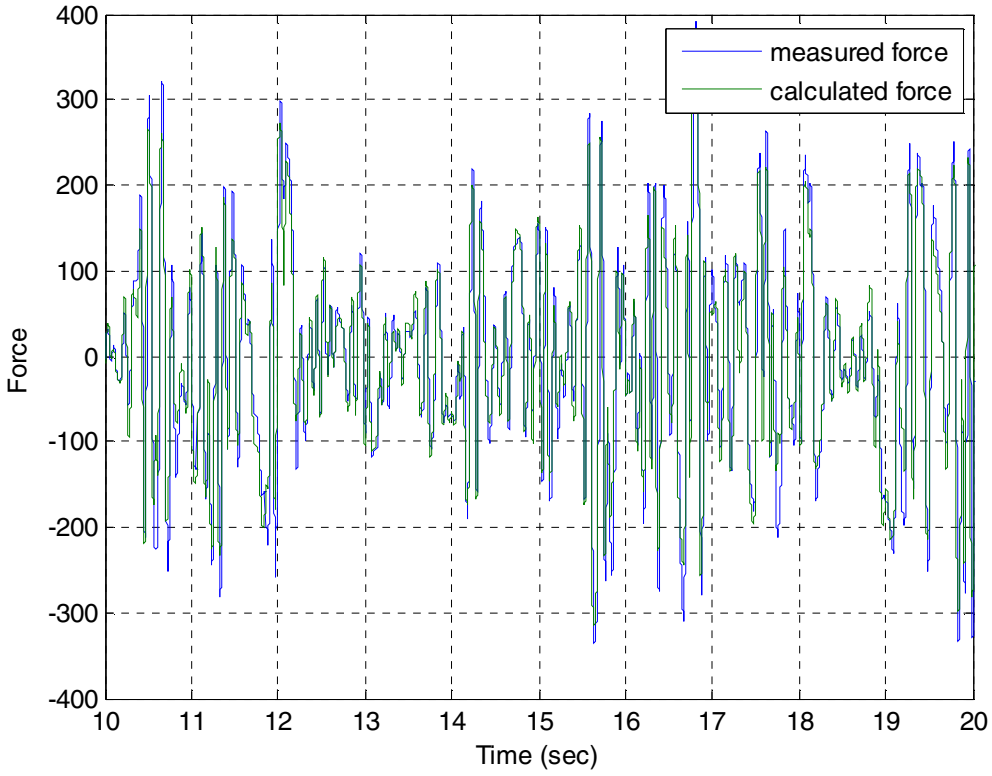

Figure 5-5. Plot of the actual force output and the predicted force output using a nonlinear model dependant on current and velocity.

When plotting the deterministic model for force along with the force data collected, it is easily apparent that a deterministic model is not going to describe all the data because the surface of the actual force has some thickness to it. The plot of this can be seen in Figure 4-4. There appears to be a very large effect of hysteresis, especially at high values of current, which can be easily seen by tracing the path of the signal. It is clear that the force response to velocity and current took a much different path going one way than the other. In addition, it seems that there are more data points lying above the deterministic surface at negative velocities than at positive velocities. Upon further examination, though, this is not a problem with the model, but a characteristic of possible hysteresis or dynamic effects that are not always prevalent. This will be discussed in further detail in the following section.

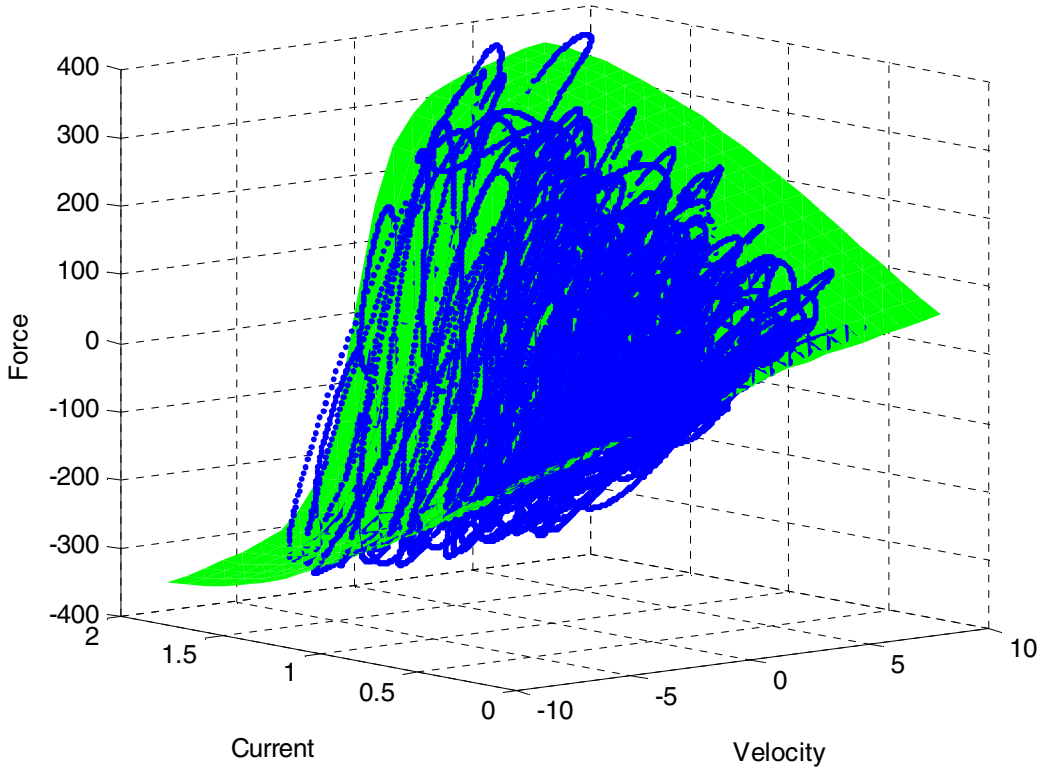

Figure 5-6. Plot of the deterministic model of the force, shown as the green surface, with the force data plotted in blue.

The thickness of this plot is visible from this three dimensional plot, but it is difficult to quantify. The difficulty arises from the fact that we cannot determine the factors that are causing it, so the force response of the damper is different in every test. It is possible to define an envelope of possible forces by lumping the data into discrete sections. In this case, a grid is created with each square encompassing one hundredth of the total range of force, one hundredth of the total range of velocity, and one tenth of the total range of current. By finding the number of points in all the data values that are inside each cube of the grid, we can create a probability density function (PDF) of the data. While not a true PDF in that the range the densities are calculated in is fixed, It provides a representation of the data that is easily compared to different types of models. The trace of the deterministic model force versus velocity relationship at a current of 1.5 A is shown on the graph. You can see that the PDF has a higher density for force values

greater than the deterministic model predicts; however, the area that the PDF covers appears to be evenly distributed above and below the values predicted by the model.

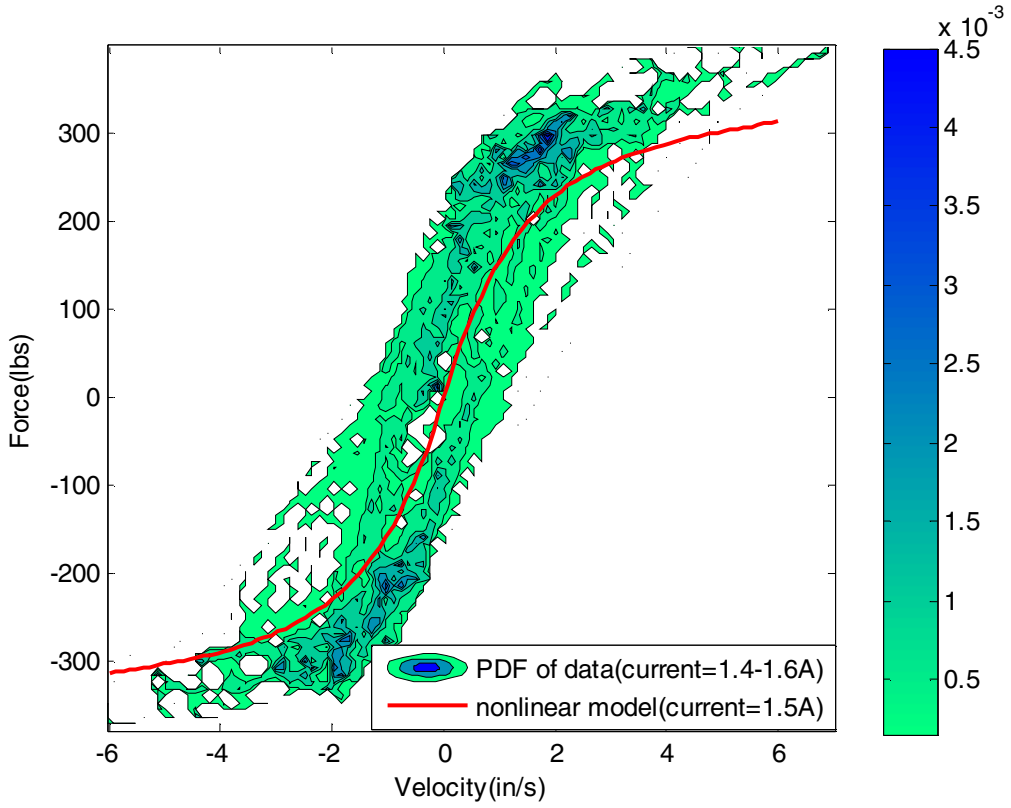

Figure 5-7. Non-linear damper model solved for a current of 1.5 A overlaid on the empirical PDF data at a current of 1.4 to 1.6 A.

5.3 Hysteretic Function

Using a Nonlinear function provided a much closer approximation of the actual behavior of the damper than a linear current dependent model. The error was significantly less in the nonlinear model, and the shape of the exponential model seemed to approximate the average of the data when viewed from the cross section, as seen in Figure 5-7. You can see from this graph that at higher currents, there is noticeable void in the center of the graph, at a velocity and force value of zero. This is a very noticeable hysteresis effect. Possible causes of this behavior are mentioned in the introduction and background sections of this paper, however, it is beyond the scope of this thesis to isolate the actual cause.

It is possible to model hysteresis with a spring in series with a damper. The proof for this will be carried out using a linear viscous damper for easier notation and calculation, but the result can be extended to the nonlinear case as well. A model of the system is shown in Figure 5-8. The system is assumed to have negligible mass.

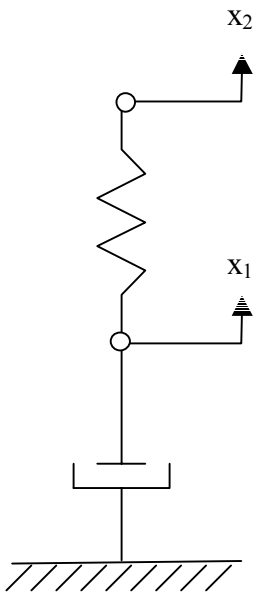

Figure 5-8. Model of damper with hysteresis included by placing a spring in series with the damper. The spring acts as a compliance in the system; all hysteresis can be modeled this way regardless of the physical cause.

Because the system is free on both ends, a reference frame was arbitrarily assigned to one end of the damper. This was chosen because the positions we are interested in are the length of just the damper and the length of the overall system. Choosing this reference frame will decrease the number of variables in the equations of motion.

Because there is negligible mass, the equations of motion will be first order differential equations. It also is apparent that there is no term for inertial force in the equations. This gives us

$$F_{x_1} = 0 = -c\dot{x}_1 - k(x_1 - x_2)$$
$$F_{x_2} = k(x_1 - x_2)$$

In this case we are interested in velocity, so we can combine these equations and rewrite in terms of velocity, v

$$\frac{F_{total}}{F_{damping}} = \frac{k\int v_1 - v_2}{cv_1 + k\int v_1 - v_2}$$

This is the same form as the differential equation describing a low pass filter. Therefore, we can make the same transformation into current domain [14]. This gives us the frequency response transfer function

$$\frac{F_{total}}{F_{damping}} = \frac{a}{s+a}$$

Where *a* is a lumped parameter to be determined.

Using the same algorithm as the previous model, but using the transfer function to add hysteresis to the model, we get the following equation.

$$F_d = \left[\left(A_1 I^3 + A_2 I^2 + A_3 I + A_4\right)\left(\operatorname{sgn}(v_{rel})\left(1 - e^{-|v_{rel}|/v_0}\right)\right) + cv_{rel}\right]\left[\frac{a}{s+a}\right]$$

With the variables optimized to minimize the square of the error with the test data, the result is,

$$F_d = \left[\left(-32.23I^3 + 53.72I^2 + 167.5I + 1.54\right)\left(\operatorname{sgn}(v_{rel})\left(1 - e^{-|v_{rel}|/0.741}\right)\right) + 9.413v_{rel}\right]\left[\frac{147.5}{s+147.5}\right]$$

The total RMS error was 45.67 lbs. This is half the error of a deterministic model based on current and velocity. This result confirms that hysteresis is a contributor to the damper's force response.

As in the previous section, it is important to interpret the model graphically as well as numerically. Figure 5-9 shows the predicted signal overlaid on the actual signal. It appears very similar to the deterministic nonlinear model, matching the actual signal at all peaks, exhibiting the same frequency, and showing little difference between the values of force.

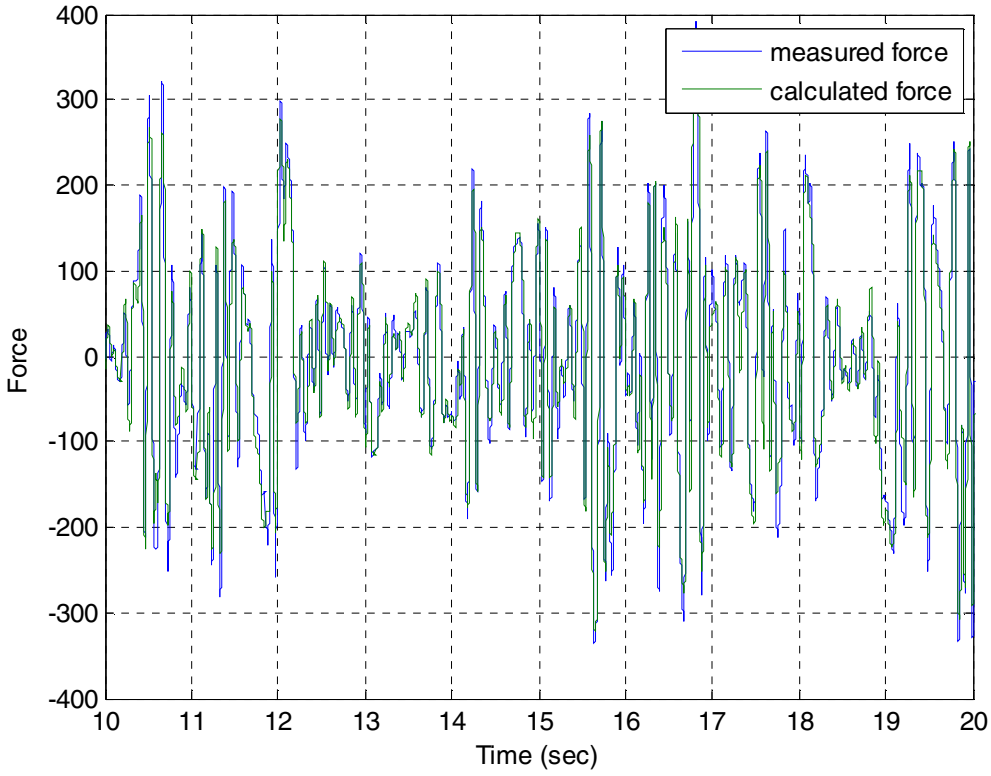

Figure 5-9. Force response of the actual MR damper and the hysteretic model of the damper.

Additional information about how the model is approximating the actual signal can be seen when the model is shown in a two dimensional plot. Because including hysteresis in the model causes some thickness to the surface, it is not possible to plot it as a surface like the deterministic model. However, the 2-D plot of the hysteresis model, shown in Figure 5-10, has the plot of the original data to the side for comparison. Following the signal through its velocity-current sweep you can see that the trace of the force data has a very similar shape, and the model exhibits a thickness that appears very similar to the thickness of the surface created by the observed data. There are noticeable differences between the two plots. The model with hysteresis has a consistent shape, differing only because the point at which the velocity or current changes direction has an effect on how much the hysteresis changes the amplitude of the force. In the actual data, shown in the subset of Figure 5-10, the shape of the surface is not consistent. Sometimes

it appears more linear, other times it more closely follows the shape of the nonlinear model. This is not captured with the hysteresis model.

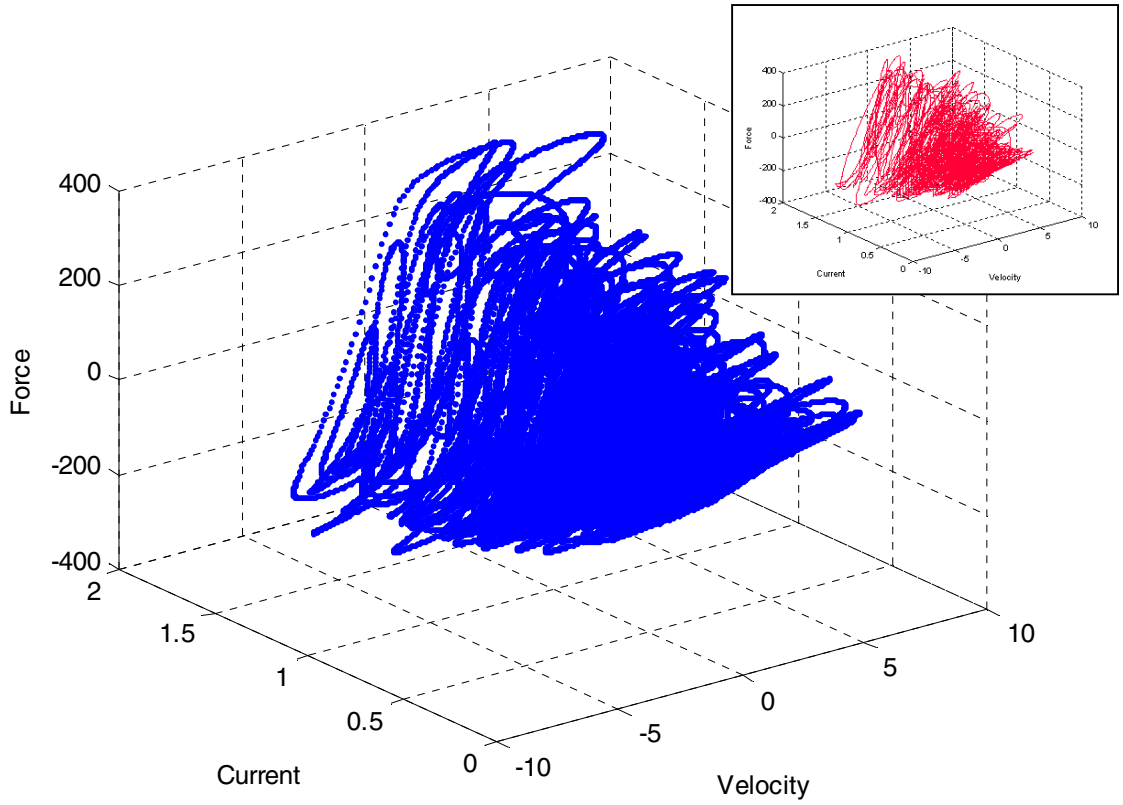

Figure 5-10. Plot of the force response of a nonlinear MR damper model with a first order filter used to simulate hysteresis. In the subset image is the response of the actual MR damper, shown in red.

The final way of evaluating the model is by comparing the PDF of the model to the PDF of the data. The comparison can be seen in Figure 5-11. The PDFs in this figure are shown for a current range of 1.6 A to 1.8 A. In this plot the inaccuracies of a hysteresis model are more apparent. The figure on the left is the probability density function of the data; the one at the right is the model. The PDF for the data clearly shows that more data points fall at higher magnitudes with the range of data. Conversely, the PDF for the model with hysteresis is evenly distributed above and below the centerline. Another difference in the plots is there is more data at the centerline of the area of possible force output in the data than the model predicts.

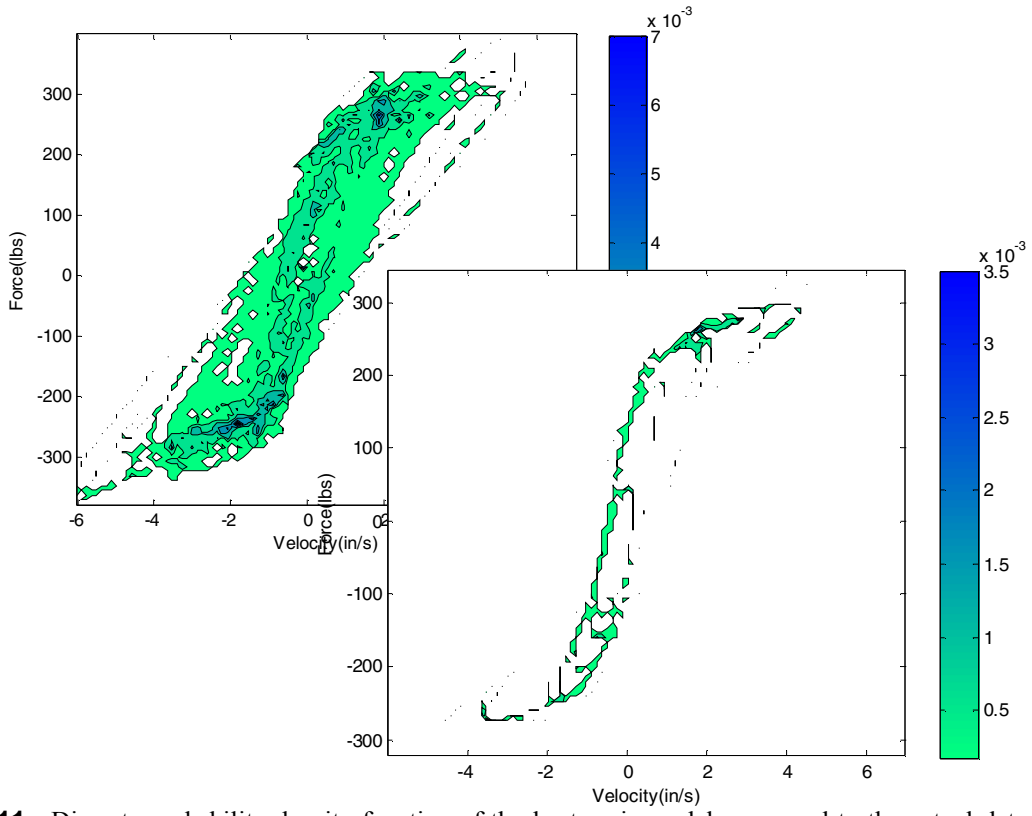

Figure 5-11. Discrete probability density function of the hysteresis model compared to the actual data. The foreground picture shows the PDF for the model, and the background picture shows the distribution of the recorded data. The scale for the number of points at a location that each color corresponds to is shown in the bar on the right of each plot.

Figure 5-12 shows the same comparison between the PDF of the data and the PDF of the model with hysteresis. This plot has more points in the area, which shows a current of 0.4 A to 0.6 A, and some effects are more apparent. In particular, there is a noticeable difference in the number of points that occur at the origin.

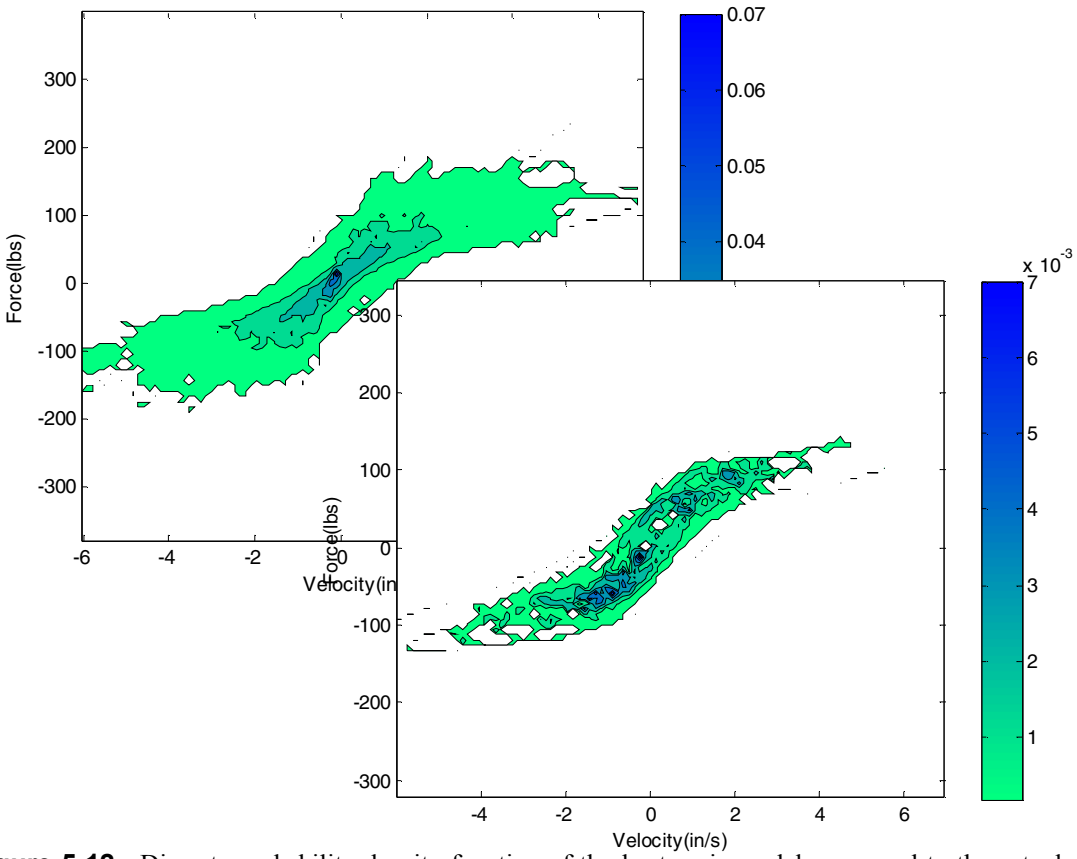

Figure 5-12. Discrete probability density function of the hysteresis model compared to the actual data. The foreground picture shows the PDF for the model, and the background picture shows the distribution of the recorded data. The scale for the number of points at a location that each color corresponds to is shown in the bar on the right of each plot.

5.4 Probability Function

In the previous section a model was developed to describe the data using a continuous function dependant on time and velocity. This model closely resembles existing models and while it has the potential to be a better approximation of MR dampers during normal modes of operation than existing models, all of the dynamic effects of the damper's dependence on velocity and current are lost. That is to say, a continuous first order function cannot account for hysteresis or any other inconsistencies in the damper. However, the dynamometer test results contain all of this information. In the continuous model, the velocity and current components of the equation are separable which would allow for a sensitivity analysis of each variable. For the data set, the random input signals limit the number of data points that occur all at the same velocity

and current. Consequently, it is not possible to attribute the dynamic effects to velocity or current. The solution presented in this research effort is to treat the damper model as stochastic, and develop a probability model of the damper across the range of current and velocity tested.

The methodology used in the previous sections to find appropriate models is not valid to find the probabilistic model. A probability model cannot be compared to a recorded force signal because the random variation in a probability model will not necessarily match random variations in the real signal. The comparison of significance is the frequency that the data hits a particular point in the current-velocity-force space.

The focus of model fitting previously used in this study is to minimize the total error between the actual data and the force output of the model. This approach results in a model that is robust; the magnitude of the error at any point in the model is minimized as much as possible for that type of model. However, actually using a model to simulate the behavior of an MR damper may require a different approach than minimizing the error over the entire range of values.

The question in analyzing the error from a probability perspective instead of a force error perspective is what type of behavior is the damper most likely to exhibit. The relevance of this question to creating an appropriate model is beyond the scope of this thesis. However, this section will quantify the accuracy of the deterministic model from a probability standpoint.

The first step to creating the probability model is selecting a parameter to track the probability. This part of the study will start with the deterministic model described previously. Recall equation for the deterministic model is

$$F_d = \left(-22.96I^3 + 21.42I^2 + 194.3I + 7.462\right)\left(\operatorname{sgn}\left(v_{rel}\right)\left(1 - e^{-|v_{rel}|/1.173}\right)\right) + 7.53v_{rel}$$

Since there are multiple parameters that are dependent on each other for the current part of the equation, individual probabilities cannot be determined for this term. This leaves the velocity terms. Choosing one is based on which parameter has a greater influence on the shape of the model. A simple sensitivity analysis can be done to find which parameter to vary. The change in the sum of the force will be found when each parameter is varied. The result is

$$\Delta F_1 = \sum_{i=1}^{n} \left| \left(-22.96 I_i^{\,3} + 21.42 I_i^{\,2} + 194.3 I_i + 7.462\right) \left(\operatorname{sgn}\left(v_{rel\,i}\right) \left(1 - e^{-|v_{rel\ i}| / 1.173 + \Delta v0}\right)\right) + 7.53 v_{rel\,i} - F_i \right|$$

$$\Delta F_2 = \sum_{i=1}^{n} \left| \left(-22.96 I_i^{\,3} + 21.42 I_i^{\,2} + 194.3 I_i + 7.462\right) \left(\operatorname{sgn}\left(v_{rel\,i}\right) \left(1 - e^{-|v_{rel\ i}| / 1.173}\right)\right) + 7.53 v_{rel\,i} \Delta k - F_i \right|$$

$$\Delta F_1 = 1.7327 \times 10^5$$

$$\Delta F_2 = 9054$$

Clearly, the deterministic model has a much higher sensitivity to the v0 parameter. Therefore, this parameter will be the focus of this probability study.

A model with a v0 that varies cannot be directly compared to the data taken. Here the model creation will be a different approach from previous models. Models with different *v0* values will be compared to the PDF of the actual data. The first step in this comparison is to select the values of *v0* to compare to the PDF. The PDF, as described earlier, is a count of the number of data points that fall into a predefined "bin," or range of velocity, current, and force. For the appropriate number of samples where the parameter is compared to the data, a difference of one half of the size of each bin in the force dimension will be between each *v0* curve at its maximum value. In addition, this will be measured at the maximum current value; in order to compare it to the PDF, this value is set at the average current value for the highest value bin, e.g. 1.9 A. Expecting a linear change in force when varying the value of the parameter *v0* requires a nonlinear change between each *v0* value. A Matlab script was written to check for v0 values that result in the desired change in the force output. A plot of these v0 values versus the number of total points is shown in Figure 5-13. Taking into consideration repeatability and programming simplicity, the curve can be approximated by spacing the *v0* values evenly in the logarithmic scale. The green line in Figure 5-13 shows this trace.

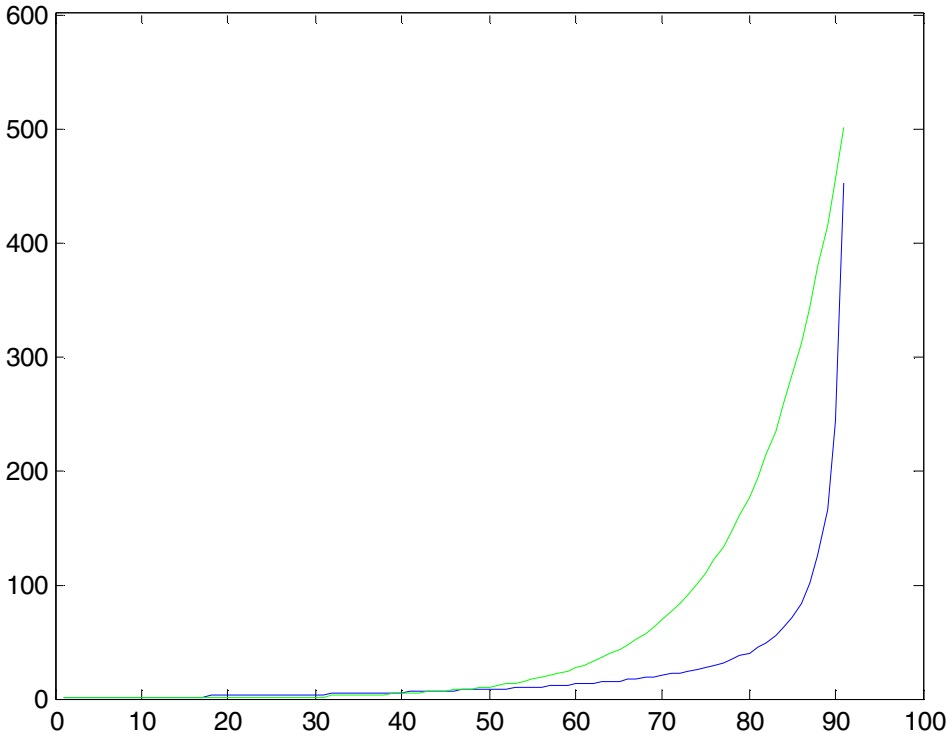

Figure 5-13. Logarithmically space values of vo (green) versus the number of values, which will be used to approximate the values of v0 (blue) that create a linearly spaced change in force in the deterministic model.

An appropriate range of values for v0 has now been created for which to compare to the data. Applying these v0 values in the deterministic model, optimized in a previous section, results in range of possible forces at each velocity, for a particular current. At the current of 1.9 A that was used to find the appropriately spaced values of *v0*, the area covered by the force versus velocity plot of the different *v0* can be seen in Figure 5-14. In addition, the PDF of the data at that current is plotted underneath. Comparing these two areas shows that not all data points can be modeled by varying the *v0* parameter. It can be seen that this new model will cover a large amount of the data.

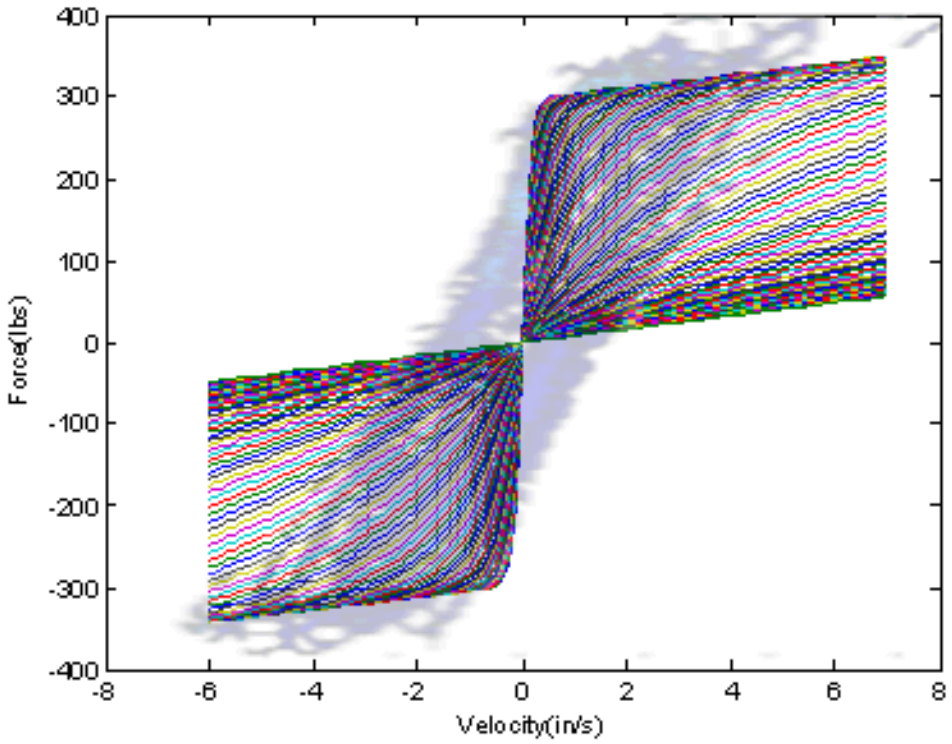

Figure 5-14. The area covered by the deterministic function when the *v0* parameter is varied. This can be compared to the PDF plot of the actual data.

To find the probability that the data is best modeled by a certain value of *v0*, the probability density will be summed wherever they intersect with a curve of the deterministic model for each parameter value. This sum of densities gives the relative frequency that the value of *v0* will accurately represent the data. Figure 5-15 shows the frequency versus *v0* value when the intersection points are summed along the entire current and velocity dimensions. In addition, this plot shows the value of *v0* found by minimizing the error in force output. The plot surprisingly shows that the value of *v0* found by minimizing the error in force appears identical to the *v0* that has the highest probability of describing the real data.

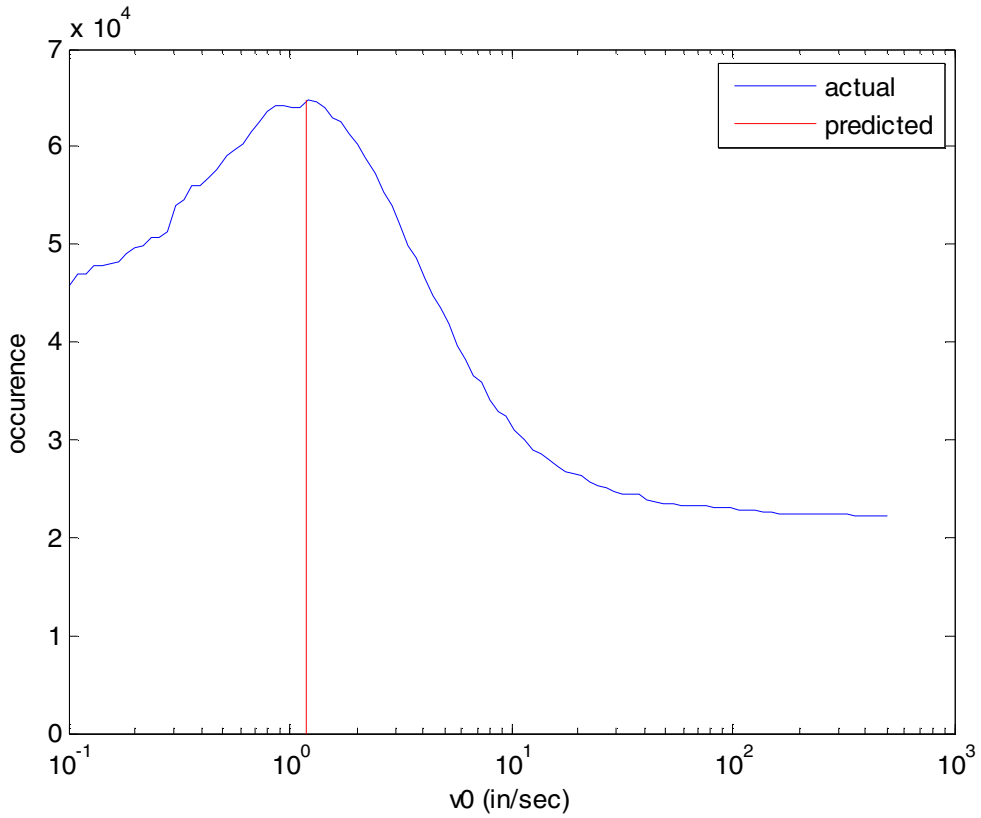

Figure 5-15. Comparison of the value found for the parameter *v0* in the deterministic equation, in red, and the number of data points that are accurately described by different parameter values, in blue.

While the *v0* parameter in the deterministic model coincides with the maximum occurrence for data points described by a certain *v0*, there is a wide range of parameter values that also have high occurrence values. Further examination of the data shows that the value of *v0* that has the highest occurrence changes when current changes. This can be seen in Figure 5-16. When current is lower, the *v0* value with the highest occurrence is higher than the parameter value predicted with the deterministic model. For higher currents, the value is lower than predicted.

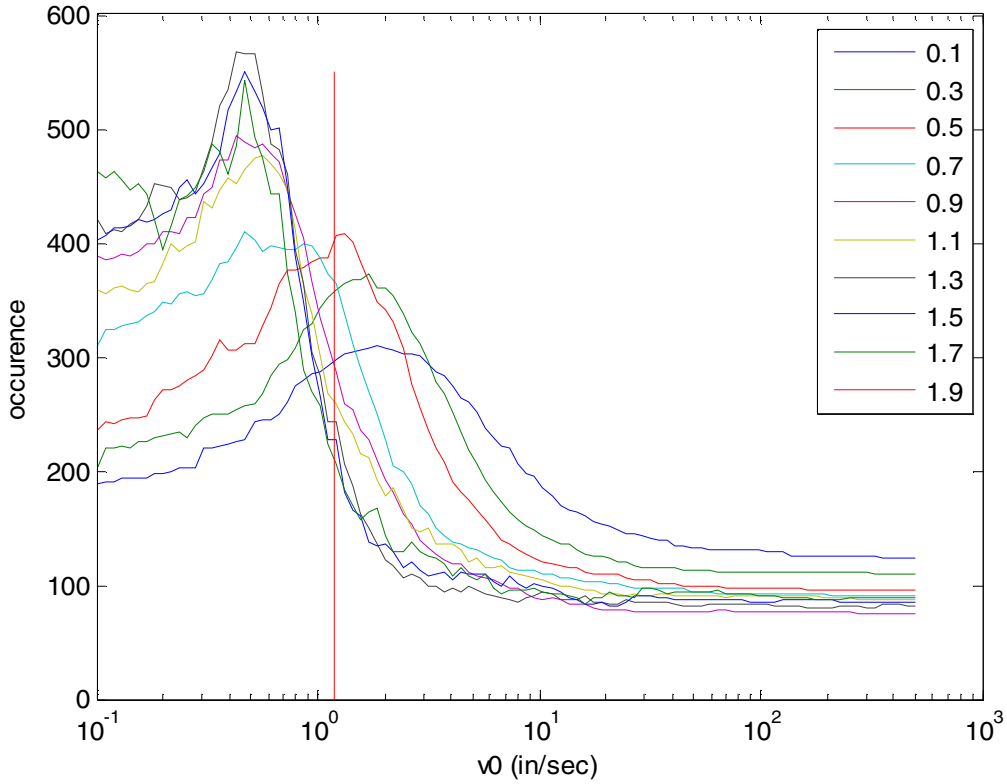

Figure 5-16. The value of the parameter *v0* that describes the highest number of data points varies with the input current (the legend shows the value of current for each trace). For comparison, the deterministic model predicts a value of 1.173 for *v0*.

The probability study of the parameter value for *v0* can be expanded to include creating a probability model and finding the effect of the other parameters. An analysis of considerations for future research can be found in Appendix C.

6 Conclusions and Recommendations

The general conclusion of this thesis is that using a deterministic model to simulate the behavior of an MR damper is insufficient. There are dynamic effects on the force response of an MR damper. Measuring their response at a fixed current or a periodic velocity function will result in an incomplete picture of a damper's force response. Using a deterministic model will not provide an output that mimics the shape of the force response of an actual damper. The number of parameters required for a phenomenological model that includes all the dynamic effects will be too high to be practical.

Using two parameter models to simplify the control strategy shows the importance of including dynamic effects. A liner model based solely on current has an extremely larger error compared to more detailed models. It represents a situation with the least controllability issues but the results would not be representative of the force output in a real world application. Using a nonlinear model decreases the error significantly. There is a high correlation in the shape of the force output by the model and the actual force output of the damper. Further examination of the probability space shows, however that is a large error between the predicted force and the actual force. Dramatic improvements can again be seen by adding a dynamic term to the model. Including hysteresis in the nonlinear model reduce the error by 80%.

Any deterministic model based on input current and velocity will still fall short of matching the probability density of force output for a real damper. Creating an empirical nonparametric PDF to replace the v0 parameter in the nonlinear model shows that the distribution of the parameter is not constant across the range of current. Suggestions for further research and considerations can be seen in Appendix D.

The result of this study clearly shows the importance of nonlinear and dynamic effects in a MR damper. Applications that require high precision in the response of the system must take these effects into account. Hopefully this study will provide a resource for improved MR damper control systems as well as more accurate modeling in MR damper simulations.

A Experimental Data

This appendix shows the results of the experiment displayed graphically. The first plot shows the 5 signals recorded, with the raw data in blue, and the filtered data used in the study in green. All ten trials of the experiment are shown below. After each plot of the raw data is the 3D plot of current, velocity, and force.

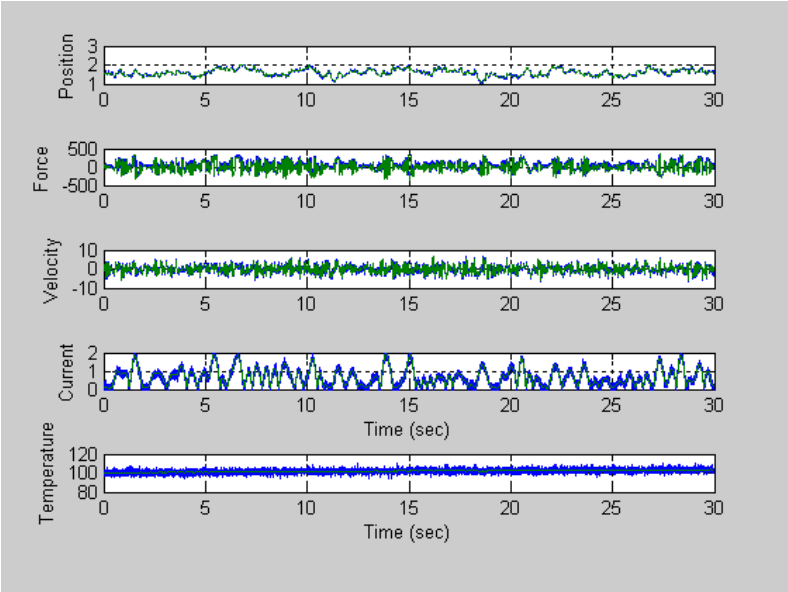

Figure A-1. Plot of the data, with the unfiltered data shown in blue and the filtered data shown in green, for the first trial of the experiment.

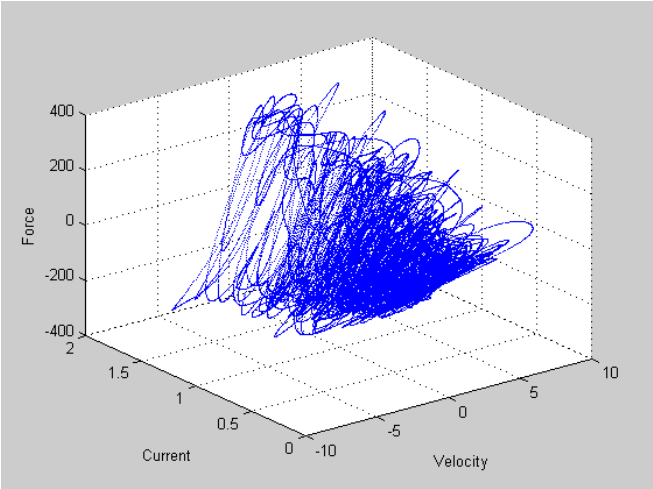

Figure A-2. 3D plot of force, velocity, and current for the first trial of the experiment

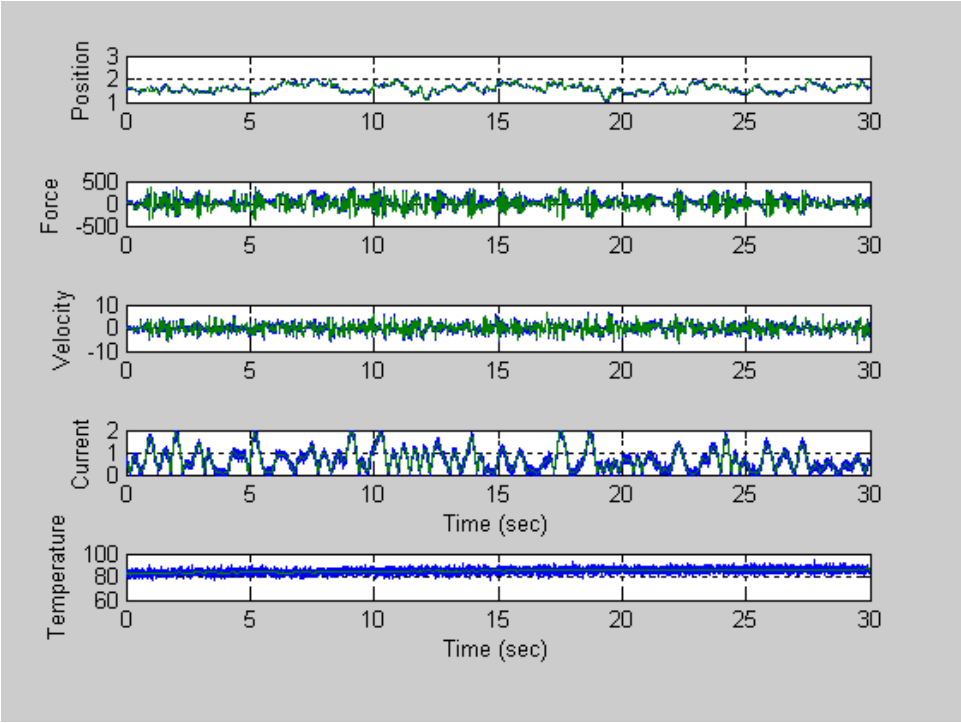

Figure A-3. Plot of the data, with the unfiltered data shown in blue and the filtered data shown in green, for the second trial of the experiment.

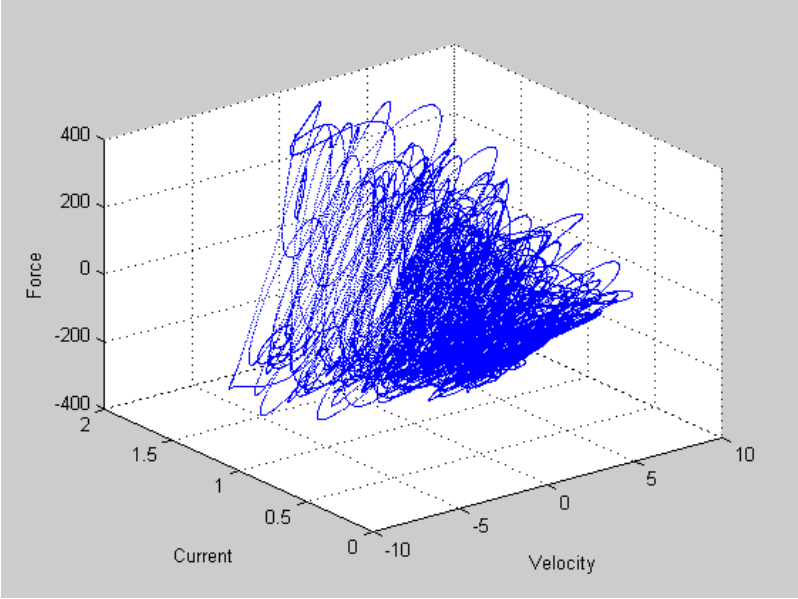

Figure A-4. 3D plot of force, velocity, and current for the second trial of the experiment

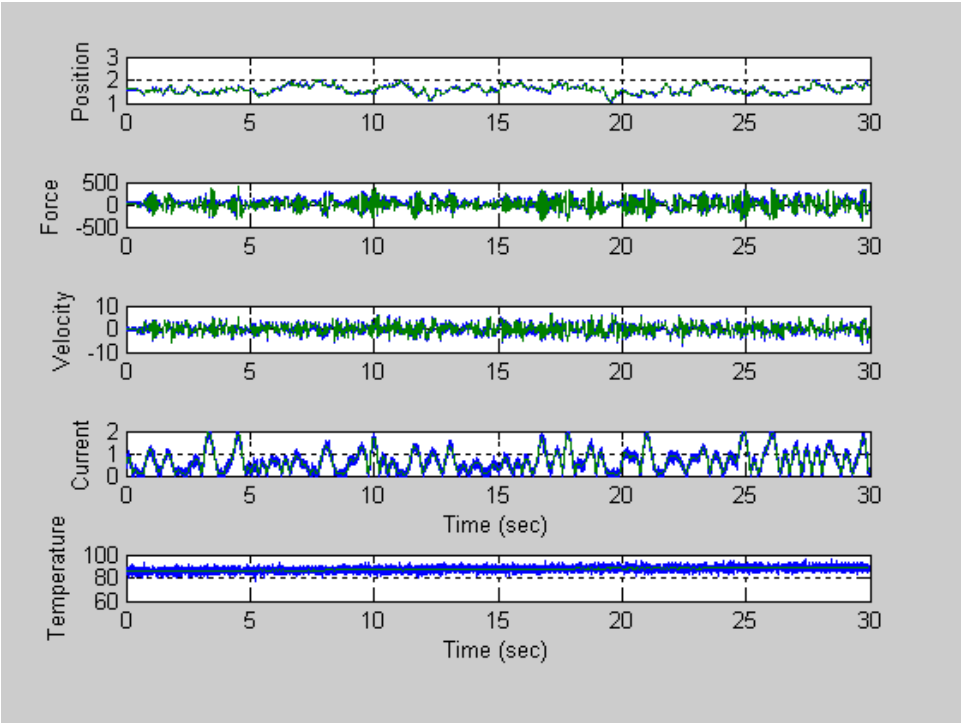

Figure A-5. Plot of the data, with the unfiltered data shown in blue and the filtered data shown in green, for the third trial of the experiment.

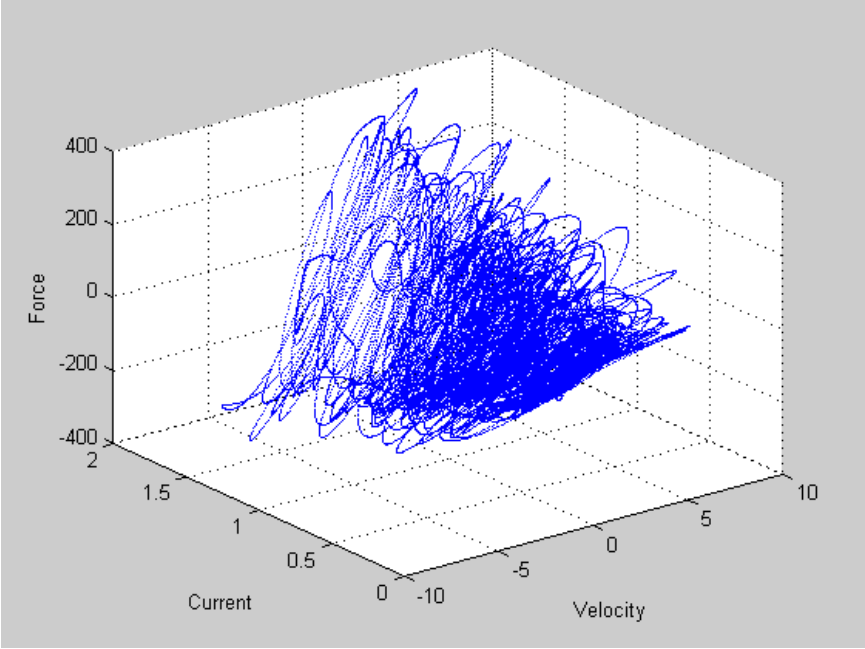

Figure A-6. 3D plot of force, velocity, and current for the third trial of the experiment

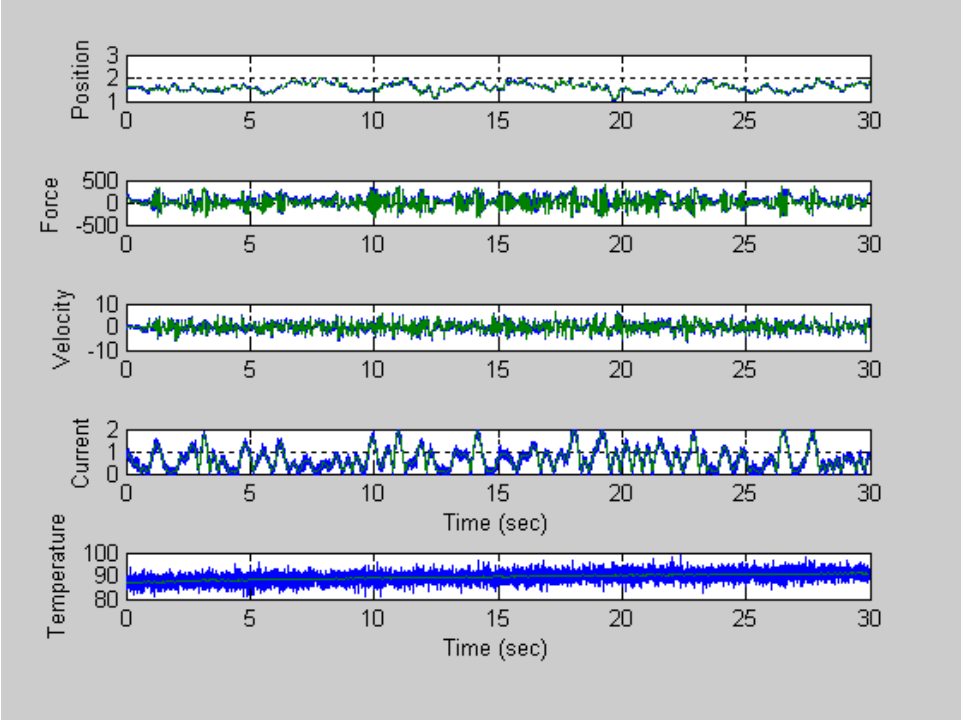

Figure A-7. Plot of the data, with the unfiltered data shown in blue and the filtered data shown in green, for the fourth trial of the experiment.

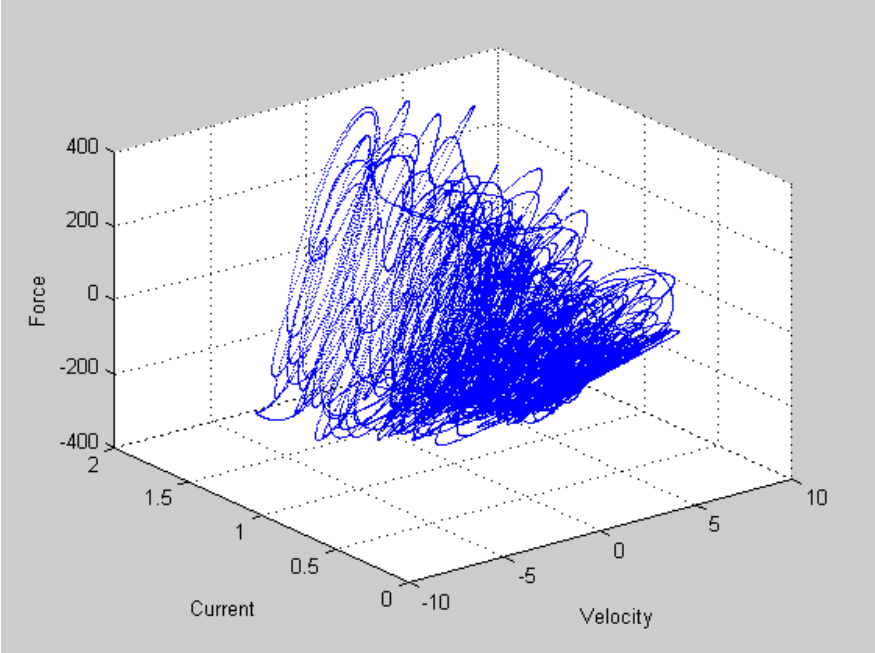

Figure A-8. 3D plot of force, velocity, and current for the fourth trial of the experiment

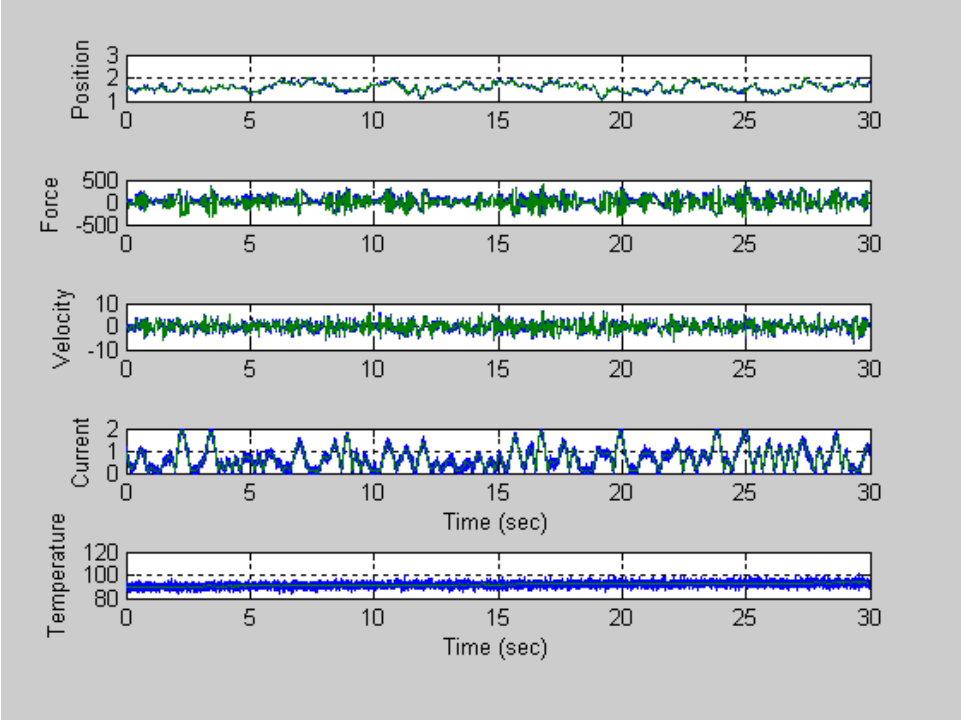

Figure A-9. Plot of the data, with the unfiltered data shown in blue and the filtered data shown in green, for the fifth trial of the experiment.

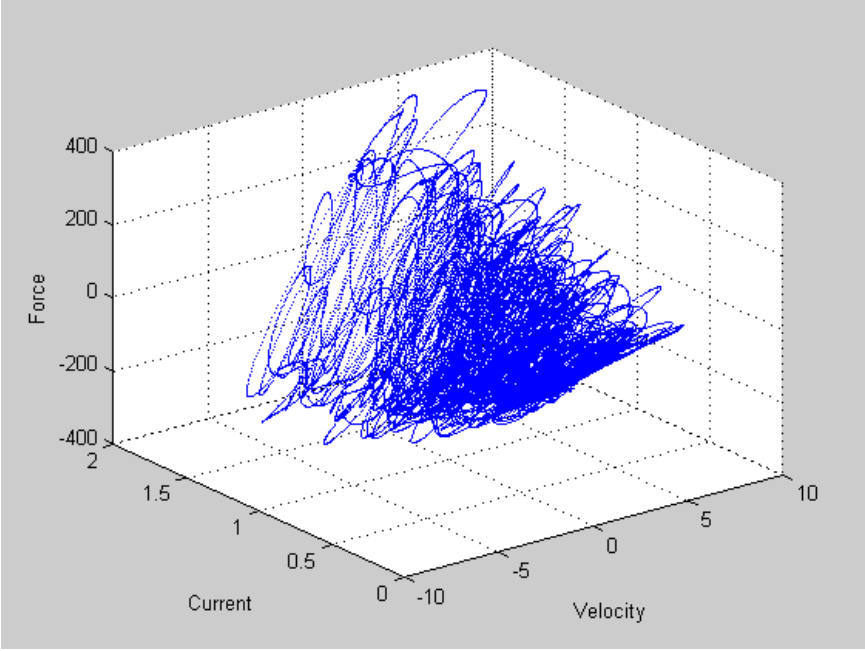

Figure A-10. 3D plot of force, velocity, and current for the fifth trial of the experiment

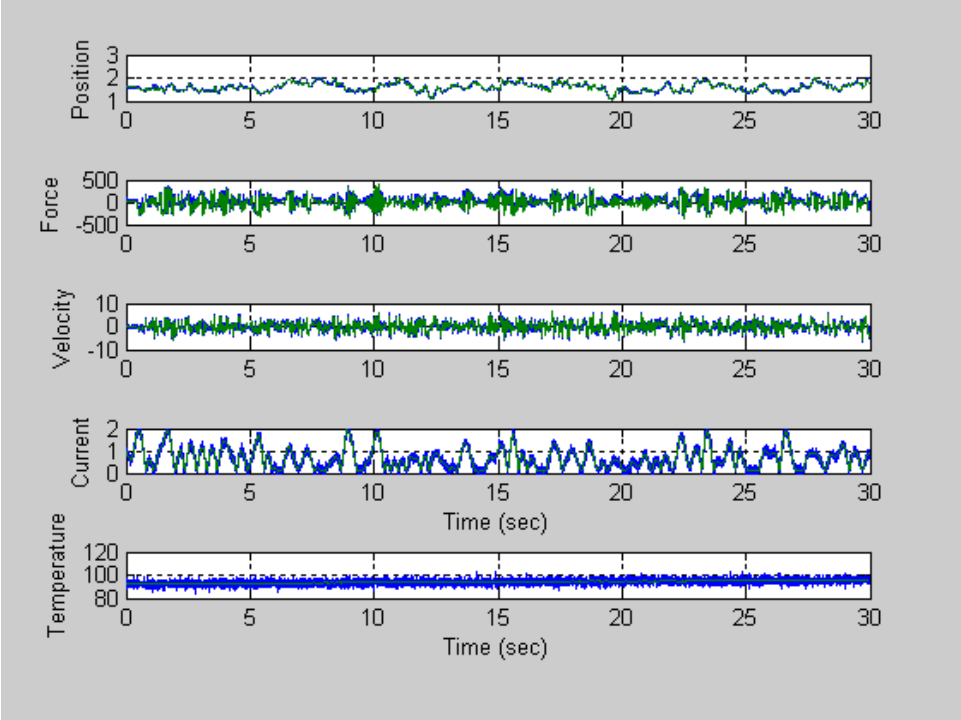

Figure A-11. Plot of the data, with the unfiltered data shown in blue and the filtered data shown in green, for the sixth trial of the experiment.

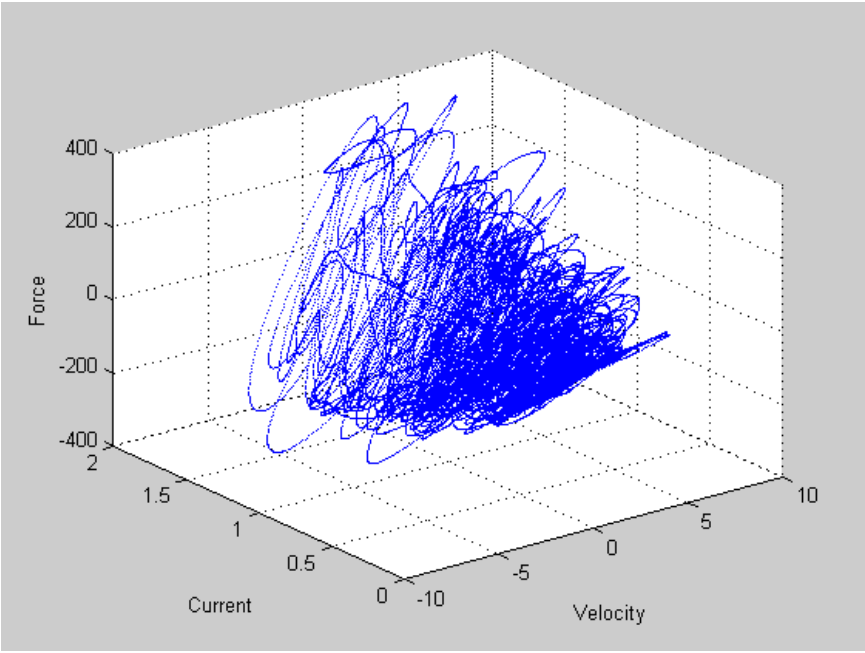

Figure A-12. 3D plot of force, velocity, and current for the sixth trial of the experiment

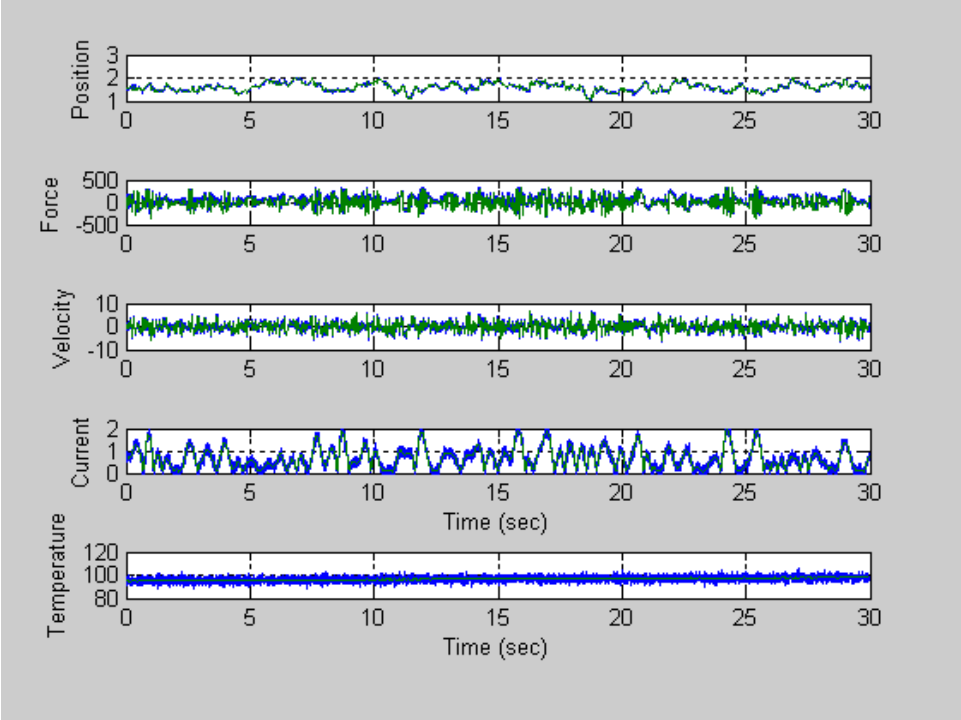

Figure A-13. Plot of the data, with the unfiltered data shown in blue and the filtered data shown in green, for the seventh trial of the experiment.

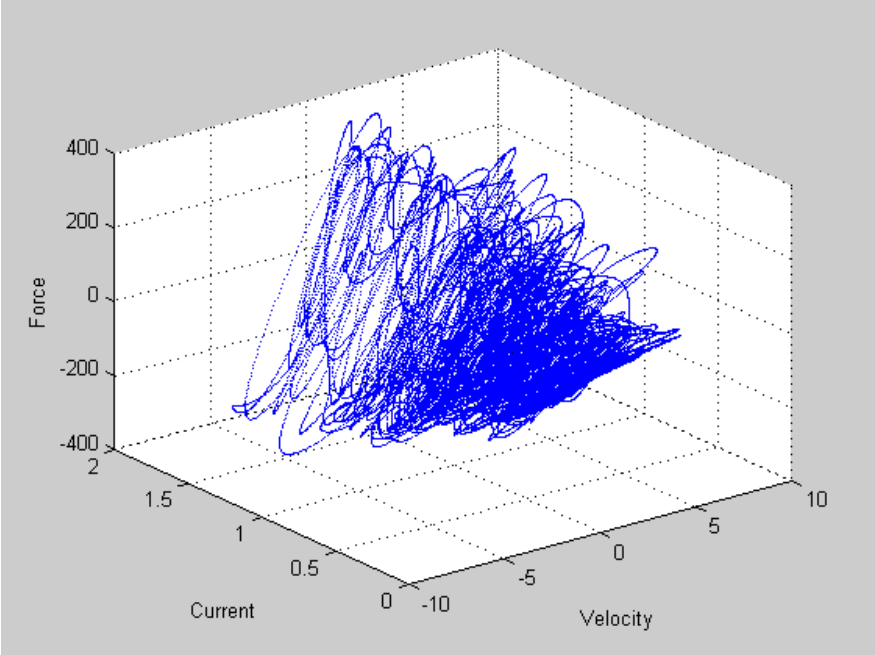

Figure A-14. 3D plot of force, velocity, and current for the seventh trial of the experiment

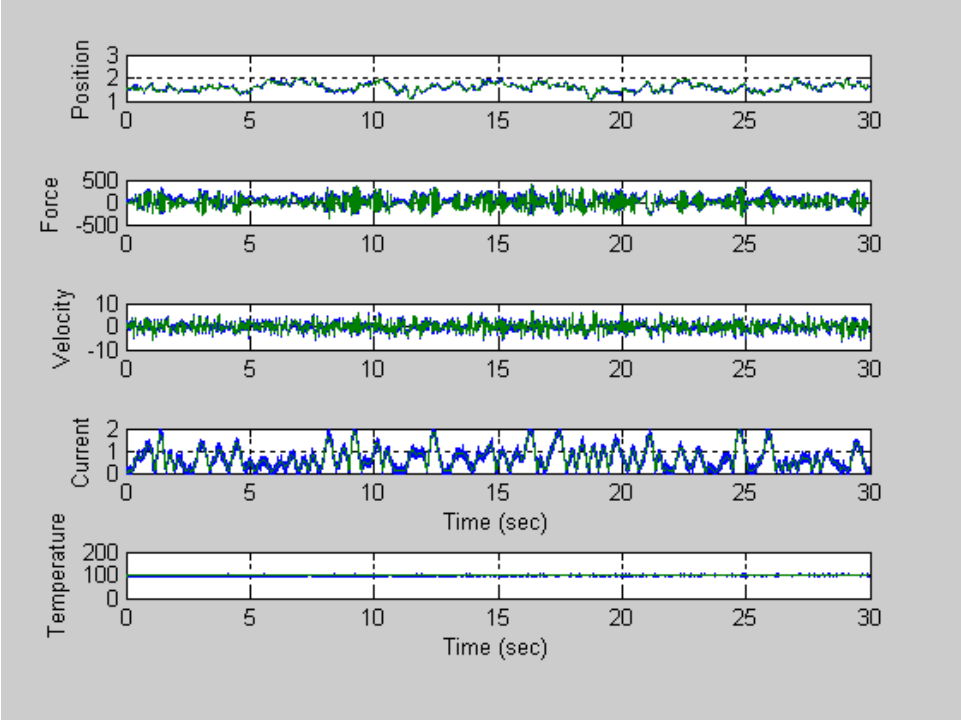

Figure A-15. Plot of the data, with the unfiltered data shown in blue and the filtered data shown in green, for the eighth trial of the experiment.

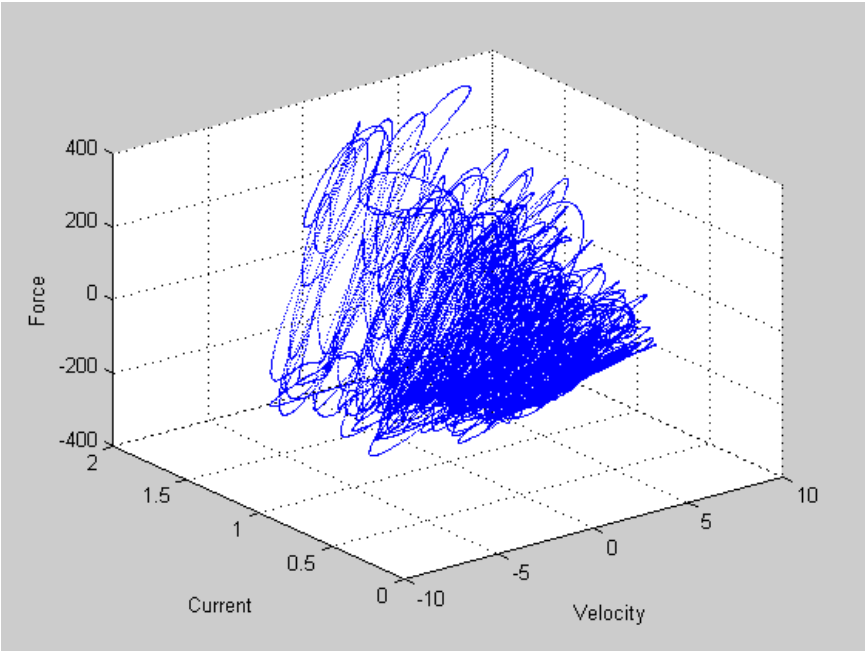

Figure A-16. 3D plot of force, velocity, and current for the eighth trial of the experiment

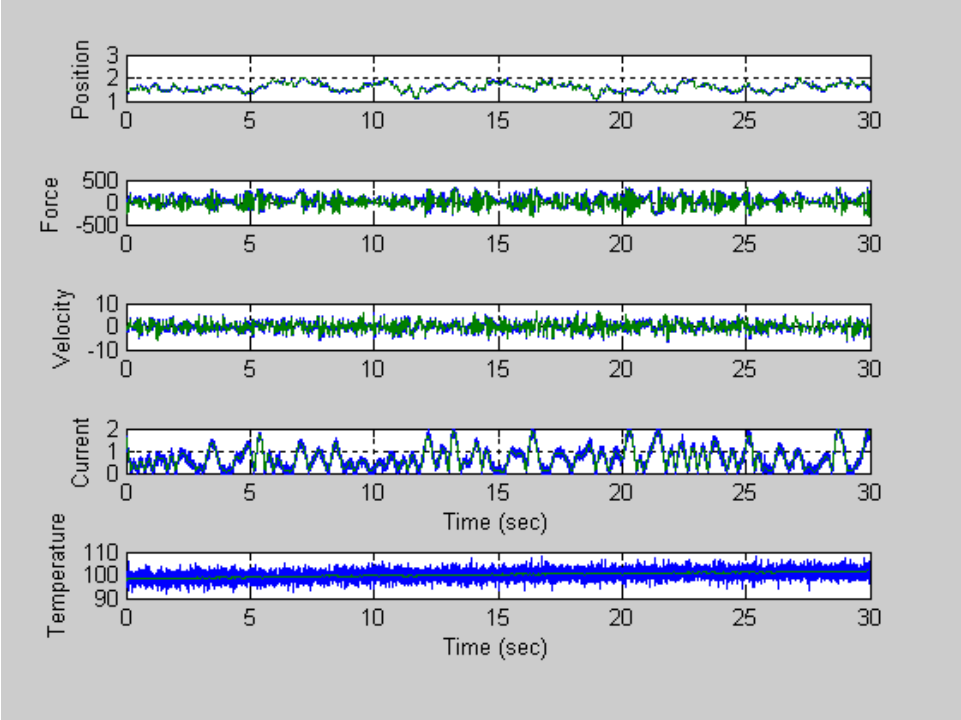

Figure A-17. Plot of the data, with the unfiltered data shown in blue and the filtered data shown in green, for the ninth trial of the experiment.

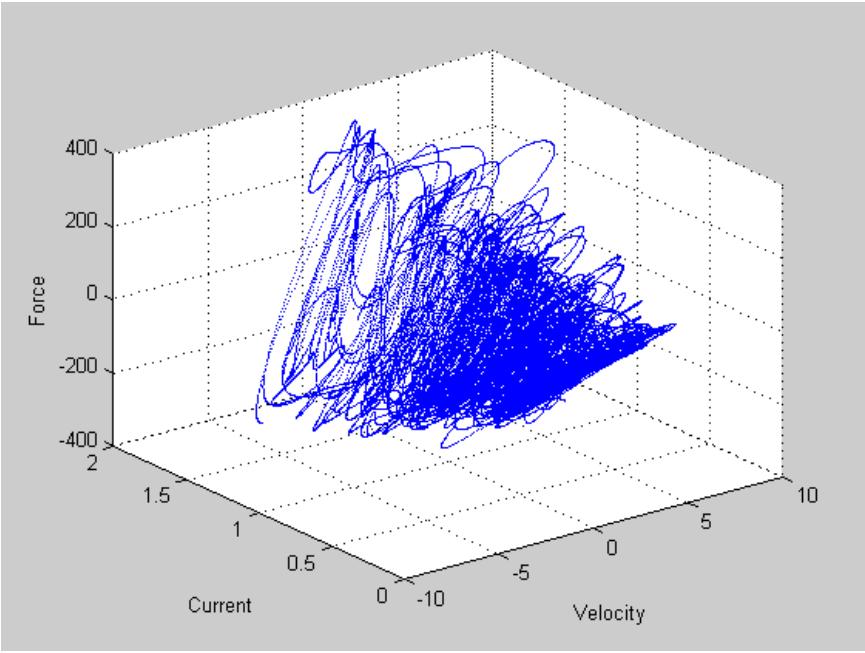

Figure A-18. 3D plot of force, velocity, and current for the ninth trial of the experiment

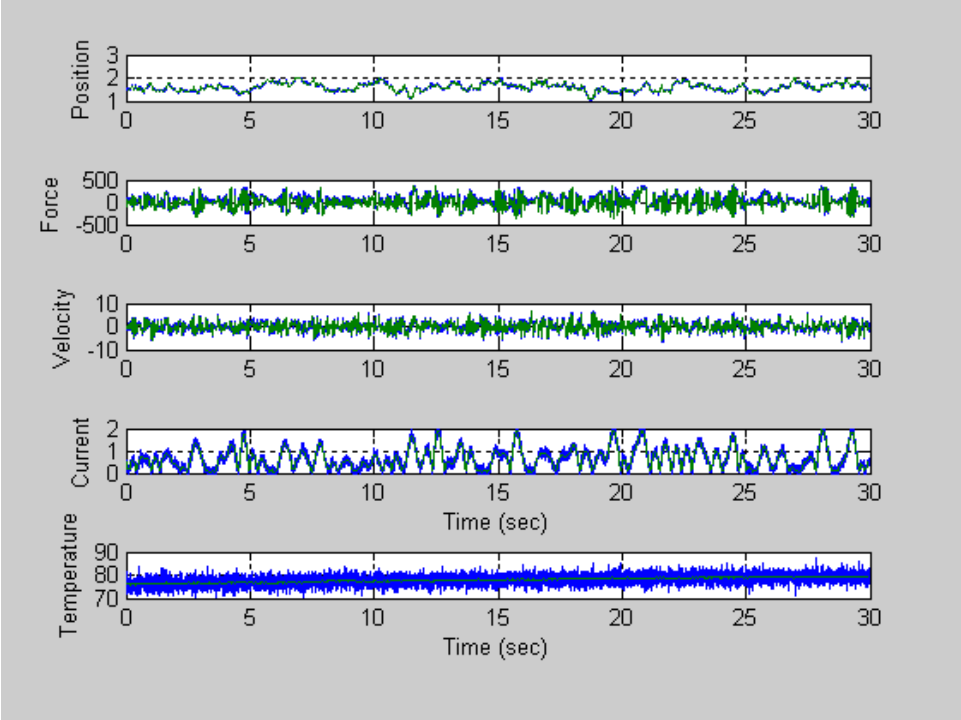

Figure A-19. Plot of the data, with the unfiltered data shown in blue and the filtered data shown in green, for the tenth trial of the experiment.

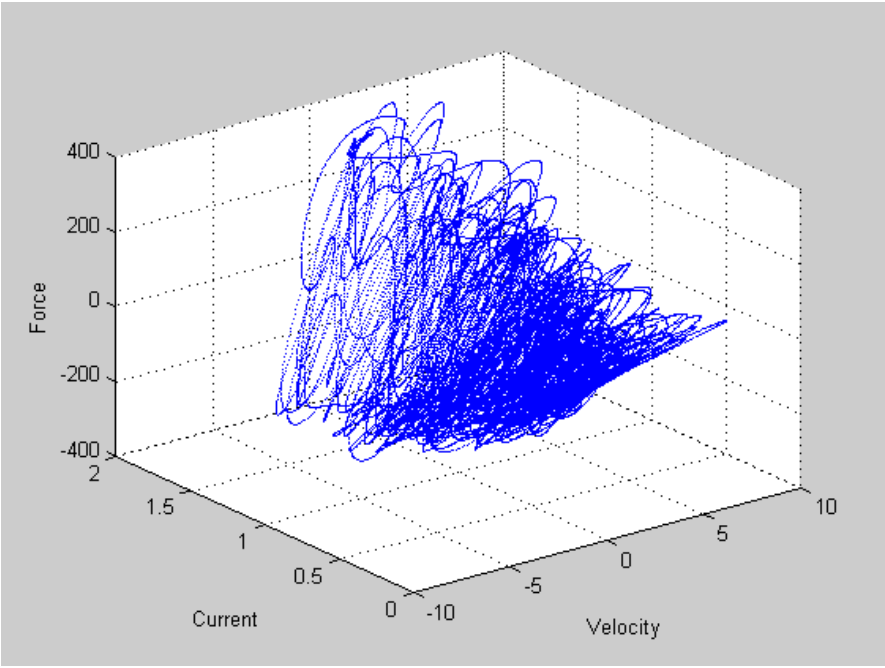

Figure A-20. 3D plot of force, velocity, and current for the tenth trial of the experiment

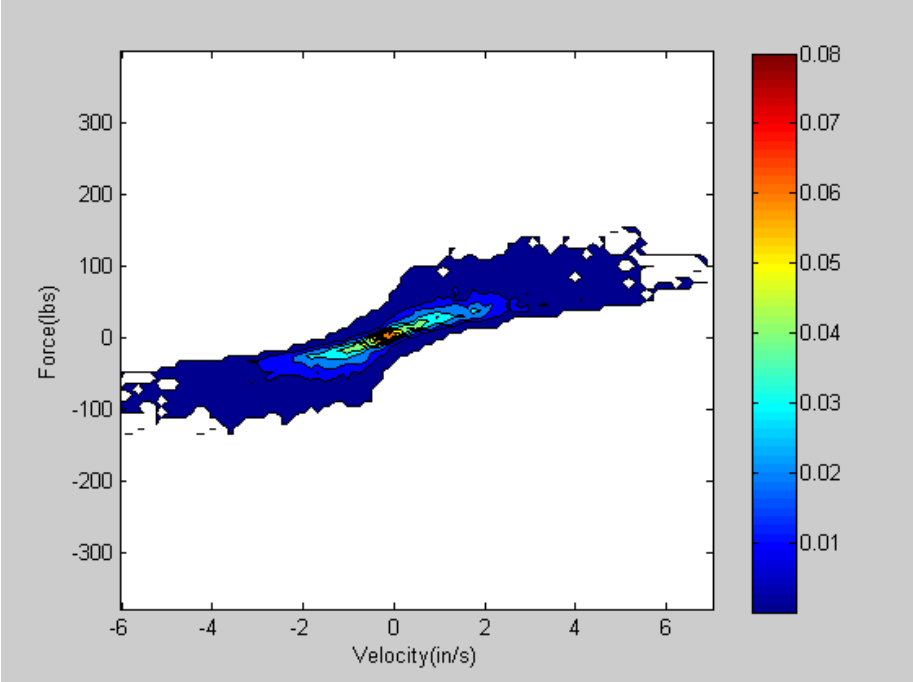

Figure A-21. Histogram PDF of the data for a current range of 0 to 0.2 A.

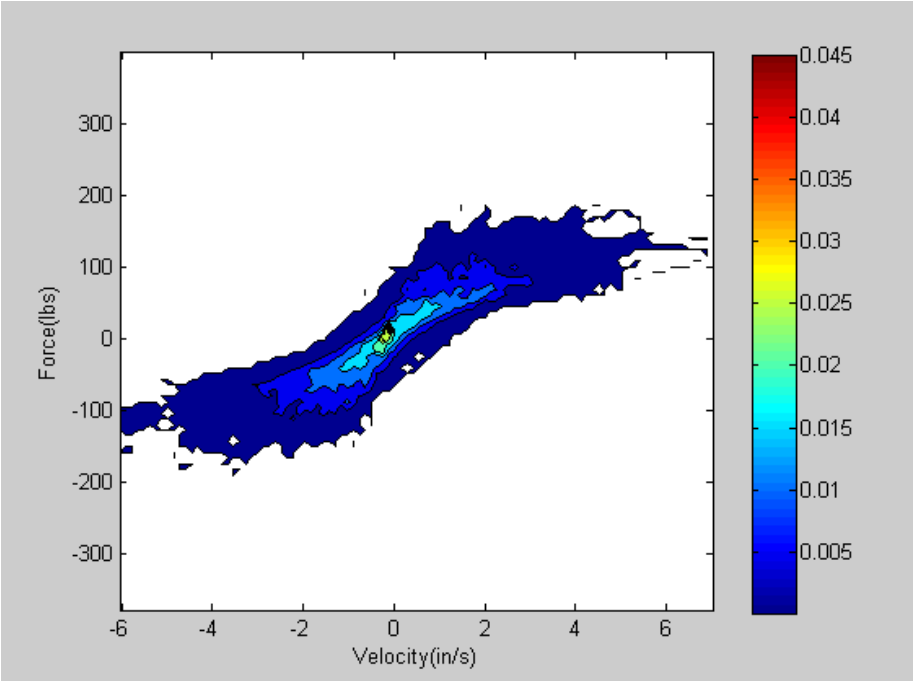

Figure A-22. Histogram PDF of the data for a current range of 0.2 to 0.4 A.

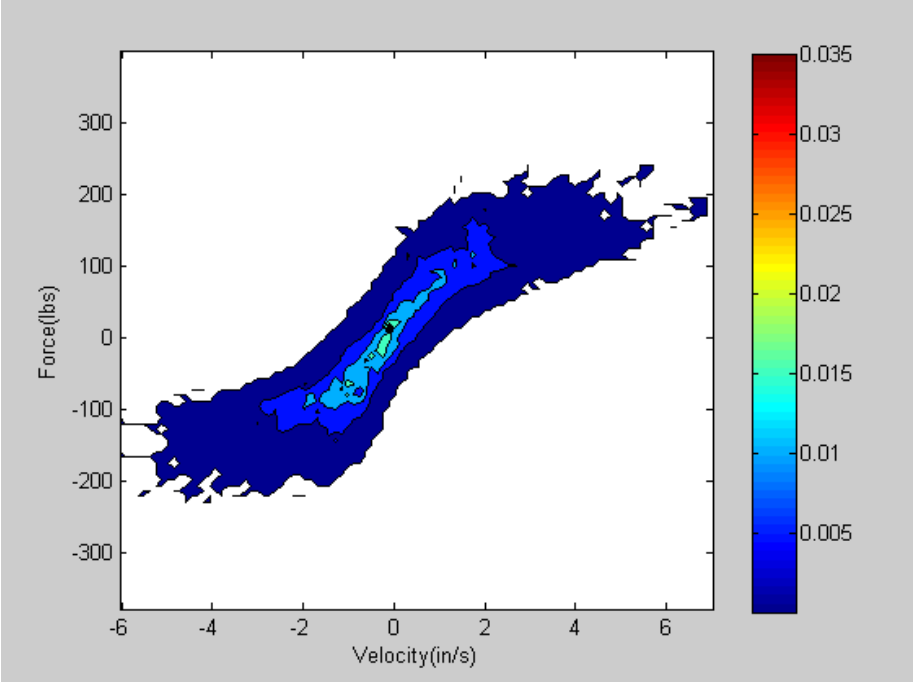

Figure A-23. Histogram PDF of the data for a current range of 0.4 to 0.6 A.

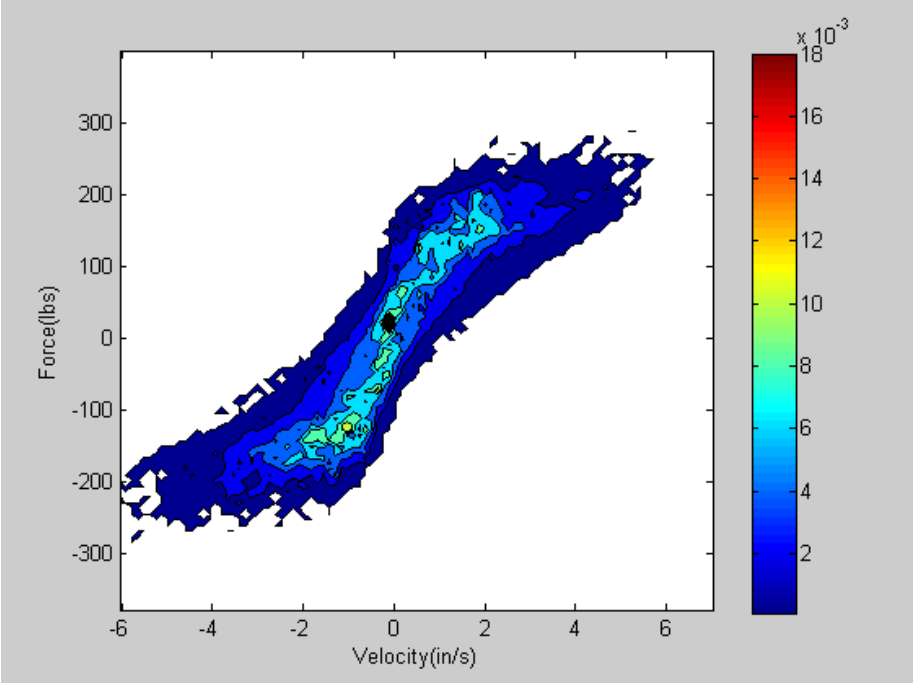

Figure A-24. Histogram PDF of the data for a current range of 0.6 to 0.8 A.

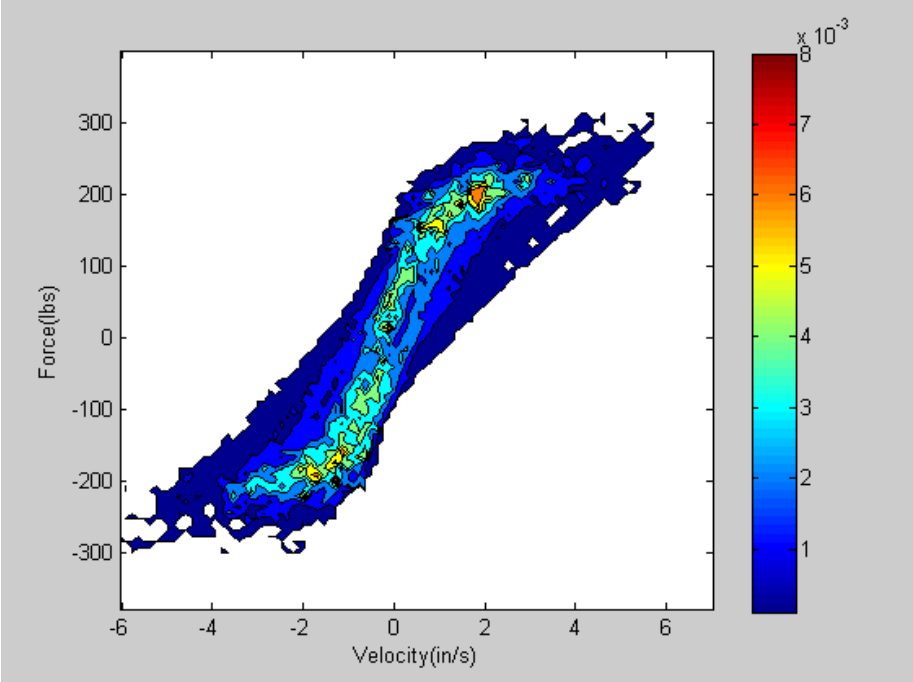

Figure A-25. Histogram PDF of the data for a current range of 0.8 to 1.0 A.

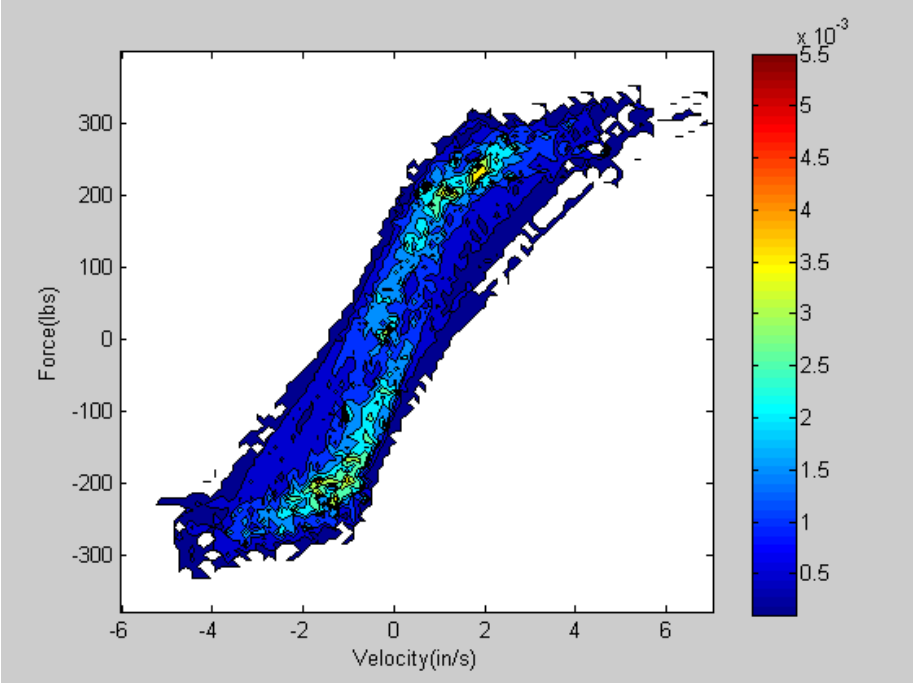

Figure A-26. Histogram PDF of the data for a current range of 1.0 to 1.2 A.

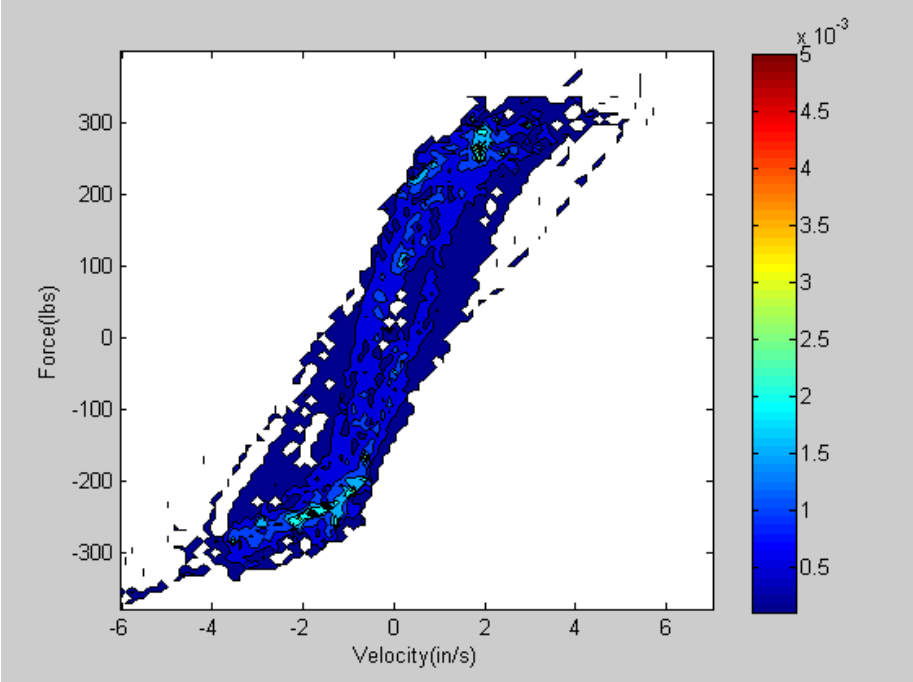

Figure A-27. Histogram PDF of the data for a current range of 1.2 to 1.4 A.

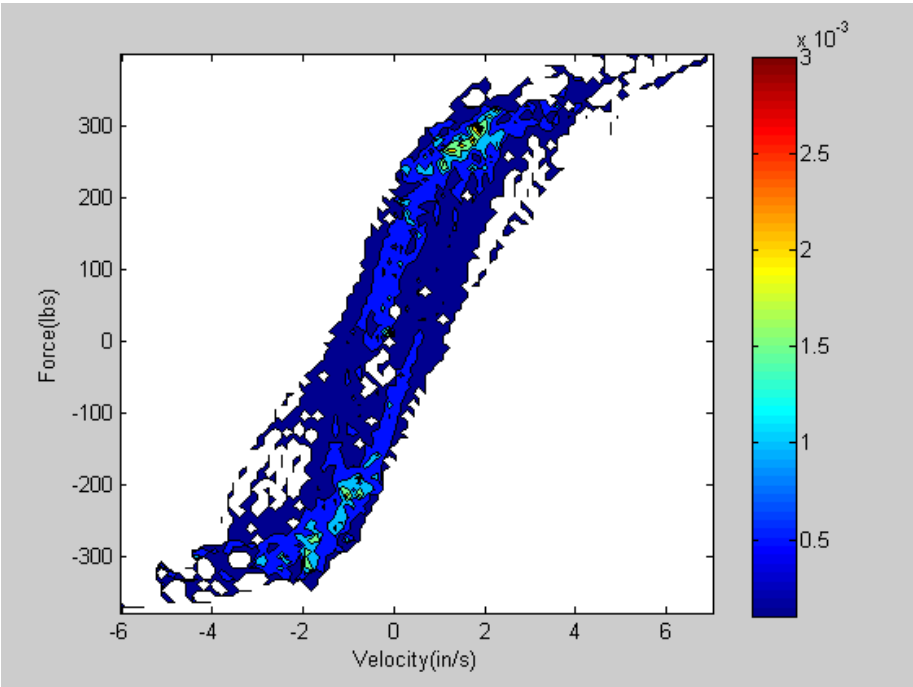

Figure A-28. Histogram PDF of the data for a current range of 1.4 to 1.6 A.

B Matlab Code

All computer simulation was done using Matlab. This appendix contains the code for all the functions used in this study that are not part of the built in library of Matlab v7.3.

B.1 Experimental Model

To prepare for creating the models, two Matlab files were written. The first is a script, called curr_test.m, uses existing data on the relationship between current and force in an MR damper to find an appropriate order polynomial model to describe the relationship. The second is an m-file that is called to create a 3D histogram of the force-velocity current plots of the data from the damper test.

curr_test.m

```
%  This script finds the accuracy of polynomial functions of different
%  order that relate change in current to change in force output of an
MR
%  damper

%  Rusty Richards

clear, clc

%  --load the position data

curr = 0:0.2:1.8;
force = [40.625 50 78.125 125 181.25 234.375 293.75 356.25 409.375
459.375];

%  --prepare for the optimization

options = optimset( ...
    'Display','iter', ...   % want to display lots of resuls
    'MaxFunevals',4000, ...  % maximum number of iterations
    'TolCon',1e-10, ...     % termination tolerance for constraint
violation
    'TolFun',1e-10, ...     % termination tolerance for f
    'TolX',1e-6);           % termination tolerance for x

%  --define the initial parameter guess and search bounds
```

```
x0=[-2 250];
lb=[-5 240];
ub=[0 250];

%  --find the optimal parameter vector

xopt = fmincon('curmod',x0,[],[],[],[],lb,ub,[],options,curr,force);

[tot_e,e,f_calc] = curmod(xopt,curr,force);

figure(1)
plot(curr,force,curr,f_calc)
xlabel('Current')
ylabel('Force')
grid on

x0=[24 153 53];
lb=[23 152 52];
ub=[25 154 54];

xopt2 = fmincon('curmod',x0,[],[],[],[],lb,ub,[],options,curr,force);

[tot_e2,e2,f_calc2] = curmod(xopt2,curr,force);

figure(2)
plot(curr,force,curr,f_calc2)
xlabel('Current')
ylabel('Force')
grid on

x0=[38 16 253 -73];
lb=[37 15 252 -74];
ub=[39 17 254 -72];

xopt3 = fmincon('curmod',x0,[],[],[],[],lb,ub,[],options,curr,force);

[tot_e3,e3,f_calc3] = curmod(xopt3,curr,force);

figure(3)
plot(curr,force,curr,f_calc3)
xlabel('Current')
ylabel('Force')
grid on

x0=[.01 .01 300 .01 .01];
lb=[-100 -100 200 -200 -100];
ub=[100 100 400 100 100];

xopt4 = fmincon('curmod',x0,[],[],[],[],lb,ub,[],options,curr,force);

[tot_e4,e4,f_calc4] = curmod(xopt4,curr,force);
```

```
figure(4)
plot(curr,force,curr,f_calc4)
xlabel('Current')
ylabel('Force')
grid on

figure(5)
subplot(4,1,1)
plot(curr,e,'.')
subplot(4,1,2)
plot(curr,e2,'.')
subplot(4,1,3)
plot(curr,e3,'.')
subplot(4,1,4)
plot(curr,e4,'.')
xlabel('Current')
ylabel('Error')
grid on


xopt
tot_e
xopt2
tot_e2
xopt3
tot_e3
xopt4
tot_e4
```

histogram.m

```
function hist_damper = histogram(current, velocity, force, g, col_map)

%Histogram creates a 3-D histogram (discrete PDF) of signal

%Histogram takes velocity, current, and force data for damper and
arranges
%into a 10x100x100 matrix of bins which store the number of data points
%that all in the range of each bin

minv=min(min(velocity));
minc=min(min(current));
minf=min(min(force));
maxv=max(max(velocity));
maxc=max(max(current));
maxf=max(max(force));

dv = linspace(minv,maxv,100);       %divisions for velocity
di = linspace(minc,maxc,10);            %divisions for current
dfc = linspace(minf,maxf,100);        %divisions for force
df = fliplr(dfc);                      %flip vector to align correctly
for graph

if maxc==minc
    hist_damper = zeros(length(df),length(dv));
```

```
else
    hist_damper = zeros(length(df),length(dv),length(di));
end

[a,b]=size(force);

for i = 1:a
    for j = 1:length(velocity)
        for k = 1:(length(df)-1)
            if (force(i,j)<df(k)) && (force(i,j)>=df(k+1))
                for l = 1:(length(dv)-1)
                    if (velocity(i,j)>dv(l)) &&
(velocity(i,j)<=dv(l+1))
                        if maxc==minc
                            hist_damper(k,l)=hist_damper(k,l)+1;
                        else
                            for m = 1:(length(di)-1)
                                if (current(i,j)>di(m)) &&
(current(i,j)<=di(m+1))
                                    hist_damper(k,l,m)=
hist_damper(k,l,m)+1;
                                end
                            end
                        end
                    end
                end
            end
        end
    end
end

n=length(df)*length(dv)*length(di);
bin_size=(maxf-minf)*(maxv-minv)*(maxc-minc)/n;

hist_damper=hist_damper./(n*bin_size);

if nargin<4
    [a,b,c]=size(hist_damper);
    g=1:c;
end

if nargout==0
    hist_damper(find(hist_damper<1.e-4))=NaN;
    for k=1:length(g);
        figure
        cs = contourf(dv,df,(hist_damper(:,:,g(k))));
        if nargin > 4
            colormap(col_map)
        end
        colorbar('vert');
        xlabel('Velocity(in/s)');
        ylabel('Force(lbs)');
        zlabel('Probability density (# of data points)');
    end
end
```

The stand alone first piece of code was written to load the data from the experiment, filter the noise, and plot the data appropriately. The Matlab script can be seen below.

data_fit.m

```
%  This script loads all the Tektronix CSV file data from the 6/3/06
%  testing of an MR damper with current and velocity excitation.
%  Data is plotted appropriately.

%  Rusty Richards - modified from S. C. Southward

close all
clear, clc

%  --load the position data

load rustest1.mat;
B(1,:,:)=A;
load rustest2.mat;
B(2,:,:)=A;
load rustest3.mat;
B(3,:,:)=A;
load rustest4.mat;
B(4,:,:)=A;
load rustest5.mat;
B(5,:,:)=A;
load rustest6.mat;
B(6,:,:)=A;
load rustest7.mat;
B(7,:,:)=A;
load rustest8.mat;
B(8,:,:)=A;
load rustest9.mat;
B(9,:,:)=A;
load rustest10.mat;
B(10,:,:)=A;


%%  Filter and scale Data Sets %%

% set scalars to convert data

sv = 25.6;              % (in/s)/volt
sf = 1024.3;              % (lbs)/volt
sp = 0.901;             % (in)/volt
sc = 10.0;             % (A)/volt
st = 180;             % (F)/volt
```

```
ov = 0.0221;            % offset (in/s)
of = 38.601;            % offset (lbs)
op = 3.7925;            % offset (in)
oc = 0;             % offset (A)
ot = 32;             % offset (F)

%  --create time data
length(B(1,:,1));
sample_rate = 2000;  %Hz
t = 0:1/sample_rate:(length(B(1,:,1))-1)/sample_rate;

%loop to extract and scale data from each data set
for i = 1:10

    raw_vel1 = B(i,:,1);
    raw_force1 = B(i,:,2);
    raw_pos1 = B(i,:,3);
    comm_current1 = B(i,:,4);
    raw_current1 = B(i,:,5);
    raw_temp1 = B(i,:,6);

    raw_vel(i,:) = sv.*raw_vel1+ov;
    raw_force(i,:) = sf.*raw_force1+of;
    raw_pos(i,:) = sp.*raw_pos1+op;
    raw_current(i,:) = sc.*raw_current1+oc;
    raw_temp(i,:) = st.*raw_temp1+ot;

    %  --clean up the data with a zero-phase low-pass filter

    [b,a] = butter(4,15/(sample_rate/2));        % 4th order, 80 Hz
break frequency

    pos(i,:) = filtfilt(b,a,raw_pos(i,:));
    force(i,:) = filtfilt(b,a,raw_force(i,:));
    vel(i,:) = filtfilt(b,a,raw_vel(i,:));
    current(i,:) = filtfilt(b,a,raw_current(i,:));
    temp(i,:) = filtfilt(b,a,raw_temp(i,:));

    force(i,:) = detrend(force(i,:),'constant');           %subtracts
DC offset from force data

end

%%  --plot the data

a=10;     %data set to plot

figure(1)
subplot(5,1,1)
plot(t,[raw_pos(a,:);pos(a,:)])
grid on
ylabel('Position')
subplot(5,1,2)
plot(t,[raw_force(a,:);force(a,:)])
```

```
grid on
ylabel('Force')
subplot(5,1,3)
plot(t,[raw_vel(a,:);vel(a,:)])
grid on
ylabel('Velocity')
subplot(5,1,4)
plot(t,[raw_current(a,:);current(a,:)])
grid on
ylabel('Current')
xlabel('Time (sec)')
ylim([0,2])
subplot(5,1,5)
plot(t,[raw_temp(a,:);temp(a,:)])
grid on
ylabel('Temperature')
xlabel('Time (sec)')

figure(2)
plot3(vel(a,:),current(a,:),force(a,:),'.','MarkerSize',3)
xlabel('Velocity')
ylabel('Current')
zlabel('Force')
grid on

histogram(current, vel, force, 1:10);
```

The following code was used to create a model for the damper and then display it graphically. The first three models, for linear, nonlinear, and hysteretic models, use three separate files of code. The first piece of code is an M-file that accepts parameters for a model, current data, velocity data, and force data; it returns the total error in force squared, the error in force at each point, and the force output of the model at each point for the given velocity and current. The second code is a script that uses the built in Matlab function *fmincon* to find the parameters of the model and the error. The third piece of code takes this information and displays it graphically.

fhat_l.m

```
function [f,e,f_calc] = fhat_l(x,current,velocity,force)

g = x(1);

f_calc = g.*current.*sign(velocity);

e = f_calc-force;

f = sum(e.*e);
```

```
return
```

lin_fit.m

```
%  This script loads all the Tektronix CSV file data from the 6/3/06
%  testing of an MR damper with current and velocity excitation.
%  Data is then fit to a linear model dependant on current.

%  Rusty Richards - modified from S. C. Southward

close all
clear, clc

%  --load the position data

load rustest1.mat;
B(1,:,:)=A;
load rustest2.mat;
B(2,:,:)=A;
load rustest3.mat;
B(3,:,:)=A;
load rustest4.mat;
B(4,:,:)=A;
load rustest5.mat;
B(5,:,:)=A;
load rustest6.mat;
B(6,:,:)=A;
load rustest7.mat;
B(7,:,:)=A;
load rustest8.mat;
B(8,:,:)=A;
load rustest9.mat;
B(9,:,:)=A;
load rustest10.mat;
B(10,:,:)=A;


%%  Filter and scale Data Sets %%

% set scalars to convert data

sv = 25.6;            % (in/s)/volt
sf = 1024.3;            % (lbs)/volt
sp = 0.901;           % (in)/volt
sc = 10.0;           % (A)/volt
st = 180;           % (F)/volt

ov = 0.0221;            % offset (in/s)
of = 38.601;            % offset (lbs)
op = 3.7925;            % offset (in)
oc = 0;           % offset (A)
ot = 32;           % offset (F)
```

```
%  --create time data
length(B(1,:,1));
sample_rate = 2000;  %Hz
t = 0:1/sample_rate:(length(B(1,:,1))-1)/sample_rate;

%loop to extract and scale data from each data set
for i = 1:10

    raw_vel = B(i,:,1);
    raw_force = B(i,:,2);
    raw_pos = B(i,:,3);
    comm_current = B(i,:,4);
    raw_current = B(i,:,5);
    raw_temp = B(i,:,6);

    raw_vel = sv.*raw_vel+ov;
    raw_force = sf.*raw_force+of;
    raw_pos = sp.*raw_pos+op;
    raw_current = sc.*raw_current+oc;
    raw_temp = st.*raw_temp+ot;

    %  --clean up the data with a zero-phase low-pass filter

    [b,a] = butter(4,15/(sample_rate/2));        % 4th order, 15 Hz
break frequency

    pos(i,:) = filtfilt(b,a,raw_pos);
    force(i,:) = filtfilt(b,a,raw_force);
    vel(i,:) = filtfilt(b,a,raw_vel);
    current(i,:) = filtfilt(b,a,raw_current);
    temp(i,:) = filtfilt(b,a,raw_temp);

    force(i,:) = detrend(force(i,:),'constant');           %subtracts
DC offset from force data

end

%%  fit data to linear model

%  --define the initial parameter guess and search bounds

g0=[127.4];
lb=[125];
ub=[130];

%  --prepare for the optimization

options = optimset( ...
    'Display','iter', ...   % want to display lots of resuls
    'MaxFunevals',1000*length(g0), ...  % maximum number of iterations
    'TolCon',1e-10, ...     % termination tolerance for constraint
violation
    'TolFun',1e-10, ...     % termination tolerance for f
    'TolX',1e-6);           % termination tolerance for x
```

```
%  --find the optimal parameter vector

a=2;                    %choose the data sets to optimize from
b=7;

gopt = fmincon('fhat_l',g0,[],[],[],[],lb,ub,[],options,[current(a,:)
current(b,:)],[vel(a,:) vel(b,:)],[force(a,:) force(b,:)]);

[tot_e,e,f_calc] = fhat_l(gopt,[current(a,:) current(b,:)],[vel(a,:)
vel(b,:)],[force(a,:) force(b,:)]);

gopt
tot_e
```

lin_graph.m

```
%  This script loads all the Tektronix CSV file data from the 6/3/06
%  testing of an MR damper with current and velocity excitation.
%  Data is then fit to a linear model dependant on current.

%  Rusty Richards - modified from S. C. Southward

close all
clear, clc

%  --load the position data

load rustest1.mat;
B(1,:,:)=A;
load rustest2.mat;
B(2,:,:)=A;
load rustest3.mat;
B(3,:,:)=A;
load rustest4.mat;
B(4,:,:)=A;
load rustest5.mat;
B(5,:,:)=A;
load rustest6.mat;
B(6,:,:)=A;
load rustest7.mat;
B(7,:,:)=A;
load rustest8.mat;
B(8,:,:)=A;
load rustest9.mat;
B(9,:,:)=A;
load rustest10.mat;
B(10,:,:)=A;


%%  Filter and scale Data Sets %%

% set scalars to convert data
```

```
sv = 25.6;            % (in/s)/volt
sf = 1024.3;            % (lbs)/volt
sp = 0.901;            % (in)/volt
sc = 10.0;            % (A)/volt
st = 180;            % (F)/volt

ov = 0.0221;            % offset (in/s)
of = 38.601;            % offset (lbs)
op = 3.7925;            % offset (in)
oc = 0;            % offset (A)
ot = 32;            % offset (F)

%  --create time data
length(B(1,:,1));
sample_rate = 2000;  %Hz
t = 0:1/sample_rate:(length(B(1,:,1))-1)/sample_rate;

%loop to extract and scale data from each data set
for i = 1:10

    raw_vel = B(i,:,1);
    raw_force = B(i,:,2);
    raw_pos = B(i,:,3);
    comm_current = B(i,:,4);
    raw_current = B(i,:,5);
    raw_temp = B(i,:,6);

    raw_vel = sv.*raw_vel+ov;
    raw_force = sf.*raw_force+of;
    raw_pos = sp.*raw_pos+op;
    raw_current = sc.*raw_current+oc;
    raw_temp = st.*raw_temp+ot;

    %  --clean up the data with a zero-phase low-pass filter

    [b,a] = butter(4,15/(sample_rate/2));        % 4th order, 15 Hz
break frequency

    pos(i,:) = filtfilt(b,a,raw_pos);
    force(i,:) = filtfilt(b,a,raw_force);
    vel(i,:) = filtfilt(b,a,raw_vel);
    current(i,:) = filtfilt(b,a,raw_current);
    temp(i,:) = filtfilt(b,a,raw_temp);

    force(i,:) = detrend(force(i,:),'constant');           %subtracts
DC offset from force data

end

%  --create linear model

g=[127.4125];
```

```
[tot_e,e, f_calc] = fhat_1(g,current(5,:),vel(5,:),force(5,:));

c=0:2/20:2;
v=-8:16/20:8;

fcalc2D=zeros(length(c),length(v));

for i = 1:length(c),
    for j = 1:length(v),
        [temp1,temp2,f_calc2D(i,j)] =
fhat_1(g,c(i),v(j),zeros(1,2000));
    end
end

%  --plot the data

figure(1)

plot(t,[force(5,:);f_calc])
grid on
ylabel('Force')
xlabel('Time (sec)')
xlim([10,20])
legend('measured force','calculated force','location','NorthEast')

%  --plot the damper function

figure(2)

vc = [-400:200:400];       % array of contour lines for the damper
force
vw = [-40,10];              % 3D view:  [aximuth, elevation] (degrees)
ms = 3;                     % marker size for plotting points

h = surf(v,c,f_calc2D);      % 3D surface plot
hold on
set(h(1),'facealpha',0.7)      % make it transparent
shading interp                  % smooth the colors

%colormap('jet')         % use this for a range of colors
colormap([0,1,0])      % use this for a constant color

contour3(v,c,f_calc2D,vc)     % draw the contour lines on the surface

view(vw)

plot3(vel(5,:),current(5,:),force(5,:),'.b','MarkerSize',ms)
xlabel('Velocity')
ylabel('Current')
zlabel('Force')
grid on
```

fhat.m

```
function [f,e,f_calc] = fhat(x,current,velocity,force)

A1 = x(1);
A2 = x(2);
A3 = x(3);
A4 = x(4);
v0 = x(5);
k1 = x(6);

Acurr = A1*current.^3+A2*current.^2+A3*current.^1+A4*current.^0;

f_calc = Acurr.*sign(velocity).*(1-exp(-
abs(velocity)/v0))+k1.*velocity;

e = f_calc-force;

f = sum(e.*e);

return
```

nonlin_fit.m

```
%  This script loads all the Tektronix CSV file data from the 6/3/06
%  testing of an MR damper with current and velocity excitation.
%  Data is then fit to a linear model dependant on current.

%  Rusty Richards - modified from S. C. Southward

close all
clear, clc

%  --load the position data

load rustest1.mat;
B(1,:,:)=A;
load rustest2.mat;
B(2,:,:)=A;
load rustest3.mat;
B(3,:,:)=A;
load rustest4.mat;
B(4,:,:)=A;
load rustest5.mat;
B(5,:,:)=A;
load rustest6.mat;
B(6,:,:)=A;
load rustest7.mat;
B(7,:,:)=A;
load rustest8.mat;
B(8,:,:)=A;
load rustest9.mat;
B(9,:,:)=A;
load rustest10.mat;
B(10,:,:)=A;
```

```
%%  Filter and scale Data Sets %%

% set scalars to convert data

sv = 25.6;            % (in/s)/volt
sf = 1024.3;            % (lbs)/volt
sp = 0.901;            % (in)/volt
sc = 10.0;            % (A)/volt
st = 180;            % (F)/volt

ov = 0.0221;            % offset (in/s)
of = 38.601;            % offset (lbs)
op = 3.7925;            % offset (in)
oc = 0;            % offset (A)
ot = 32;            % offset (F)

%  --create time data
length(B(1,:,1));
sample_rate = 2000;  %Hz
t = 0:1/sample_rate:(length(B(1,:,1))-1)/sample_rate;

%loop to extract and scale data from each data set
for i = 1:10

    raw_vel = B(i,:,1);
    raw_force = B(i,:,2);
    raw_pos = B(i,:,3);
    comm_current = B(i,:,4);
    raw_current = B(i,:,5);
    raw_temp = B(i,:,6);

    raw_vel = sv.*raw_vel+ov;
    raw_force = sf.*raw_force+of;
    raw_pos = sp.*raw_pos+op;
    raw_current = sc.*raw_current+oc;
    raw_temp = st.*raw_temp+ot;

    %  --clean up the data with a zero-phase low-pass filter

    [b,a] = butter(4,15/(sample_rate/2));        % 4th order, 15 Hz
break frequency

    pos(i,:) = filtfilt(b,a,raw_pos);
    force(i,:) = filtfilt(b,a,raw_force);
    vel(i,:) = filtfilt(b,a,raw_vel);
    current(i,:) = filtfilt(b,a,raw_current);
    temp(i,:) = filtfilt(b,a,raw_temp);

    force(i,:) = detrend(force(i,:),'constant');           %subtracts
DC offset from force data

end
```

```
%%  fit data to linear model

%  --define the initial parameter guess and search bounds

x0=[-23 21 194 7 1.2 8];
lb=[-30 20 150 5 1 5];
ub=[-20 25 200 10 2 10];

%  --prepare for the optimization

options = optimset( ...
    'Display','iter', ...   % want to display lots of resuls
    'MaxFunevals',1000*length(x0), ...  % maximum number of iterations
    'TolCon',1e-10, ...     % termination tolerance for constraint
violation
    'TolFun',1e-10, ...     % termination tolerance for f
    'TolX',1e-6);           % termination tolerance for x


%  --find the optimal parameter vector

a=2;                    %choose the data sets to optimize from
b=7;

xopt = fmincon('fhat',x0,[],[],[],[],lb,ub,[],options,[current(a,:)
current(b,:)],[vel(a,:) vel(b,:)],[force(a,:) force(b,:)]);

[tot_e,e,f_calc] = fhat(xopt,[current(a,:) current(b,:)],[vel(a,:)
vel(b,:)],[force(a,:) force(b,:)]);

xopt
tot_e
```

nonlin_graph.m

```
%  This script loads all the Tektronix CSV file data from the 6/3/06
%  testing of an MR damper with current and velocity excitation.
%  Data is then fit to a linear model dependant on current.

%  Rusty Richards - modified from S. C. Southward

close all
clear, clc

%  --load the position data

load rustest1.mat;
B(1,:,:)=A;
load rustest2.mat;
B(2,:,:)=A;
load rustest3.mat;
B(3,:,:)=A;
```

```
load rustest4.mat;
B(4,:,:)=A;
load rustest5.mat;
B(5,:,:)=A;
load rustest6.mat;
B(6,:,:)=A;
load rustest7.mat;
B(7,:,:)=A;
load rustest8.mat;
B(8,:,:)=A;
load rustest9.mat;
B(9,:,:)=A;
load rustest10.mat;
B(10,:,:)=A;


%%  Filter and scale Data Sets %%

% set scalars to convert data

sv = 25.6;            % (in/s)/volt
sf = 1024.3;            % (lbs)/volt
sp = 0.901;           % (in)/volt
sc = 10.0;            % (A)/volt
st = 180;           % (F)/volt

ov = 0.0221;            % offset (in/s)
of = 38.601;            % offset (lbs)
op = 3.7925;            % offset (in)
oc = 0;           % offset (A)
ot = 32;           % offset (F)

%  --create time data
length(B(1,:,1));
sample_rate = 2000;  %Hz
t = 0:1/sample_rate:(length(B(1,:,1))-1)/sample_rate;

%loop to extract and scale data from each data set
for i = 1:10

    raw_vel = B(i,:,1);
    raw_force = B(i,:,2);
    raw_pos = B(i,:,3);
    comm_current = B(i,:,4);
    raw_current = B(i,:,5);
    raw_temp = B(i,:,6);

    raw_vel = sv.*raw_vel+ov;
    raw_force = sf.*raw_force+of;
    raw_pos = sp.*raw_pos+op;
    raw_current = sc.*raw_current+oc;
    raw_temp = st.*raw_temp+ot;

    %  --clean up the data with a zero-phase low-pass filter
```

```
    [b,a] = butter(4,15/(sample_rate/2));        % 4th order, 15 Hz
break frequency

    pos(i,:) = filtfilt(b,a,raw_pos);
    force(i,:) = filtfilt(b,a,raw_force);
    vel(i,:) = filtfilt(b,a,raw_vel);
    current(i,:) = filtfilt(b,a,raw_current);
    temp(i,:) = filtfilt(b,a,raw_temp);

    force(i,:) = detrend(force(i,:),'constant');           %subtracts
DC offset from force data

end

%  --create linear model

x=[-22.9592 21.4234 194.2564 7.4617 1.1734 7.5345];

[tot_e,e, f_calc] = fhat(x,current(5,:),vel(5,:),force(5,:));
a=sum(abs(f_calc))

x=[-22.9592 21.4234 194.2564 7.4617 1.2734 7.5345];

[tot_e,e, f_calc1] = fhat(x,current(5,:),vel(5,:),force(5,:));
b=sum(abs(f_calc1))

b-a

c=0:2/20:2;
v=-8:16/20:8;

fcalc2D=zeros(length(c),length(v));

for i = 1:length(c),
    for j = 1:length(v),
        [temp1,temp2,f_calc2D(i,j)] = fhat(x,c(i),v(j),zeros(1,2000));
    end
end

%  --plot the data

figure(1)

plot(t,[force(5,:);f_calc])
grid on
ylabel('Force')
xlabel('Time (sec)')
xlim([10,20])
legend('measured force','calculated force','location','NorthEast')

%  --plot the damper function

figure(2)
```

```
vc = [-400:200:400];       % array of contour lines for the damper
force
vw = [-40,10];              % 3D view:  [aximuth, elevation] (degrees)
ms = 3;                     % marker size for plotting points

h = surf(v,c,f_calc2D);      % 3D surface plot
hold on
set(h(1),'facealpha',0.7)      % make it transparent
shading interp                  % smooth the colors

%colormap('jet')         % use this for a range of colors
colormap([0,1,0])      % use this for a constant color

contour3(v,c,f_calc2D,vc)     % draw the contour lines on the surface

view(vw)

plot3(vel(5,:),current(5,:),force(5,:),'.b','MarkerSize',ms)
xlabel('Velocity')
ylabel('Current')
zlabel('Force')
grid on

histogram(current, vel, force, [8]);
hold on
vel2=linspace(-6,6);
cur2=1.5;
[tot_e,e, f_calc2]=fhat(x,cur2, vel2, zeros(1,100));
plot(vel2,f_calc2,'r','LineWidth',2)
legend(' ','nonlinear model(current=1.5A)','location','NorthWest')
```

fhat_h.m

```
function [f,e,f_hat] = fhat_h(x,current,velocity,force)

A1 = x(1);
A2 = x(2);
A3 = x(3);
A4 = x(4);
v0 = x(5);
k1 = x(6);
a = x(7);

Acurr = A1*current.^3+A2*current.^2+A3*current.^1+A4*current.^0;

f_calc = Acurr.*sign(velocity).*(1-exp(-
abs(velocity)/v0))+k1.*velocity;

h = tf(a,[1 a]);
t = 0:1/2000:(length(f_calc)-1)/2000;
f_hat = lsim(h,f_calc,t);

e = f_hat'-force;
```

```
f = sum(e.*e);

return
```

hyst_fit.m

```
%  This script loads all the Tektronix CSV file data from the 6/3/06
%  testing of an MR damper with current and velocity excitation.

%  S. C. Southward - modified by Rusty Richards

close all
clear, clc

%  --load the position data

load rustest1.mat;
B(1,:,:)=A;
load rustest2.mat;
B(2,:,:)=A;
load rustest3.mat;
B(3,:,:)=A;
load rustest4.mat;
B(4,:,:)=A;
load rustest5.mat;
B(5,:,:)=A;
load rustest6.mat;
B(6,:,:)=A;
load rustest7.mat;
B(7,:,:)=A;
load rustest8.mat;
B(8,:,:)=A;
load rustest9.mat;
B(9,:,:)=A;
load rustest10.mat;
B(10,:,:)=A;


%%  Filter and scale Data Sets %%

% set scalars to convert data

sv = 25.6;            % (in/s)/volt
sf = 1024.3;            % (lbs)/volt
sp = 0.901;           % (in)/volt
sc = 10.0;           % (A)/volt
st = 180;           % (F)/volt

ov = 0.0221;            % offset (in/s)
of = 38.601;            % offset (lbs)
op = 3.7925;            % offset (in)
oc = 0;           % offset (A)
ot = 32;           % offset (F)
```

```
%  --create time data
length(B(1,:,1));
sample_rate = 2000;  %Hz
t = 0:1/sample_rate:(length(B(1,:,1))-1)/sample_rate;

%loop to extract and scale data from each data set
for i = 1:10

    raw_vel = B(i,:,1);
    raw_force = B(i,:,2);
    raw_pos = B(i,:,3);
    comm_current = B(i,:,4);
    raw_current = B(i,:,5);
    raw_temp = B(i,:,6);

    raw_vel = sv.*raw_vel+ov;
    raw_force = sf.*raw_force+of;
    raw_pos = sp.*raw_pos+op;
    raw_current = sc.*raw_current+oc;
    raw_temp = st.*raw_temp+ot;

    %  --clean up the data with a zero-phase low-pass filter

    [b,a] = butter(4,15/(sample_rate/2));        % 4th order, 15 Hz
break frequency

    pos(i,:) = filtfilt(b,a,raw_pos);
    force(i,:) = filtfilt(b,a,raw_force);
    vel(i,:) = filtfilt(b,a,raw_vel);
    current(i,:) = filtfilt(b,a,raw_current);
    temp(i,:) = filtfilt(b,a,raw_temp);

    force(i,:) = detrend(force(i,:),'constant');           %subtracts
DC offset from force data

end

%%  fit data to hysteretic model

%  --define the initial parameter guess and search bounds

x0=[-32 53 167 1.54 .74 9.4 147];
lb=[-33 53 167 1 .5 9 147];
ub=[-32 54 168 1.6 1 10 148];

%  --prepare for the optimization

options = optimset( ...
    'Display','iter', ...   % want to display lots of resuls
    'MaxFunevals',1000*length(x0), ...  % maximum number of iterations
    'TolCon',1e-10, ...     % termination tolerance for constraint
violation
    'TolFun',1e-10, ...     % termination tolerance for f
```

```
    'TolX',1e-6);           % termination tolerance for x


%  --find the optimal parameter vector

a=2;                    %choose the data sets to optimize from
b=7;

xopt = fmincon('fhat_h',x0,[],[],[],[],lb,ub,[],options,[current(a,:)
current(b,:)],[vel(a,:) vel(b,:)],[force(a,:) force(b,:)]);

[tot_e,e,f_calc] = fhat_h(xopt,[current(a,:) current(b,:)],[vel(a,:)
vel(b,:)],[force(a,:) force(b,:)]);

xopt
tot_e
```

hyst_graph.m

```
%  This script loads all the Tektronix CSV file data from the 6/3/06
%  testing of an MR damper with current and velocity excitation.

%  Rusty Richards - modified from S. C. Southward

close all
clear, clc

%  --load the position data

load rustest1.mat;
B(1,:,:)=A;
load rustest2.mat;
B(2,:,:)=A;
load rustest3.mat;
B(3,:,:)=A;
load rustest4.mat;
B(4,:,:)=A;
load rustest5.mat;
B(5,:,:)=A;
load rustest6.mat;
B(6,:,:)=A;
load rustest7.mat;
B(7,:,:)=A;
load rustest8.mat;
B(8,:,:)=A;
load rustest9.mat;
B(9,:,:)=A;
load rustest10.mat;
B(10,:,:)=A;


%%  Filter and scale Data Sets %%
```

```
% set scalars to convert data

sv = 25.6;            % (in/s)/volt
sf = 1024.3;            % (lbs)/volt
sp = 0.901;           % (in)/volt
sc = 10.0;            % (A)/volt
st = 180;           % (F)/volt

ov = 0.0221;            % offset (in/s)
of = 38.601;            % offset (lbs)
op = 3.7925;            % offset (in)
oc = 0;           % offset (A)
ot = 32;           % offset (F)

%  --create time data
length(B(1,:,1));
sample_rate = 2000;  %Hz
t = 0:1/sample_rate:(length(B(1,:,1))-1)/sample_rate;

%loop to extract and scale data from each data set
for i = 1:10

    raw_vel = B(i,:,1);
    raw_force = B(i,:,2);
    raw_pos = B(i,:,3);
    comm_current = B(i,:,4);
    raw_current = B(i,:,5);
    raw_temp = B(i,:,6);

    raw_vel = sv.*raw_vel+ov;
    raw_force = sf.*raw_force+of;
    raw_pos = sp.*raw_pos+op;
    raw_current = sc.*raw_current+oc;
    raw_temp = st.*raw_temp+ot;

    %  --clean up the data with a zero-phase low-pass filter

    [b,a] = butter(4,15/(sample_rate/2));        % 4th order, 15 Hz
break frequency

    pos(i,:) = filtfilt(b,a,raw_pos);
    force(i,:) = filtfilt(b,a,raw_force);
    vel(i,:) = filtfilt(b,a,raw_vel);
    current(i,:) = filtfilt(b,a,raw_current);
    temp(i,:) = filtfilt(b,a,raw_temp);

    force(i,:) = detrend(force(i,:),'constant');           %subtracts
DC offset from force data

end

%%  fit data to hysteretic model

%  --define the initial parameter guess and search bounds
```

```
x=[-32.2332 53.7158 167.5422 1.5455 0.7406 9.4129 147.4786];

[tot_e,e,f_calc] = fhat_h(x,current(5,:),vel(5,:),force(5,:));

%  --plot the data

figure(1)

plot(t,[force(5,:);f_calc'])
grid on
ylabel('Force')
xlabel('Time (sec)')
xlim([10,20])
legend('measured force','calculated force','location','NorthEast')

%  --plot the damper function

figure(2)

ms = 3;                    % marker size for plotting points

plot3(vel(5,:),current(5,:),f_calc,'.','MarkerSize',ms)
xlabel('Velocity')
ylabel('Current')
zlabel('Force')
grid on

histogram(current, vel, force, [7,2]);
histogram(current(5,:), vel(5,:), f_calc', [7,2]);
```

The final script generates the empirical PDFs for the v0 parameter for the probability model.

Prob_fit.m

```
%  This script loads all the Tektronix CSV file data from the 6/3/06
%  testing of an MR damper with current and velocity excitation.

%  Rusty Richards - modified from S. C. Southward

close all
clear, clc

%  --load the position data

%  --load the position data

load rustest1.mat;
B(1,:,:)=A;
load rustest2.mat;
B(2,:,:)=A;
```

```
load rustest3.mat;
B(3,:,:)=A;
load rustest4.mat;
B(4,:,:)=A;
load rustest5.mat;
B(5,:,:)=A;
load rustest6.mat;
B(6,:,:)=A;
load rustest7.mat;
B(7,:,:)=A;
load rustest8.mat;
B(8,:,:)=A;
load rustest9.mat;
B(9,:,:)=A;
load rustest10.mat;
B(10,:,:)=A;


%%  Filter and scale Data Sets %%

% set scalars to convert data

sv = 25.6;            % (in/s)/volt
sf = 1024.3;            % (lbs)/volt
sp = 0.901;           % (in)/volt
sc = 10.0;           % (A)/volt
st = 180;           % (F)/volt

ov = 0.0221;            % offset (in/s)
of = 38.601;            % offset (lbs)
op = 3.7925;            % offset (in)
oc = 0;           % offset (A)
ot = 32;           % offset (F)

%  --create time data
length(B(1,:,1));
sample_rate = 2000;  %Hz
t = 0:1/sample_rate:(length(B(1,:,1))-1)/sample_rate;

%loop to extract and scale data from each data set
for i = 1:10

    raw_vel = B(i,:,1);
    raw_force = B(i,:,2);
    raw_pos = B(i,:,3);
    comm_current = B(i,:,4);
    raw_current = B(i,:,5);
    raw_temp = B(i,:,6);

    raw_vel = sv.*raw_vel+ov;
    raw_force = sf.*raw_force+of;
    raw_pos = sp.*raw_pos+op;
    raw_current = sc.*raw_current+oc;
    raw_temp = st.*raw_temp+ot;
```

```
    %  --clean up the data with a zero-phase low-pass filter

    [b,a] = butter(4,15/(sample_rate/2));        % 4th order, 15 Hz
break frequency

    pos(i,:) = filtfilt(b,a,raw_pos);
    force(i,:) = filtfilt(b,a,raw_force);
    vel(i,:) = filtfilt(b,a,raw_vel);
    current(i,:) = filtfilt(b,a,raw_current);
    temp(i,:) = filtfilt(b,a,raw_temp);

    force(i,:) = detrend(force(i,:),'constant');           %subtracts
DC offset from force data

end

hist_f=histogram(current, vel, force);

minv=min(min(vel));
minf=min(min(force));
maxv=max(max(vel));
maxf=max(max(force));

vc=linspace(minv,maxv,100);       %divisions for velocity

prob=zeros(100,10);
f_calc=zeros(100,100,10);
v0=logspace(-1,2.7,100);

for i=1:1:10
    cur=i/5-0.1;
    for j=1:100

        x=[-22.9 21.4 194.3 7.462 v0(j) 7.5];
        [temp, temp2,
f_calc(:,j,i)]=fhat(x,cur,vc,zeros(1,length(vc)));

        f_temp=horzcat(f_calc(:,j,i)',minf,maxf);
        v_temp=horzcat(vc,maxv,minv);
        hist_fc=histogram(i*ones(1,length(v_temp)), v_temp, f_temp);

        prob(j,i)=sum(sum(hist_fc.*hist_f(:,:,i)));
    end
end


prob_tot=sum(prob,2);
figure(1)
semilogx(v0,prob_tot',[1.1734,1.1734],[0,max(prob_tot)],'r')
xlabel('v0 (in/sec)')
ylabel('occurence')
legend('actual','predicted')

sc=sum(prob(1))./sum(prob);
```

```
sc=ones(length(prob),1)*sc;

figure(2)
semilogx(v0,prob.*sc)
hold on
semilogx([1.1734,1.1734],[0,550],'r')
xlabel('v0 (in/sec)')
ylabel('occurence')
legend('0.1','0.3','0.5','0.7','0.9','1.1','1.3','1.5','1.7','1.9')

figure(3)
plot(vc,f_calc(:,:,i))
```

B.2 Simulink Model

The input signals for the Roehrig dynamometer and the Lord damper were created using the Simulink toolbox in Matlab. The following code sets the parameters and captures the data from the simulation.

Roehrig_inputs.m

```
tc=1/150;
tfv=10;
tfc=10;
velmax=15;
curmax=2;
posmax=1;
pos_gain=1;
pos_off=0;
cur_gain=1;
cur_off=0;

npi=.01;
npv=.01;

cutoff_c=15;
f = [0 cutoff_c cutoff_c 1];
m = [1 1 0 0];
[numc,demc]=butter(4,cutoff_c,'s');

cutoff_v=60;
f = [0 cutoff_v cutoff_v 1];
m = [1 1 0 0];
[numv,demv]=butter(4,cutoff_v,'s');

cur_val=1000;
vel_val=1000;

sim('velocity_generator',tfv);
```

```
sim('current_generator',tfc);

diff = max(position)-min(position);
pos_gain = posmax/diff;
pos_off=posmax/2-(max(position)+min(position))/2*pos_gain;
diff = max(current)-min(current);
cur_gain = curmax/diff;
cur_off=curmax/2-(max(current)+min(current))/2*cur_gain

sim('velocity_generator',tfv);
sim('current_generator',tfc);

figure(1)
plot(current)
figure (2)
plot(position)
figure (3)
plot(velocity)
figure (4)
plot(velocity,current,'.-','MarkerSize',2)
grid on


time_vel = [0:tc:tfv]';
time_cur = [0:tc:tfc]';
position = [time_vel position];
current = [time_cur current];

csvwrite('rand_pos.csv',position);
csvwrite('rand_cur.csv',current);
```

The Simulink models to generate the velocity and current signals is pictured in Figure B-1 and Figure B-2.

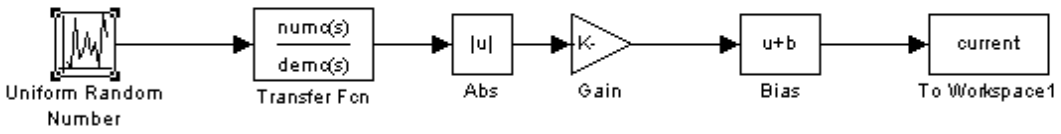

Figure B-1. Simulink model used to generate the current signal for the experiment.

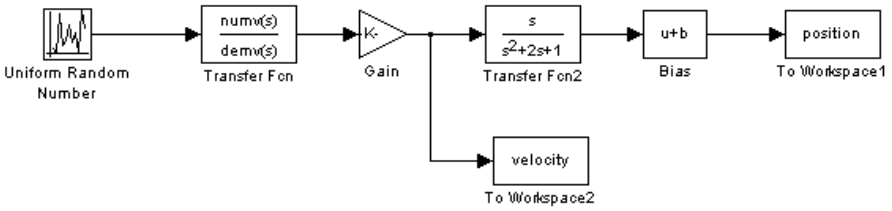

Figure B-2. Simulink model used to generate the velocity signal for the experiment.

C Data Sheets for Experiment Equipment

The following section has the data sheets for the equipment used in the data collection.

Table C-1. Datasheet for the AEMC current probe.

MODEL	SL261
ELECTRICAL	
Nominal Range	10A & 100A
Measurement Range	100mA to 100A
Transformation Ratio	Voltage output
Output Signal	10A: 100mV/A 100A: 10mV/A
Accuracy (100mV/A Range) 50mA to 10A Peak	3% of Reading ± 50mA
500mA to 40A Peak	±4% of Reading ± 50mA
40A to 100A Peak	±15% max @ 100A
Phase Shift (10mV/A Range) DC	to 65Hz 1.5°
Overload	Red LED indicates input greater than the selected range
Frequency Range	DC to 100kHz (-3dB with current derating)
Load Impedance	>1MΩ/100pF
Working/Common Mode Voltage	600Vrms
Output Termination	6.5 ft coaxial cable
MECHANICAL	
Operating Temperature	32° to 122°F (0° to 50°C)
Storage Temperature	-22° to 176°F (-30° to 80°C)
Operating Relative Humidity	10° to 30°C: 85 ± 5% RH (without condensation) 40° to 50°C: 45 ± 5% RH (without condensation)
Maximum Conductor Size	0.46" (11.8mm)
Dimensions	9.09 x 1.42 x 2.64" (231 x 36 x 67mm)
Weight	11.6 oz (330g) with battery
Polycarbonate Material	Handle: Lexan® 920A, UL94 V2
SAFETY	
Electrical	EN 61010-2-32
UL Approval	Yes – Canada and United States
Double Insulation ⧈	Yes
CE Mark	Yes

Note: Reference conditions:
Model SL261: 23°C ± 5°K, 20 to 75% RH, DC to 1kHz, probe zeroed, 1 minute warm-up, battery at 9V ± 0.1V, external magnetic field < 40A/m, no DC component, no external current carrying conductor, 1MΩ/100pF load, conductor centered.

Table C-2. Data Sheet for the Tektronix TDS3054B

Form Factor	Benchtop
Bandwidth	500 MHz
Number of Channels	4 ch
Simultaneous Channels	4 ch
Simultaneous Maximum Sampling Rate/ch	5 GSa/s
One ch. only max. sampling rate	5 GSa/s
Max. Single Shot bandwidth	500 MHz
Max. Record Length	10000 pt/sec
Min. Vertical Sensitivity	1 mV/div
Maximum Vertical Sensitivity	10 V/div
Number of Bits	9 bits
Input Impedance	1 MOhm
Input Impedance (alternate)	50 Ohm
Input Coupling	AC,DC,GND
Maximum Input Voltage	150 Vrms
Main time base - lowest	1 ns/div
Main time base - highest	10 s/div
Timebase accuracy	0.002 %
Trigger Source	External,Internal
Minimum Trigger Holdoff	13.2 ns
Minimum Glitch Trigger	39.6 ns
Display Type	Color LCD
Display modes	Dot,Persistence,Vector

Also in this section is the calibration data for the Lord transconductance amplifier and the Roehrig dynamometer. **Error! Reference source not found.** contains the input voltage to the current output for the Lord Wonderbox.

Typical Performance, 4 ohm load

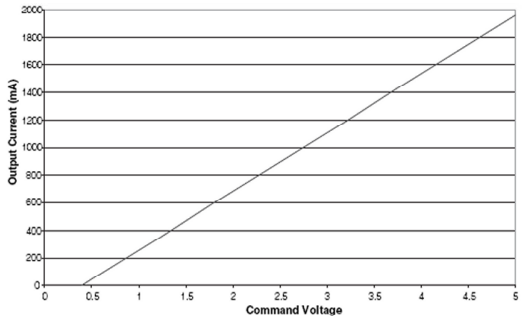

Input Voltage	Output Current (4 ohm)
~ 0.4-0.6 V	0 mA
2 V	750 mA
4.3 V	1800 mA

Input Voltage	Output Current (8 ohm)
~ 0.4-0.6 V	0 mA
1.6 V	600 mA
3.2 V	1300 mA

Figure C-1. Lord Wonderbox calibration curve.

The next figures are the calibration curves for the Roehrig. The first, **Error! Reference source not found.**, shows the relationship of the current output to the

displacement of the damper. Following that, **Error! Reference source not found.** shows the velocity, **Error! Reference source not found.** the force, and **Error! Reference source not found.**, the temperature.

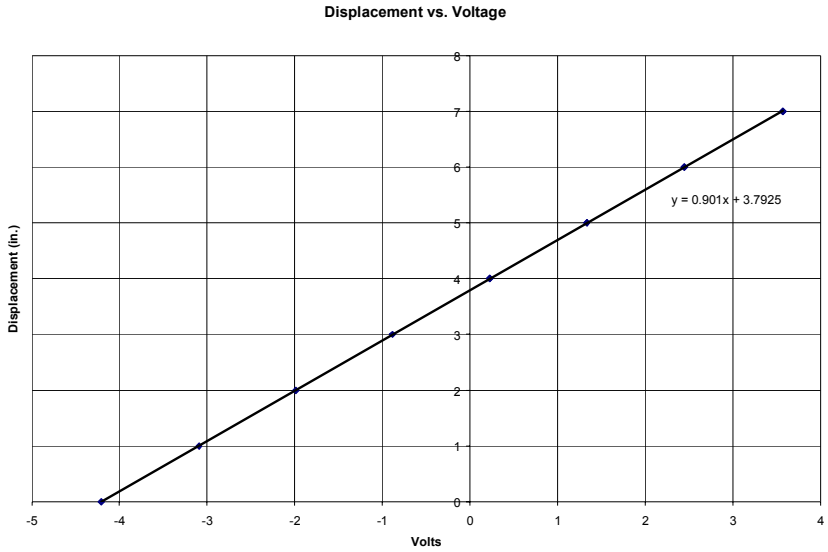

Figure C-2. Calibration curve for the displacement output of the Roehrig dynamometer.

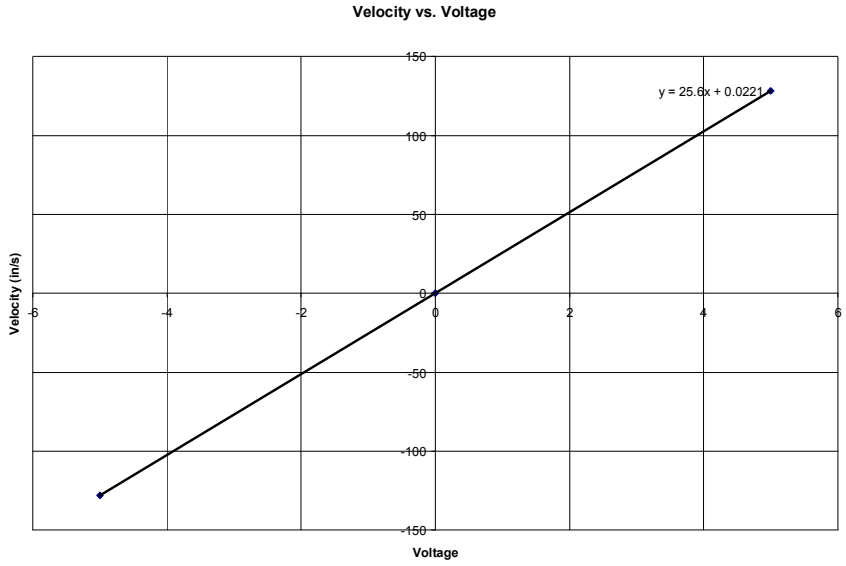

Figure C-3. Calibration curve for the velocity output of the Roehrig dynamometer

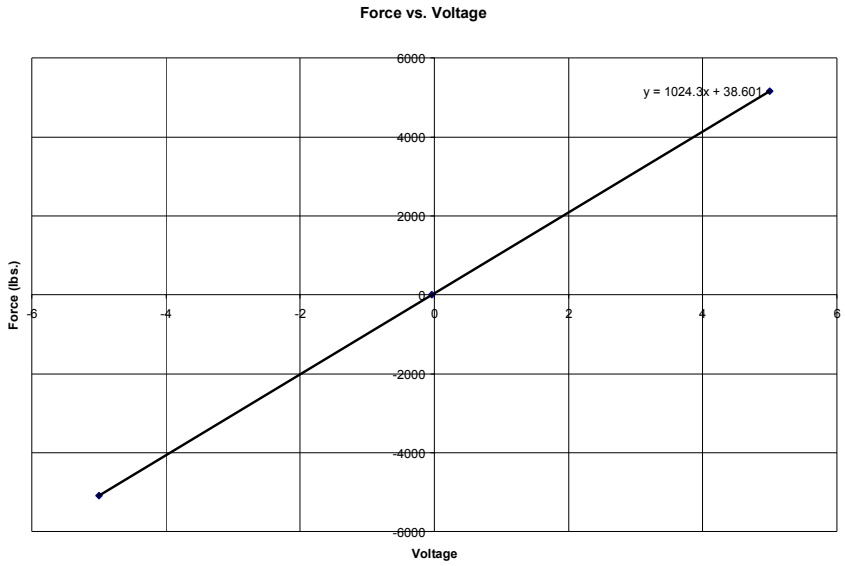

Figure C-4. Calibration curve for the force output of the Roehrig dynamometer

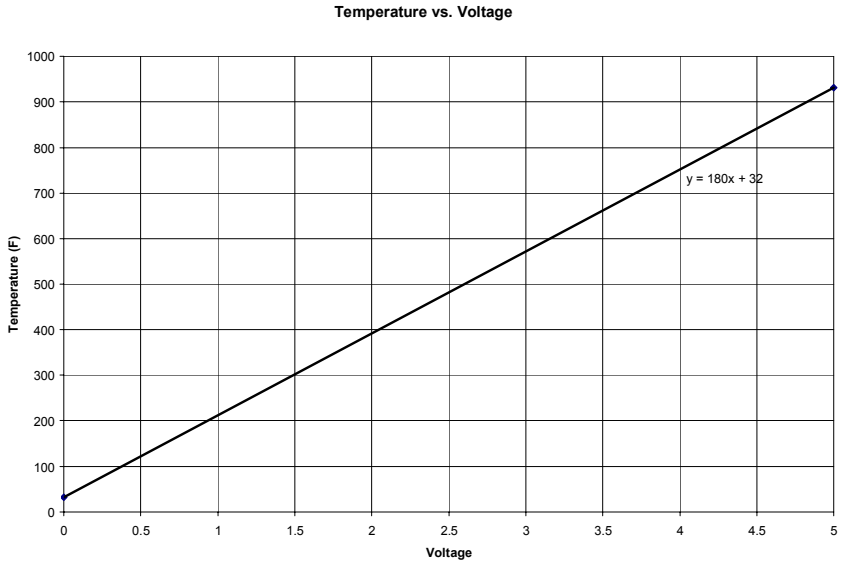

Figure C-5. Calibration curve for the temperature output of the Roehrig dynamometer

D Future Research and Considerations

Creating an appropriate probability model for the data is difficult due because a nonparametric approach must be taken. Again we will consider the problem in only one parameter, and by the same logic assume that *v0* is the most appropriate one to be governed by a probability function. We know the general shape of the density function for the parameter *v0*, and that it is bounded by 0 and infinity. Using Matlab's *dfittool* built in probability solver, we can compare the likelihood of parametric PDF function describing the data. F shows the graphical interface of *dfittool*.

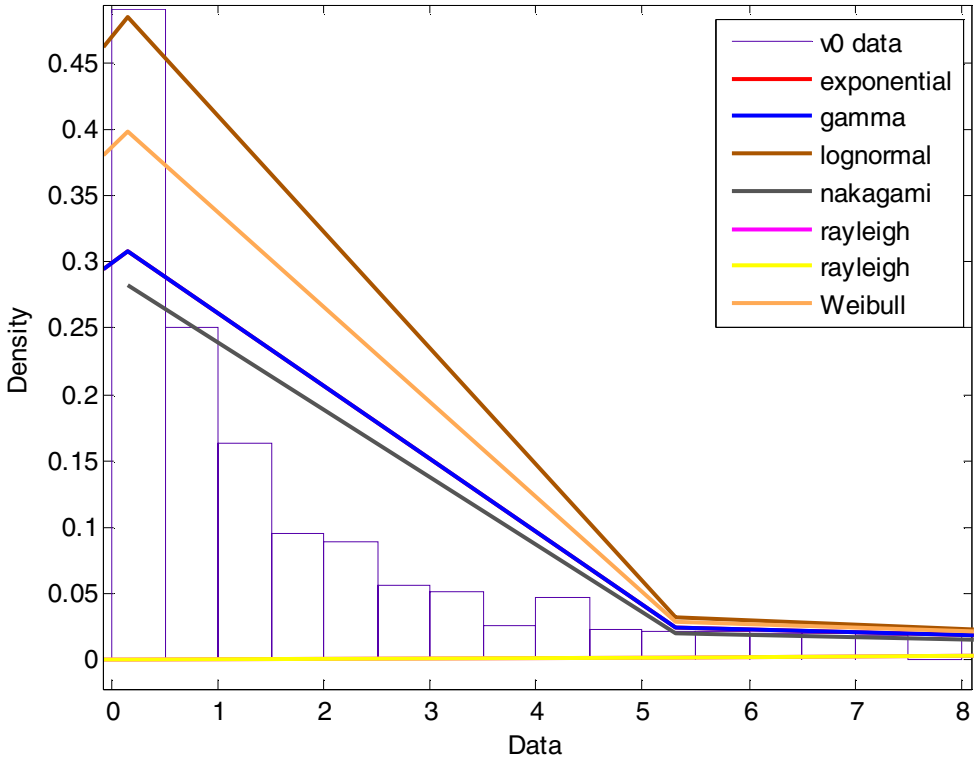

Figure D-1. Matlab approximation of probability distributions. Note that Matlab sets bin size independent of source data.

The downfall of the Matlab functions is that they expect a linear scale for the data. Because the *v0* data is logarithmically distributed, important characteristics of the empirical PDF are lost in the parametric estimation. An appropriate window and smoothing technique may be needed to get accurate results. Running the *dfittool* solver

without adjusting the data results in PDF functions that vary greatly in mean value and variation. The results can be seen in Table D-1.

Table D-1. Log likelihoods and parameter values for the types of probability distributions that match v0

Distribution	Log Likelihood	Mean	Variance	Parameter value(s)		
Exponential	-1.80E+07	35.60	1267.69	μ	=	35.6046
Gamma	-1.42E+07	35.60	4480.03	a	=	0.282964
				b	=	125.827
Lognormal	-1.32E+07	40.75	296585.00	μ	=	1.1122
				σ	=	2.2783
Nakagami	-1.45E+07	49.68	6538.14	μ	=	0.115796
				ω	=	9006.29
Rayleigh	-3.27E+07	84.10	1932.77	b	=	67.1055
Weibull	-1.37E+07	28.96	6955.67	a	=	10.0274
				b	=	0.421922

Another consideration for future research is examining the preyield/postyield characteristics of the damper. Figure D-2 shows the PDF of the data from a different direction, slicing along velocity, which relates current to force. This section is taken at a velocity range of -0.54 to 0.14 in/s. There is a much higher range of possible force output from the damper at higher currents. This could be attributable to hysteresis or the yield characteristic of the damper. At high driving frequencies for the damper, the preyield/postyield transition point occurs at a certain velocity. However, at driving frequencies close to zero, the damper may exert a force even at zero velocity. The large range of forces at zero velocity in the PDF could be in part because of the different driving frequencies contained in the velocity input signal.

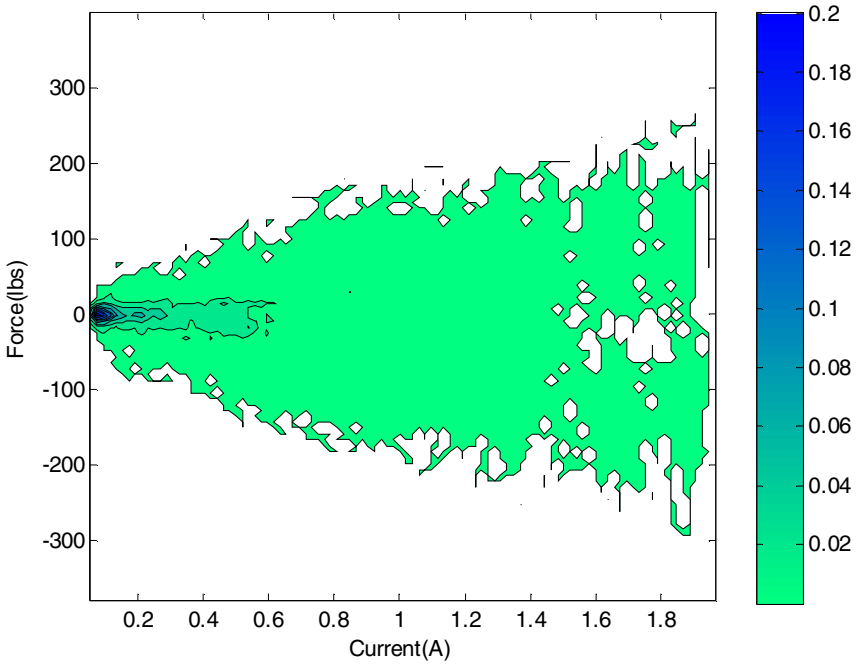

Figure D-2. PDF of current versus force for the MR damper at a velocity range of -0.5 to 0.1 in/s. The range of possible force outputs at higher currents could be attributable to hysteresis, or a frequency dependant yield transistion.

References

[1] Poyner, J.C., "Innovative Designs for Magneto-Rheological Dampers," Master of Science Thesis, Department of Mechanical Engineering, Virginia Tech, August 2001.

[2] Goncalves, F. "Dynamic Analysis of Semiactive Control Techniques for Vehicle Applications," Master of Science Thesis, Department of Mechanical Engineering, Virginia Tech, August 2001.

[3] Dixon, J., *The Shock Absorber Handbook,* Society of Automotive Engineers, Inc. Warrendale, PA, 1999.

[4] Lord Corporation, "Rheonetic™ MR Damper RD-1005-3," http://www.rheonetic.com/devices_damper_begin.htm,

[5] Simon, D., "Investigation of the Effectiveness of Skyhook Suspension for Controlling Roll Dynamics of Sport Utility Vehicles using Magneto-Rheological Dampers," Ph.D. Dissertation, Department of Mechanical Engineering, Virginia Tech, December 2001.

[6] Masi, J.W., "Affective of Control Techniques on the Performance of Semiactive Dampers," Master of Science Thesis, Department of Mechanical Engineering, Virginia Tech, December 2001.

[7] Paré, C.A., Ahmadian, M. "A Quarter-Car Experimental Analysis of Alternative Semiactive Control Methods," *Journal of Intelligent Material Systems and Structures*, Vol. 11, 2000, pp 604-612.

[8] Ma, X.Q., Wang, E.R., Rakheja, S., and Su, C.Y., "Modeling Hysteretic Characteristics of MR Fluid Damper and Model Validation," *Proceedings of the 41st IEEE Conference on Decision and Control*, Las Vegas, NV, December 2002.

[9] Spencer, B.F., Dyke, S.J., Sain, M.K., and Carlson, J.D., "Phenomenological model for a Magnetorheological Damper," *J. Eng. Mech. Am. Soc. Civil Eng.* Vol 123, pp. 230–52

[10] Dominguez, A., Sedaghati, R., and Stiharu, I., "Modeling the Hysteresis Phenomenon of Megnetorheological Dampers," *Smart Materials and Structures*, Vol. 13, 2004, pp 1351-1361.

[11] Song, X., Ahmadian, M., and Southward, S., "Modeling Megneto-Rheological Dampers with Application of Nonparametric Approach," *Journal of Intelligent Material Systems and Structures*, Vol. 16, 2005, pp 421-432.

[12 Mugtussidis, I.B., "Flight Data Processing Techniques to Identify Unusual Events," Ph.D. Dissertation, Department of Aerospace Engineering, Virginia Tech, June 2000.

[13] Phillips, K.A., "Probability Density Function Estimation Applied to Minimum Bit Error Rate Adaptive Filtering," Master of Science Thesis, Department of Electrical and Computer Engineering, Virginia Tech, May 1999.

[14] Hambley, Allen, *Electrical Engineering Principles and Applications*. Prentice Hall, Upper Saddle River, NJ, 2002